INTRANASAL DELIVERY OF MACROMOLECULES TO THE RODENT BRAIN VIA OLFACTORY PATHWAYS.

A THESIS SUBMITTED IN TOTAL FULFILMENT

OF THE REQUIREMENTS OF

THE DEGREE OF DOCTOR OF PHILOSOPHY

BY

Anthony Neil Pollard

Bachelor of Science (Honours)

Department of Human Physiology,

Centre for Neuroscience;

School of Medicine, Flinders University;

Adelaide, South Australia

March 2009

TABLE OF CONTENTS

Dedicated to my Nanna,

Muriel Estella Bartle

1912-2006

THESIS SUMMARY

One of the major limitations in drug development and gene therapy for brain diseases is the natural defensive structure called the blood brain barrier (BBB), which prevents therapeutic polypeptide drugs and viral vectors from entering the brain. Intranasal delivery of therapeutic gene products into the brain offers a non-invasive alternative towards a feasible gene and protein therapy for neurological diseases. From recent studies involving axonal transport, it is tempting to speculate that therapeutic macromolecules including neurotrophic factors and viral vectors can be delivered into the brain by peripheral neurons, such as olfactory receptor neurons (ORNs), which span the BBB. It is thought that the nasal pathway into the brain involves two general mechanisms; intracellular (intraneuronal) or extracellular routes of transport. However the pathways involved have not yet been fully characterized.

In this study I firstly investigated the temporal and spatial localisation pattern of both biotinylated and I^{125} labelled ciliary neurotrophic factor (CNTF) following nasal delivery into Sprague-Dawley rats. Results showed that intranasal delivered CNTF was transported to several brain regions by both intracellular/axonal pathway through ORNs and the extracellular trigeminal pathway. Excess unlabelled CNTF competed for receptor binding in the olfactory mucosa confirming receptor mediated intracellular transport to the olfactory bulb via ORNs. Denervation of the olfactory mucosa prior to CNTF delivery failed to prevent CNTF transport to trigeminal and hypothalamic brain regions. Intranasal delivered CNTF was biologically active, resulting in activation of the STAT3 signalling pathway in the thalamus and hypothalamus.

To examine the functional activity of intranasal delivered CNTF, I conducted a weight loss trial using an obese Zucker rat (OZR) model to test whether CNTF treatment caused body weight loss. Intranasal administration of CNTF resulted in

reduced body weight in the CNTF treated OZR group compared to the BSA control group during the 12 day trial and for 3 days after. Intranasal delivery of CNTF may be a valuable method for the treatment of obesity.

In the second study, I investigated the temporal and spatial expression of Enhanced Green Fluorescent Protein (EGFP) transferred by a single nasal delivery of either a recombinant adenovirus vector (Ad5CMV-EGFP) or an adeno-associated virus vector (AAV2-EGFP) into Sprague-Dawley rats. Adenovirus mediated EGFP expression was localized in ORNs throughout the olfactory epithelium after 24 hours. EGFP in the ORNs appeared to be anterogradely transported along their axons to the olfactory bulb and transferred in glomeruli to second-order neurons. EGFP was transferred to several brain regions including the cortex, hippocampus, and brainstem after 7 days. EGFP expression co-localized with Olfactory Marker Protein and was confirmed with EGFP immunofluorescence labelling and western blotting. AAV expressed EGFP localized in similar olfactory and brain regions 6 weeks after delivery. mRNA levels suggested that the AAV-EGFP construct was only incorporated into olfactory mucosa cells and the viral vector was not present in olfactory bulb and brain regions.

In conclusion, this simple and non-invasive polypeptide and gene delivery method provides ubiquitous macromolecule distribution throughout the rodent brain and may be useful for the treatment of neurological disorders.

DECLARATION

I certify that this thesis does not incorporate without acknowledgment any material previously submitted for a degree or diploma in any university; and that to the best of my knowledge and belief it does not contain any material previously published or written by another person except where due reference is made in the text.

I give consent to this copy of my thesis, when deposited in the University Library, being available for loan and photocopying.

The author acknowledges that copyright of published work contained within this thesis resides with the copyright holder/s of those works.

Anthony N Pollard

March 2009

ACKNOWLEDGEMENTS

This PhD project has most certainly led me on a fantastic journey through the field of neuroscience, in particular, olfactory neuroscience. Firstly, I would like to acknowledge my principle supervisor, Prof. Xin-Fu Zhou, who introduced me to this exciting project and provided me support, encouragement and exceptional patience that allowed the completion of this thesis possible. I am very grateful for his excellent scientific insight, enthusiasm in this field and deep knowledge.

Secondly, many thanks to my co-supervisors, Prof. Gino Saccone and Prof. Johnno Oliver for providing excellent critical review of my thesis and great assistance and advice for my final PhD seminar. Additionally I would also like to thank my other co-supervisor, Dr. Steve Johnson, for good advice and discussions early in my candidature.

Many thanks to all the members of the Neuroregeneration lab both past and present for their good advice and technical support during my project. In particular I would like to especially thank Ernesto Aguilar, my PhD bro and running mate, for excellent friendship, support and good discussions over a few beers or sangria's. I would also certainly like to thank my other PhD brother and friend, Dr. John Wang, for his great surgical knowledge in teaching me animal surgery skills and a healthy appreciation for Chongquing (Szechuan) cuisine + Chinese rice wine. My appreciation also goes to Dr. Henry Li for good advice and assistance in fluorescent microscopy, and Michelle Norman for excellent histological advice and training. The staff of the Flinders Uni animal house provided me with good support and patience, with my thanks going to Ray, Stuart, Theresa and Peggy. For allowing me to use their lab space for my radioiodination experiments, thanks goes to Dr. Heather Barr and Prof. Bill Blessing. Quite regularly, the members of the FURACS group of level6 gave me good companionship over a few reds, and thanks to Robyn, Jen, Mary-Louise, Rainer, Rodrigo, Matty, Mal & Bren. Also thanks to Dusan who helped me channel my frustrations into healthy competition of indoor soccer.

Finally, my deepest thanks and love go to my family, Mum, Dad and Mike for their unconditional love and support throughout difficult times.

Lastly, I would like to especially thank my loving wife, Fiona for all her support, friendship, advice and tender care during this tough time. I am very blessed too have known her and cherished the time we spent together.

PERSONAL PUBLICATIONS AND CONFERENCE PRESENTATIONS

Personal Publications (2005-2009)

Refereed Journal Articles

1) **Pollard AN**, Aguilar-Salegio EA, Wang YJ, Sun Y and Zhou XF. (2009) Delivery of CNTF along olfactory pathways and the implication in the therapeutic treatment of obesity. (Submitted to J Cell Molec. Med.).

2) **Pollard AN**, Wang YJ, Aguilar-Salegio EA, and Zhou XF. (2009) Adenoviral and AAV vector gene delivery of enhanced-GFP to the brain via the olfactory receptor neurons. (in manuscript).

3) Aguilar-Salegio EA, **Pollard AN**, Smith M and Zhou XF. (2009) Depletion of macrophages prevents regeneration of pre-conditioned adult dorsal root ganglion neurons after spinal cord injury. (Submitted to Brain Behav Immun.)

4) Wang YJ, Valadares D, Sun Y, Wang X, Zhong JH, Liu XH, Majd S, Chen L, Gao CY, Chen S, Lim Y, **Pollard AN**, Aguilar E, Gai WP, Yang M, Zhou XF. (2009) Effects of proNGF on Neuronal Viability, Neurite Growth and Amyloid-beta Metabolism. **Neurotox Res.** 2009 Aug 13. [Epub ahead of print]

5) Wang YJ, Thomas P, Zhong JH, Bi FF, Kosaraju S, **Pollard AN**, Fenech M, Zhou XF. (2009) Consumption of grape seed extract prevents amyloid-beta deposition and attenuates inflammation in brain of an Alzheimer's disease mouse. **Neurotox Res.** 15:3-14.

6) Wang YJ, **Pollard AN**, Zhong JH, Dong XY, Wu XB, Zhou HD and Zhou XF. (2009) Intramuscular delivery of a single chain antibody gene reduces brain amyloid-beta burden in a mouse model of Alzheimer's disease. **Neurobiol of Aging.** 30:364-376.

7) Thomas P, Wang YJ, **Pollard AN**, Zhong JH, Kosaraju S, O'Callaghan NJ, Zhou XF, Fenech M. (2008) Grape seed polyphenols and curcumin reduce genomic instability events in a transgenic mouse model for Alzheimer's disease. **Mutat Res.** (Nov 6. Epub ahead of print)

Conference proceedings

1. Wang YJ*****, Thomas P, Zhong JH, Bi FF, Kosaraju S, **Pollard A**, Fenech M, Zhou XF. (2008) Consumption of polyphenol-rich grape seed extract prevents amyloid deposition and suppresses inflammation in the brain of a transgenic mouse model for Alzheimer's disease. Society for Neuroscience (SfN) 38th annual meeting, Washington DC, US, Nov19 (Symposium talk)

2. **Pollard AN***, Zhou FH, Zhong JH, Oliver J and Zhou XF. (2007) Intranasal delivery of ciliary neurotrophic factor to the rat brain along olfactory pathways. Society for Neuroscience (SfN) 37th annual meeting,. San Diego, Calif, US, Nov 3-7. (Poster presentation)

3. **Pollard AN***, Zhong JH, Wang YJ and Zhou XF. (2006) Adenoviral Vector Gene Delivery to the Brain via the Olfactory Sensory Receptor Neurons. Australian Neuroscience Society (ANS) 26th annual meeting, Sydney, Australia, Jan 31-Feb 3. (Poster presentation)

4. Wang YJ*, **Pollard AN**, Zhou HD, Zhong JH, and Zhou XF. (2006) Characterization of an Alzheimer's Disease Mouse Model Bearing Mutant Genes of Amyloid Precursor Protein and Human Presenilin 1. Australian Neuroscience Society (ANS) 26th annual meeting, Sydney, Australia, Jan 31-Feb 3. (Poster presentation)

5. **Pollard AN***, Li L, Zhou FH, Zhong JH, Wu XB and Zhou XF. (2005) AAV-Mediated Gene Delivery of GFP to the Brain via the Olfactory Pathway. Australian Neuroscience Society (ANS) 25th annual meeting, Perth, Australia, 30 Jan - 2 Feb 2005. (Symposium talk)

* Presenting author.

GENERAL ABBREVIATIONS

Abbreviation	Full name
AAV	adeno associated virus
ABC	avidin-biotin conjugate
AdV	adenovirus
ALS	amyotrophic lateral sclerosis
BBB	blood brain barrier
BCA	bicinchoninic acid
BSA	bovine serum albumin
cDNA	complementary DNA from mRNA
cm, mm, μm	centimetre, millimetre, micrometre
CNS, PNS	central nervous system, peripheral nervous system
rhCNTF	recombinant human ciliary neurotrophic factor
CO_2	carbon dioxide
CPM/mg	counts per minute/ milligram
CSF	cerebral spinal fluid
DAB	3'3'-diamino-benzidine tetrachloride
DAPI	4',6-diamidino-2-phenylindole
DNA	deoxyribonucleic acid
ECL	enhanced chemiluminescence
EDTA	ethylenediaminetetraacetic acid
EGFP	enhanced green fluorescence protein
H&E	haematoxylin & eosin
h, min, s	hour, minute, second
H_2O_2	hydrogen peroxide
HCl	hydrogen chloride
HRP	horse-radish peroxide
IGF	insulin growth factor
ICV, IM, IN, IPa, IT, IV	intracerebroventricular, intramuscular, intranasal, intraparenchymal, intrathecal, intravenous
IL	interleukin
KDa	kilo daltons
Kg, g, mg, μg, ng	kilogram, gram, milligram, microgram, nanogram

L, ml, µl	litre, millilitre, microlitre
M, mM, µM, nM	molar, millimolar, micromolar, nano molar
mRNA	messenger ribonucleic acid
MW	molecular weight
NaCl	sodium chloride
$NaNO_3$	sodium nitrate
NaOH	sodium hydroxide
NHS	normal horse serum
NGF	nerve growth factor
^oC	degrees celsius
OMP	olfactory marker protein
ORN	olfactory receptor neuron
OZR	obese Zucker rat
PAGE	polyacrylamide gel electrophoresis
PB	phosphate buffer
PBS	phosphate buffered saline
PBST	PBS + 0.1% tween-20
RT-PCR	reverse transcription polymerase chain reaction
pH	hydrogen ion concentration
pSTAT3	phospho- signal transduction and activation of transcription 3
RT	room temperature
SD	Sprague Dawley
SDS	sodium dodecylsulphate
pSTAT	phosphorylated signal transduction and activation of transcription
TBS	tris buffered saline
TCA	trichloracetic acid
WGA	wheat germ agglutinin
$ZnSO_4$	zinc suphate

BRAIN REGION NOMENCLATURE

Abbreviation	Full name
AOB	accessory olfactory bulb
AOV	anterior olfactory nucleus, ventral part
ArcM	arcuate nucleus, medial part
CA2	field CA2 of hippocampus
CA3	field CA3 of hippocampus
Cb	cerebellum
CPu	caudate putamen (striatum)
DEn	dorsal endopiriform cortex
DG	dentate gyrus
EPL	external plexiform layer of olfactory bulb
GL	glomerular layer of olfactory bulb
GCL	granular cell layer of olfactory bulb
IC	inferior colliculus
IPL	internal plexiform layer of olfactory bulb
LC	locus coeruleus
LEnt	lateral entorhinal cortex
LH	lateral hypothalamus
MCL	mitral cell layer of olfactory bulb
MOB	main olfactory bulb
ONL	olfactory nerve layer
Pr5VL	principal sensory trigeminal nucleus, ventrolateral part
PVP	paraventriular thalamic nucleus, posterior part
sp5	spinal trigeminal tract
VCA	ventral cochlear nucleus, anterior part
VMH	ventromedial hypothalamic nucleus
VPL	ventral postereolateral thalamic nuclei

CHAPTER 1

LITERATURE REVIEW & PROJECT AIMS

1.1 General Introduction

Prevention and cure of human brain diseases is a major goal of brain related neuroscience research. Although there has been dramatic progress in understanding the biological mechanisms underlying neurodegenerative diseases and the identification of many drug targets for these diseases, little progress has been made in developing an effective delivery of therapeutic drugs. For drug treatment therapies, the overall goal of drug delivery is to achieve and maintain therapeutic concentrations of the drug at the appropriate site of action, and also to avoid exposing other tissues to potentially deleterious concentrations of the drug. Currently, there are no effective treatments in the area of neurodegenerative diseases that have been completely approved. One of the major limitations in drug development for brain diseases is the natural defensive structure called the blood brain barrier (BBB), which prevents biologically powerful therapeutic drugs or gene vectors from penetrating the brain. In fact, many prospective drugs in preclinical and clinical trials with potential for treatment of brain diseases were terminated due to an inability to effectively deliver the drug into the brain and side effects of systemic large doses (Thoenen and Sendtner, 2002). Some drug companies have abandoned the drug development program altogether for neurological diseases and up to 40% of candidate drugs have been abandoned during development due to poor pharmacokinetic profiles (Prentis et al., 1988; Lansbury, 2004). Thus, research into overcoming the limitations of the BBB and promoting penetration of therapeutic large molecules into the brain bares paramount importance for the treatment of human neurological diseases. Surprisingly, there are few studies on this important topic within the neuroscience field.

Recently, many studies have focussed on the possibility of circumventing the BBB for the direct central delivery of macromolecules to the central nervous system

(CNS) by utilizing the potential direct transport pathway from nose to brain via the olfactory region (Mathison et al., 1998; Thorne and Frey 2nd, 2001; Illum, 2004). Much research characterizing this pathway has been done in animal models, but the mechanisms involved have not been fully elucidated and it is undecided whether similar transport occurs in humans (Merkus and van den Berg, 2007).

In this introductory chapter, a brief review of the BBB limitation on macromolecule delivery to the CNS, the concept of intranasal delivery mechanisms, and the cellular structure and pathways involved in the olfactory system will be presented. In addition, the aims and hypothesis of this project will be introduced.

1.2 The Blood Brain Barrier

The vascular system of the CNS is characterized by the presence of the BBB which divides the brain interstitial fluid from the circulating blood. The BBB not only maintains proper homeostasis by controlling influx and efflux of substances containing necessary nutrients, but also protects the brain from substances in the blood which could disrupt neurological functions. The BBB restricts macromolecule entry into the CNS from blood through several mechanisms including, a physical endothelial, enzymatic and efflux barriers (Pardridge, 2002). The multicellular BBB is formed by brain capillary endothelial cells, pericytes, astrocyte foot processes and the occasional nerve endings **(Fig. 1.1)**. Brain capillary endothelial cells are connected by epithelial-like high-resistance tight junctions which divide the endothelial plasma membrane into two domains: an abluminal membrane on the brain side of the BBB and a luminal membrane on the blood side (Brightman, 1977) (Pardridge, 2002). With minimal pinocytosis and no paracellular transport across the brain microvasculature, molecules from the blood can only cross the BBB via lipid-mediated free diffusion or catalysed transport through the endothelial cells. However,

Figure 1.1 The Blood Brain Barrier cellular structure.

These diagrams show the structural and cellular organisation of the brain capillaries. Endothelial cells in these capillaries contain tight junctions which restrict the transport of macromolecules <500 Da from the circulation. Endothelial cells are surrounded by capillary pericytes and perivascular astrocyte foot processes.

These BBB images are adapted from Principles of Human Physiology (2nd Edn.) Germann & Stanfield (2005) and Thorne & Frey 2nd (2001).

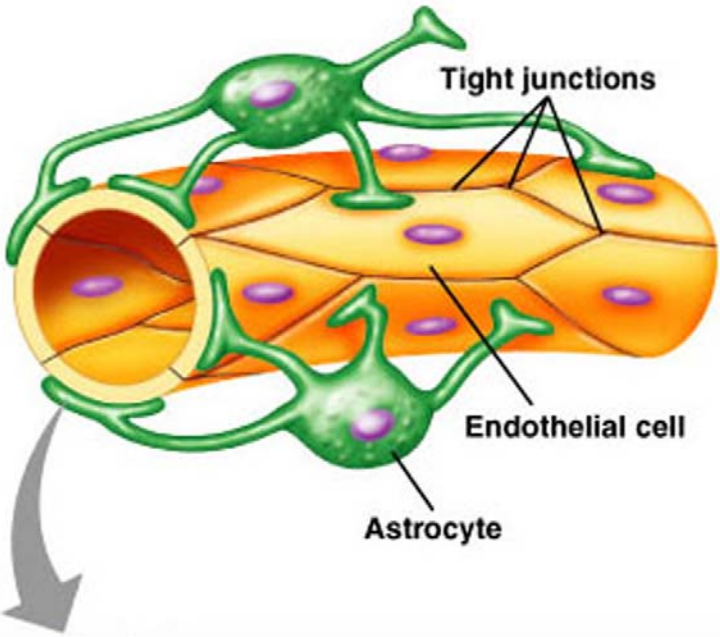
Tight junctions
Endothelial cell
Astrocyte

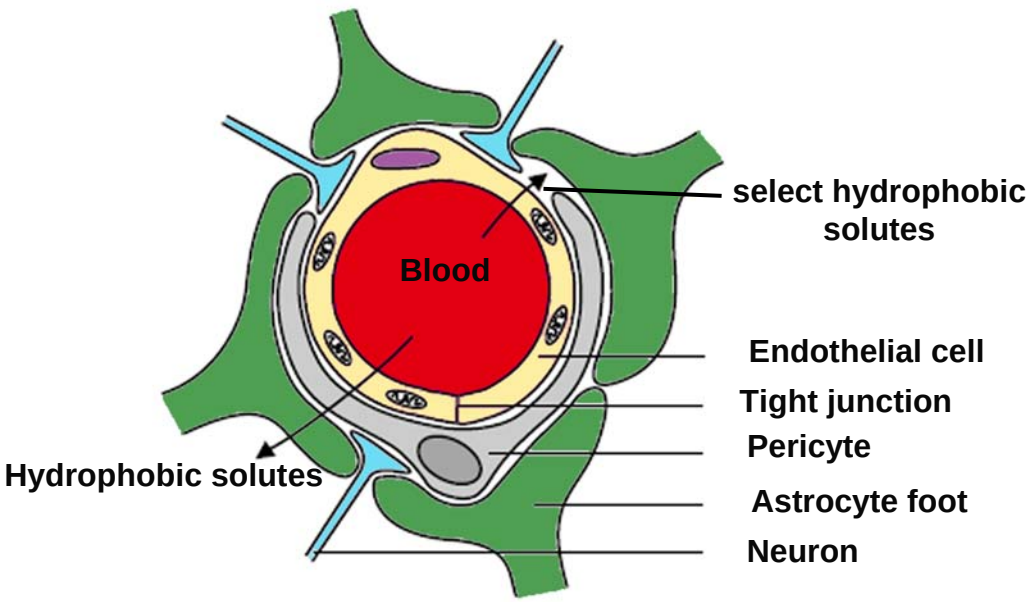
select hydrophobic solutes
Blood
Endothelial cell
Tight junction
Pericyte
Hydrophobic solutes
Astrocyte foot
Neuron

lipid-mediated free diffusion of molecules crossing the BBB requires both a molecular mass < 400-500Da and lipid solubility (Pardridge, 1998). Therefore this BBB restriction excludes almost 100% of all macromolecular neurotherapeutic drugs and > 98% small molecule drugs as well (Pardridge, 2005). In addition to the physical barrier formed by the tight junctions of the endothelial cells, an enzymatic barrier is present and consists of a variety of ecto-enzymes and peptidases expressed by the endothelial cells, astrocytes and pericytes (Brownless and Williams, 1993).

1.3 Delivery of macromolecules to the CNS

Therapeutic macromolecules, such as protein neurotrophic factors and viral vectors, which have significant potential in treatment of CNS diseases, are hindered in their clinical use by difficulties related to their delivery to the CNS. Many therapeutic macromolecules have poor pharmacokinetic profiles and short *in vivo* half-lives (Thorne and Frey 2nd, 2001). They are often restricted by enzymatic inactivation, potential immunogenicity, circulatory clearance and binding protein sequestration by factors in blood and peripheral tissues. Generally a rate-limiting step in clinical treatment of CNS diseases is the access of the therapeutic proteins to sites of action in the CNS (Pardridge, 1998). Often, undesirable or adverse side-effects result from inabilities to selectively target specific CNS sites.

Macromolecules may be delivered to the CNS via several different administration routes which can be divided into two groups. Firstly, the parenteral systemic administration routes which are restricted by the BBB and blood-cerebral spinal fluid (CSF) barrier. Secondly, the central administration routes, as shown in **Fig 1.2** (Thorne and Frey 2nd, 2001), which bypass the BBB and blood-CSF barrier. Avoiding the problems involved in systemic administration routes, attempts to target

Figure 1.2 Central drug administration routes.

Graphic representation of central administration routes offering direct access to the CNS not involving delivery via the vascular system (parenteral systemic administration) used to deliver therapeutic proteins and viral vectors. Key functional compartments include: subarachnoid space (SAS); lateral, 3rd and 4th ventricles (LV, 3V & 4V); and cortical grey matter. Intranasal delivery offers a non-invasive alternative of direct access to the CNS through the olfactory receptor neurons (Olf. nn.).

Figure was adapted and modified from Thorne & Frey 2nd (2001).

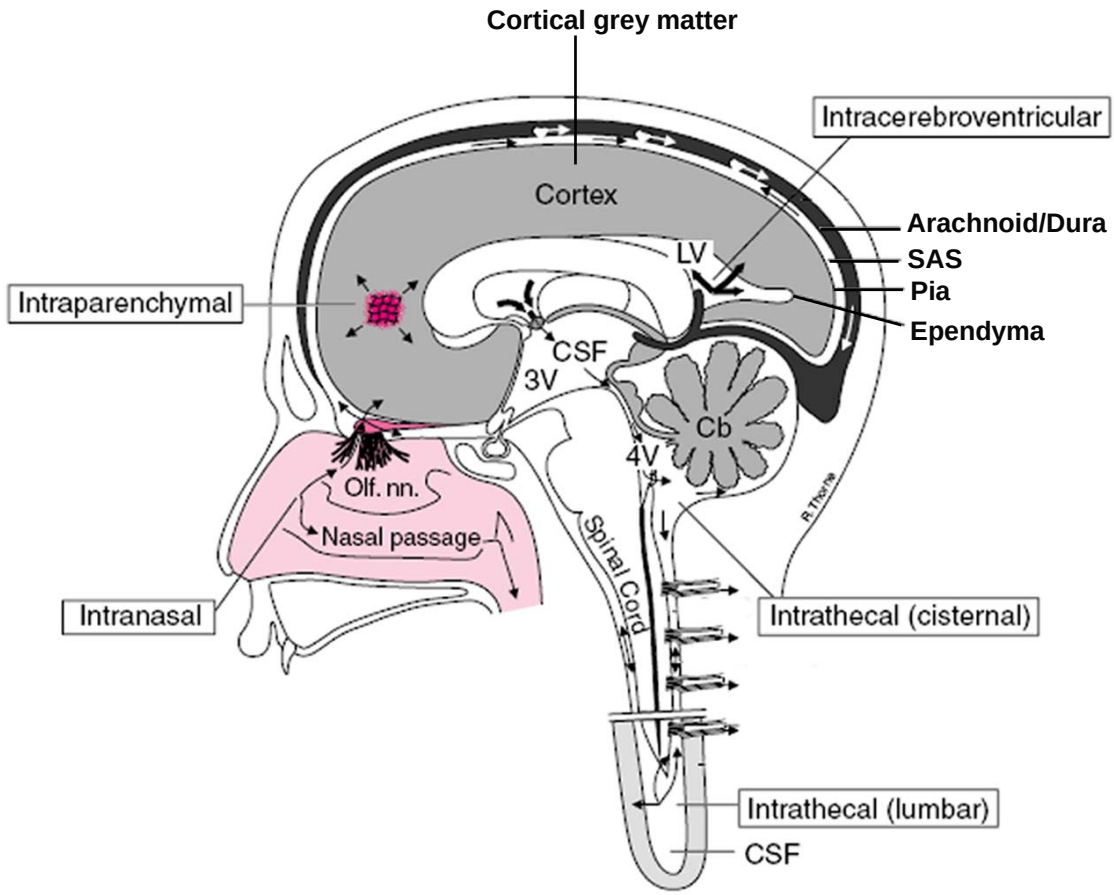
Cortical grey matter
Intracerebroventricular
Cortex
Arachnoid/Dura
SAS
Pia
Ependyma
LV
Intraparenchymal
CSF
3V
Cb
4V
Olf. nn.
Nasal passage
Spinal Cord
R.Thorne
Intranasal
Intrathecal (cisternal)
Intrathecal (lumbar)
CSF

the CNS via the central administration routes often involve invasive techniques of delivery.

1.3.1 Parenteral systemic administration

These routes of macromolecule delivery include: intravenous (IV), subcutaneous (SC) and intramuscular (IM) administration. They enable direct access to the systemic veins, bypassing the portal circulatory system and hepatic-first pass elimination. However, macromolecules delivered via these mechanisms are distributed throughout the body by the bloodstream and may influence other tissue functions in an adverse way. Entry of macromolecules into the CNS from the bloodstream only occurs following transcytosis across either the BBB or the coroidal epithelium (blood-CSF barrier), and may follow one of three general mechanisms; non-specific fluid phase endocytosis (e.g. horseradish peroxidase), adsorptive endocytosis (e.g. lectins) and receptor-mediated endocytosis (e.g. ligands) (Broadwell, 1989).

Examples of parenteral systemic administration include animal studies of both SC and IV administered basic fibroblast growth factor (bFGF) (Wagner et al., 1999; Deguchi et al., 2000). In both studies, the efficiency of brain delivery was quite low with 0.06% and <0.1% of the injected SC and IV doses reaching the CSF respectively (Wagner et al., 1999; Deguchi et al., 2000). In a phase I clinical trial examining the potential efficacy of SC administration of recombinant ciliary neurotrophic factor (rhCNTF) in amytrophic lateral sclerosis (ALS) therapy, the pharmacokinetics and toxicity were assessed (Cedarbaum et al., 1995). ALS patients experienced adverse side effects such as body weight loss, cough and fever, and antibodies to rhCNTF were found in patients' sera, indicating considerable immunogenicity of SC administered protein (Cedarbaum et al., 1996).

1.3.2 Central administration

The BBB and blood-CSF barriers are bypassed through central drug administration which directly delivers macromolecules into the CNS or CSF. Central administration targets one or several of the five different functional compartments existing in the CNS which are differentiated as: the subarachnoid space CSF, ventricular space CSF, cortical grey matter, periventricular grey matter and periventricular white matter **(Fig 1.2)**.

1.3.2.1 Intracerebroventricular (ICV) administration

Ventricular and extraventricular CSF circulation **(Fig 1.2)** allows potential delivery of either a therapeutic protein or viral vector to wide areas of the CNS through an initial ICV injection. However, the epidymal cell layer of the ventricles may be a considerable barrier to proteins delivered via ICV injection. Other factors which may limit delivery into the CNS parenchymal tissue include: diffusion limitations, venous and lymphatic system clearance before tissue penetration, binding to CSF protein components, and sequestration resulting from binding to epidymal, pial and glial tissue components (Pardridge, 1991). Studies involving ICV delivery of protein neurotrophic factors to the CNS have shown that significantly higher doses are required to produce similar effects found with intraparenchymal delivery (Morse et al., 1993; Venero et al., 1996), even with proteins which do not bind to the epidyma. Several different neurotrophic factors, including nerve growth factor (NGF), were found to be rapidly cleared from the rat CNS with a CSF half-life of <1 hour (Ferguson et al., 1991). Overall, ICV delivery using a surgical drug infusion pump offers continual drug delivery to the CNS, but is surgically invasive and has diffusional limitations (Thorne and Frey 2nd, 2001).

1.3.2.2 Intrathecal (IT) administration

Delivery of macromolecules by IT administration involves injections into the subarachnoid space CSF **(Fig. 1.2)** at the cisternal or lumbar spinal cord levels, and results in high local concentrations of the delivered substance. Although IT administration appears highly advantageous for treatment of spinal cord diseases, this delivery route may not provide therapeutic drug concentrations in other CNS regions (Kroin, 1992). Similar to ICV delivery, limitations in CNS tissue penetration include the pia and glia limitans structural barriers and diffusional limitations. An example of the clinical use of IT administration is a study that attempted delivery of CNTF in ALS patients, which did not produce the adverse effects seen in previous systemic CNTF delivery (Aebischer et al., 1996). Another study using IT CNTF in ALS patients found significantly higher lumbar concentrations of CNTF and in one patient, antibodies to the infused rhCNTF present in systemic circulation (Penn et al., 1997). In both studies, none of the ALS patients showed any clinical benefits (Aebischer et al., 1996; Penn et al., 1997).

1.3.2.3 Intraparenchymal (IPa) administration

This form of central administration delivers macromolecules directly to the CNS parenchyma **(Fig. 1.2)**, but the CNS tissue structure greatly limits distribution and hinders diffusion from the initial implantation site (Mufson et al., 1996). Some studies have developed a method of continuous neurotrophic factor supply in the brain by IPa administration of a polymer encapsulated implant of neurotrophic factors or genetically engineered cells (Mahoney and Saltzman, 1996). However the disadvantages of this method would include further invasive surgery to precisely

position the implant to maximise neurotrophic factor release into CNS target regions (Thorne and Frey 2nd, 2001)

1.3.2.4 Intranasal (IN) administration

Many recent studies have focussed on IN administration **(Fig. 1.2)**, a controversial non-invasive alternative to the other highly invasive central CNS administration routes (ICV, IPa, & IT) or traditional parenteral administration routes (IV, SC & IM) for CNS delivery of therapeutic macromolecules. Intranasal administration offers simple and effective delivery of therapeutic proteins with poor oral bioavailability, targeting the CNS and bypassing the BBB (Thorne et al., 1995; Frey 2nd et al., 1997). In the literature, much evidence exists supporting the direct entry of macromolecules, low molecular weight drugs and viruses into the brain or CSF following nasal access.

It has been known since the early 20th century that many viruses gain entry to the CNS through the nasal route. The first virus discovered utilising this route was poliomyelitis which could gain access to the brain (Landsteiner and Levaditi, 1910), CSF (Fairbrother and Hurst, 1930) and the systemic lymphatics of the olfactory mucosa (Howe and Bodian, 1941). Some of the many viruses which utilise this pathway include: rabies virus (Lafay et al., 1991), herpes simplex (Esiri and Tomlinson, 1984), hepatitis (Barnett and Perlman, 1993) and Semliki forest virus (Oliver and Fazakerley, 1997).

Growing evidence has also shown that amino acids, polypeptides and proteins can be directly transported to the CNS after intranasal administration. An example of amino acid entry via the nasal route was in 1967 when leucine was demonstrated to enter the olfactory neurons, incorporate into neural proteins and be transported to the olfactory bulb (Weiss and Holland, 1967). Proteins and polypeptides, such as HRP,

have been shown to travel along the olfactory receptor neuron (ORN) to the olfactory bulb (Kristensson and Olsson, 1971; Balin et al., 1986). When HRP is conjugated to wheat germ agglutinin, the conjugated lectin is internalised by ORNs after binding to surface receptors and transported to the olfactory bulb (Broadwell and Balin, 1985; Shipley, 1985).

Metals including aluminium (Perl and Good, 1987), colloidal gold (De Lorenzo, 1970), cadmium (Evans and Hastings, 1992) and nickel (Henriksson et al., 1997) all gain access to the CNS after nasal administration. In several investigations of olfactory nerve and neighbouring tissues, several dyes including procion and lucifer yellow (Suzuki, 1984), Evan's blue (Kristensson and Olsson, 1971) and trypan blue (Holl, 1965) have been used and found to be transported from the olfactory epithelium to the olfactory bulb.

There have been numerous rodent and human studies demonstrating the possibility of direct delivery of drugs to the brain and CNS. Several of these include IN delivery of antibiotics and antivirals which follow transport pathways from the nasal cavity to the CSF and systemic circulation (Sakane et al., 1991; Seki et al., 1994). Some studies have also explored steroid hormone uptake and transportation from the nasal mucosa to the brain, centring on transport of estradiol and progesterone (Anand Kumar et al., 1974; Anand Kumar et al., 1982; van den Berg et al., 2004). Many of the human pharmacological nasal delivery studies have been reviewed in Illum, 2004.

1.4 The Mammalian Nasal System

1.4.1 The Nasal Cavity

In humans and most mammals, the nasal cavity is longitudinally divided by a cartilaginous nasal septum, separating both halves of the cavity. The nasal passages in humans contain three scrolled, spongy-bone protrusions, collectively called turbinates, which extend laterally from the ethmoid wall. However, in the rat, there are four turbinates called endoturbinates I to IV **(Fig. 1.3A,B)** (Menco and Jackson, 1997; Shipley et al., 2004). Beneath the endoturbinates, lie a second set of turbinates called ectoturbinates 1 to 4 **(Fig. 1.3B)**.

In most mammals, substances entering the nasal cavities will accumulate at one of three functionally unique regions within the nasal cavity and these are: the vestibular, the respiratory and the olfactory regions **(Fig. 1.3A)** (Graziadei, 1970). Generally the nasal vestibule is covered in stratified squamous epithelium and is located at the opening of the nasal passages. The vestibular area contains long hairs for filtering airborne particles. Largest of the three regions in humans is the respiratory area containing an epithelium made up of ciliated cells which remove particles deposited in the mucous layer. The olfactory mucosa is located at the most dorsal and caudal region of the nasal cavity and contains a surface area of highly convoluted turbinates. Structurally, it is composed of the olfactory epithelium on the luminal side of the basal lamina and an underlying lamina propria. In humans the olfactory mucosa covers only a small area, approximately 3-5% of the total nasal cavity (Morrison and Costanzo, 1992). However in dogs, the olfactory mucosa covers 77% and in rats **(Fig. 1.3A)**, 50% of the total nasal surface area (Illum, 1996). This difference in olfactory systems between the species can clearly be seen by the relative size of the olfactory bulb in rat **(Fig. 1.3C)** and other mammals, compared to humans.

Figure 1.3 Rat brain and nasal cavity.

A. Medial view photograph of adult rat nasal cavity and brain present at the midline following sagittal dissection of the rat head. Indicated on the image are the vestibular, respiratory and olfactory regions of the rat, and the ethmoid and maxillo turbinates. Scale bar = 4mm.

B. Schematic drawing of medial view adult rat nasal cavity and brain present at the midline, including seven coronal cross-sections of different levels of the nasal cavity (1-7). Roman numerals I-IV refers to the four ethmoid endoturbinates; red numbers 1,2,2´ & 3 in the coronal sections are the ectoturbinates; and Zones 1-4 are the olfactory sensory zones, based on expression of odorant receptor genes.

Scale bar = 4mm.

C Lateral view of perfused adult rat brain. Note the size of the olfactory bulb compared to the rest of the cortex. Scale bar = 4mm.

Images in Fig. 1.3 A & B were reproduced and modified with permission from Prof. AC Puche.

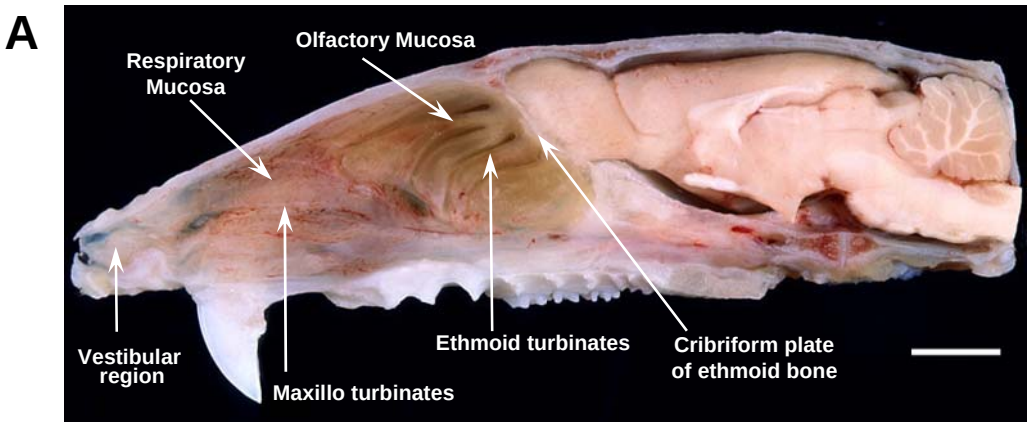
A
Respiratory Mucosa
Olfactory Mucosa
Vestibular region
Maxillo turbinates
Ethmoid turbinates
Cribriform plate of ethmoid bone

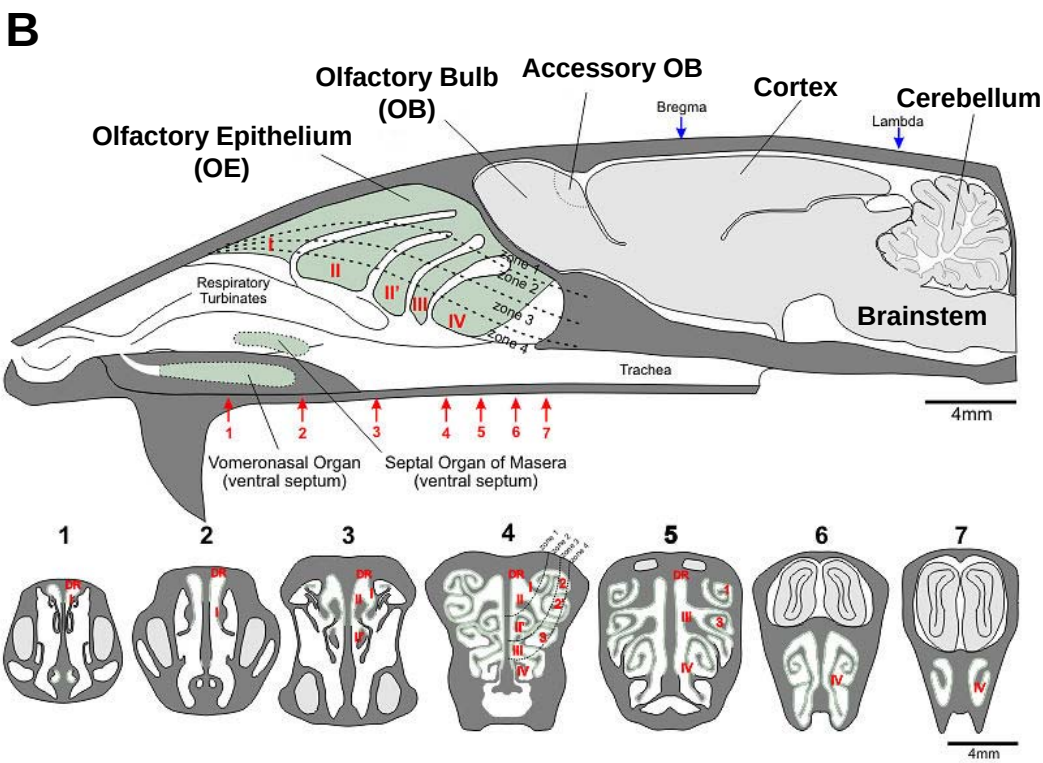
B
Olfactory Bulb (OB)
Accessory OB
Cortex
Cerebellum
Olfactory Epithelium (OE)
Bregma
Lambda
Respiratory Turbinates
Brainstem
Trachea
4mm
Vomeronasal Organ (ventral septum)
Septal Organ of Masera (ventral septum)
1
2
3
4
5
6
7

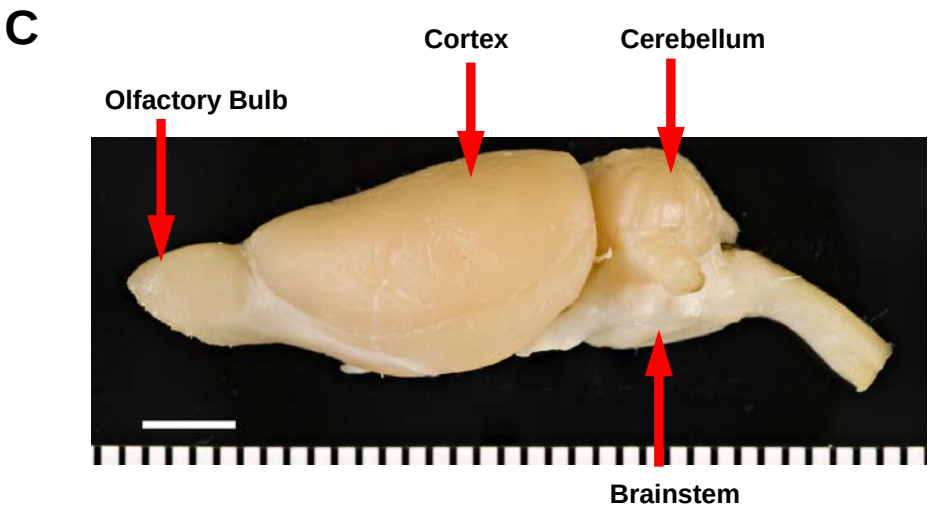
C
Olfactory Bulb
Cortex
Cerebellum
Brainstem

1.4.2 The Respiratory Epithelium

Occupying the central region of the nasal cavity **(Fig. 1.3 A,B)**, the respiratory mucosa consists of a highly vascularised, pseudostriatified columnar tissue lining the turbinate structure. It is made up of ciliated and non-ciliated columnar cells, mucus-secreting goblet cells and basal cells (Geurkink, 1983; Illum, 2000). The ciliated cells co-ordinate movement of the mucus and inhaled particles in a posterior direction, within the nasal cavity. The respiratory epithelial cells are surrounded by microvilli, which provide a high absorptive capacity. This region is a major site of systemic drug absorption due to the increasing surface area provided by the microvilli (Illum, 2004).

1.4.3 The Olfactory Epithelium

There are four olfactory systems operating in most mammals for sensing chemical odorants from the external environment. These consist of the main olfactory organ, the vomeronasal organ (Jacobson's organ), the trigeminal somatosensory system and the septal olfactory organ **(see Fig. 1.3B)**. While the main and septal olfactory organs process all general odours (Adams, 1992), the vomeronasal organ responds to chemical pheromones present in sexual activities (Evans, 2003) and the trigeminal somatosensory system deals with strongly irritative odours (Cometto-Muz and Doty, 2003). However, this thesis will only examine the transport pathways involved in the main olfactory system and parts of the trigeminal system.

The olfactory epithelium is located at the top of the mammalian nasal cavity, under the cribriform plate of the ethmoid bone which divides the cranial from the nasal cavities **(Fig. 1.3 A&B)**. This area is free of inspiratory airflow as the olfactory mucosa lies above the normal airflow path, which means that odorants and

macromolecules usually reach the olfactory neurons by diffusion (Illum, 2000). The mammalian sensory epithelium is divided roughly into four zones **(Fig. 1.3B)** based on the expression of odorant receptor genes (Buck and Axel, 1991). Generally the human olfactory epithelium shares a similar structural organisation and morphology as other mammalian species (Morrison and Costanzo, 1992).

The olfactory epithelium is a modified columnar, pseudo-stratified epithelium, similar to the respiratory epithelium. It consists of the following main cell types **(Fig. 1.4A)**: the ORNs, supporting epithelial cells (or sustentacular cells), horizontal basal cells and globose basal cells (Graziadei, 1971; Menco and Morrison, 2003). The other cell types present in the olfactory epithelium are several types of microvillous cells, including the flask-shaped microvillar cells (Moran et al., 1982) **(Fig. 1.4A)** and leukocytes (Suzuki et al., 1995). Beneath the olfactory mucosa, lies a laminar propria which contains connective tissues, blood vessels, lymphatic capillaries, ORN axon fascicles and Bowman's glands. ORN axons penetrate the basal membrane, forming larger bundles in the lamina propria which then project to the olfactory bulb.

The sustentacular cells, found in the upper epithelium **(Fig. 1.4A)**, are wide columnar cells extending to the mucous surface from their attachment to the basal membrane. They are covered with microvilli and exhibit a cellular polarity similar to ORN's (Menco et al., 1998). With sleeve-like process, the sustentacular cells often wrap around the cell bodies of the ORNs, providing structural support and maintaining normal extracellular potassium levels for neuronal activity (Graziadei, 1971). The observation of secretory granules suggests that these cells may be involved in mucus secretion along with solute transport across the epithelium (Menco, 1984).

Figure 1.4 Cellular structure of the Olfactory Epithelium.

A. Schematic diagram showing the major cell types located within the rat olfactory epithelium. These include: olfactory receptor neurons (ORNs), sustentacular cells, microvillar cells, horizontal and globose basal cells, olfactory ensheathing cells and Bowman's gland.

B. Olfactory receptor neurons

Horizontal section of rat olfactory epithelium showing green fluorescent ORNs. Cell bodies are approximately 5-7 μm wide and each have single dendrites extending towards the mucosal surface and terminating with a dendritic knob. Scale bar= 25 μm.

Image in Fig. 1.4 A was reproduced and modified with permission from Prof. AC Puche.

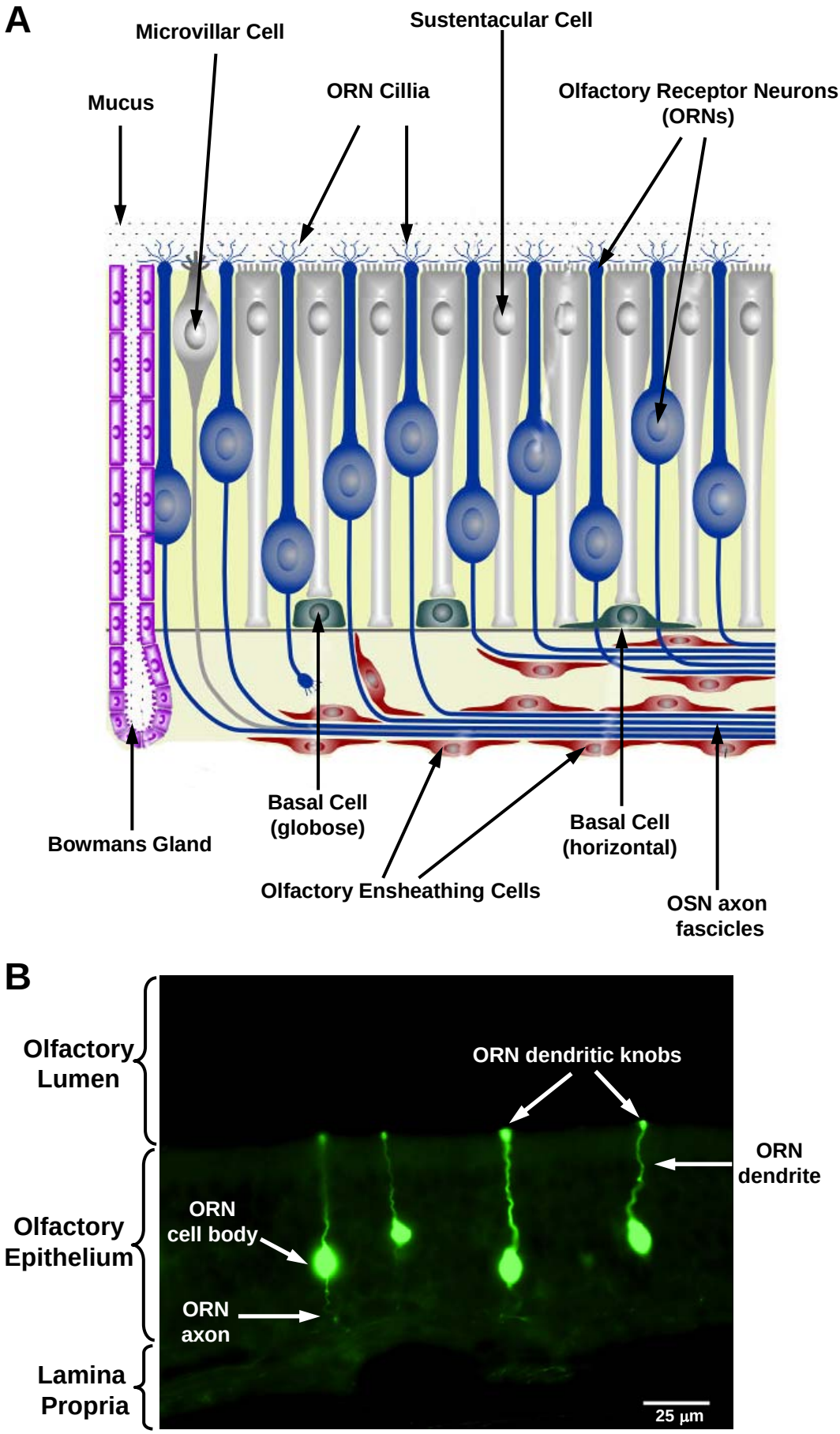
A
Microvillar Cell
Sustentacular Cell
Mucus
ORN Cillia
Olfactory Receptor Neurons
(ORNs)
Bowmans Gland
Basal Cell
(globose)
Olfactory Ensheathing Cells
Basal Cell
(horizontal)
OSN axon
fascicles
B
Olfactory
Lumen
Olfactory
Epithelium
Lamina
Propria
ORN dendritic knobs
ORN
dendrite
ORN
cell body
ORN
axon
25 µm

Horizontal and globose basal cells are located beneath the ORNs and sustentacular cells, near the basal lamina of the olfactory neuroepithelium, above the lamina propria (Graziadei and Monti-Graziadei, 1979). These basal cells are stem cells which are capable of further differentiation eventually becoming new olfactory neurons (Graziadei and Monti-Graziadei, 1979). Animal studies have shown that new ORNs arise from globose basal cells (Goldstein and Schwob, 1996). However, the relation between horizontal and globose basal cells is undecided and it seems that a candidate undifferentiated stem cell resides in the horizontal cell population (Sicard et al., 1998; Iwai et al., 2008). It has been definitively shown in mouse that horizontal basal cells function as adult olfactory neuroepithelium neural stem cells, and play a major role in olfactory neuroepithelium maintenance and regeneration (Leung et al., 2007).

Within the lamina propria, reside the Bowman's glands which are composed of mucus-secreting serous cells. This mucous layer covers the olfactory epithelium, providing a suitable microenvironment for sensory transduction (Getchell and Getchell, 1992).

1.4.4 The Olfactory Receptor Neuron

The first order neurons (cranial nerve 1), embedded within the olfactory epithelium which transduce odorant and other macromolecules are the ORNs **(Fig. 1.4 A,B)**. With an elongated, columnar-like cell body, single dendritic process and axon, ORNs are considered bipolar sensory neurons. The single dendritic process twists between other receptor cells and supporting cells, extending towards the mucosal surface and terminating in a small knob-like swelling **(Fig. 1.4B)** (Menco, 1984). From this peripheral dendritic tip, several long non-motile cilia extend into the mucous layer (Menco, 1984). Mammalian olfactory cilia do not appear to be

motile, unlike those of other vertebrates which vary in length and motility (Lidow and Menco, 1984). The olfactory cilia contain intramembranous particles which include many different odorant receptors (Buck, 1996). There are approximately 1000 genes expressed by different ORNs belonging to a large multigene family of odorant receptor genes (Buck and Axel, 1991). In the basal regions of the receptor cell bodies, ORNs taper into unbranched and unmyelinated axons eventually forming small bundles with other ORN axons. Passing through the basal lamina, the axon bundles combine into larger fascicles (fila olfactoria) and are surrounded by specialized Schwann cells, called olfactory ensheathing cells **(Fig. 1.4A & Fig. 1.5B)** (De Lorenzo, 1957; Doucette, 1993). These unique cells, which resemble both Schwann cells and astrocytes, wrap bundles of olfactory axon fibres in extended cytoplasmic tongues (Doucette, 1993). The olfactory axon fascicles project through small holes in the cribriform plate, entering a perineural space **(Fig. 1.5 A,B)** and are surrounded by a perineural epithelial sleeve which is an extension of the pia-arachnoid membrane (Davson, 1967; Shantha and Bourne, 1968). Eventually the olfactory axons enter the olfactory bulb and terminate in spherical neuropils called glomeruli, synapsing with second order mitral and tufted neuronal cells **(Fig. 1.5 A,B)**.

Olfactory marker protein is a low molecular weight protein uniquely expressed in mature ORNs (Keller and Margolis, 1975; Buiakova et al., 1994). Although the function of OMP is not fully understood, it is thought that OMP may be involved in olfactory signal transduction pathways (Ivic et al., 2000).

Setting them apart from other neurons in the CNS and PNS, olfactory neurons have several unique characteristics. 1) ORNs are in direct contact with the external environment due to their peripheral location, which makes them vulnerable compared to internal sensory neurons. 2) With their peripherally located dendrites

Figure 1.5 Olfactory epithelial connections with the olfactory bulb.

A. Diagram of the basic olfactory epithelium structure and connections of the ORN with mitral cells in the glomeruli of the olfactory bulb.

B. Diagram of the pathway taken by ORN axon fascicles (fila olfactoria) from the olfactory epithelium through holes in the cribiform plate. This figure shows the perineural spaces and anatomical connections between the olfactory epithelium and the subarachnoid space CSF.

Figures were extracted from Illum (2004).

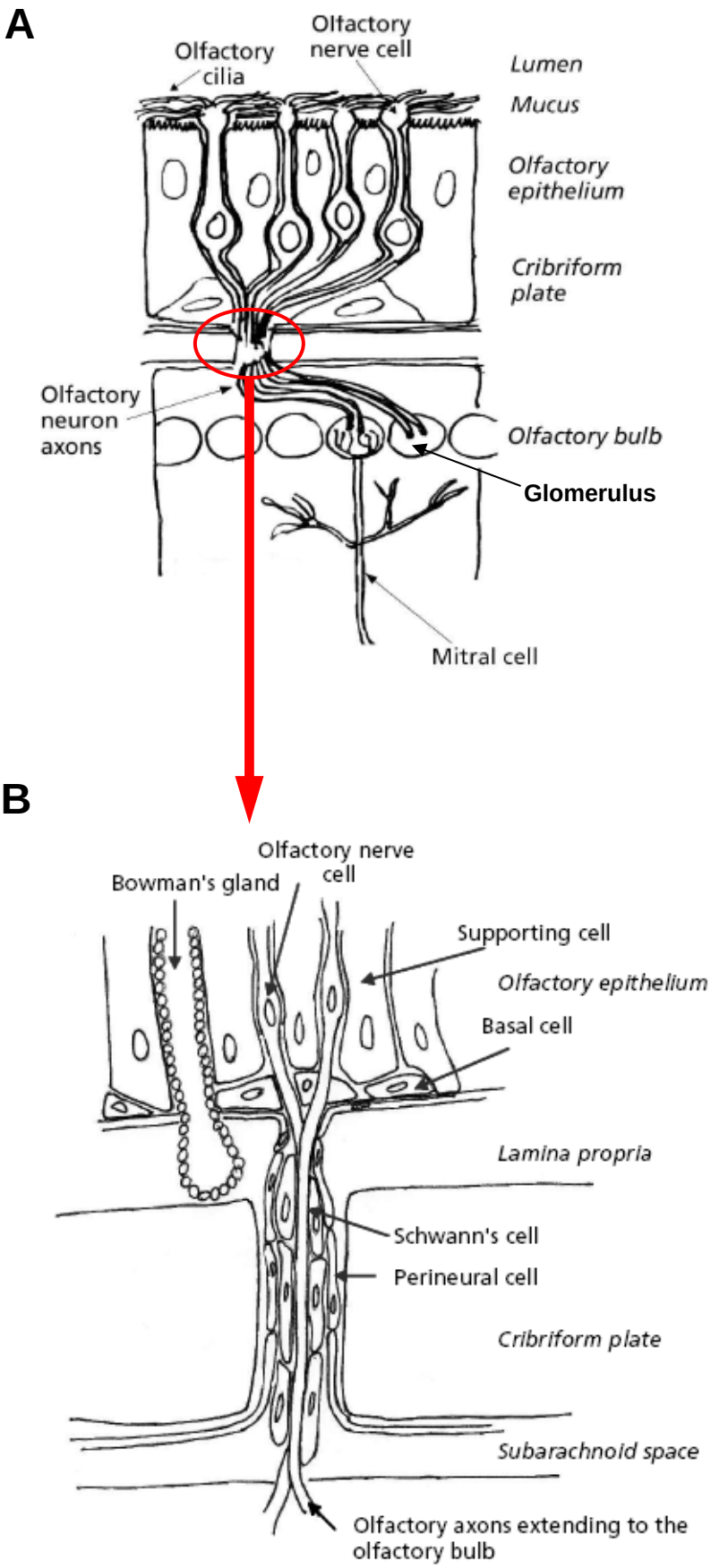
A
Olfactory cilia
Olfactory nerve cell
Lumen
Mucus
Olfactory epithelium
Cribriform plate
Olfactory neuron axons
Olfactory bulb
Glomerulus
Mitral cell
B
Olfactory nerve cell
Bowman's gland
Supporting cell
Olfactory epithelium
Basal cell
Lamina propria
Schwann's cell
Perineural cell
Cribriform plate
Subarachnoid space
Olfactory axons extending to the olfactory bulb

and direct projection of axons centrally to the forebrain, ORNs form a direct pathway for entry of exogenous substances into the brain (Mathison et al., 1998; Thorne and Frey 2nd, 2001; Illum, 2004). 3) ORNs are able to regenerate themselves through continued postnatal neurogenesis which involves neurotrophic, growth and adhesive factors (Plendl and Sinowatz, 1998; Mackay-Sim and Chuah, 2000; Newman et al., 2000). The steady loss of the sense of smell in mammals is prevented by a continual neurogenesis of ORN precursors located in the olfactory epithelium (Mackay-Sim and Chuah, 2000; Schwob, 2002). It was originally thought that ORNs were short-lived, undergoing replacement every 30 days (Graziadei and Monti-Graziadei, 1979). However more recent animal studies have challenged this view, providing evidence that the olfactory neurons live at least up to 90 days (Mackay-Sim A. and Kittel, 1991) or for one year depending on environmental factors (Hinds et al., 1984).

1.4.5 The Olfactory Bulb

The primary olfactory structure involved in processing the physiological signals delivered by ORNs and transmitting these signals directly to centres in the olfactory cortex, is the paired oval structure called the olfactory bulb. Located at the rostral end of the telencephalon, the olfactory bulb consists of 2 components in macrosmatic mammals, a main olfactory bulb (MOB) and an accessory olfactory bulb (AOB). Where the MOB is innervated by ORNs of the main olfactory epithelium, the AOB, located at the dorsocaudal limit of the MOB, is innervated by ORNs located in the vomeronasal organ. Generally in humans, which are microsmatic, the vomeronasal organ and AOB are rudimentary and non-functional (Trotier et al., 2000).

The main olfactory bulb has a characteristic laminar organisation and an overall allocortex structure. The basic laminar organisation consists of six distinctive layers **(Fig. 1.6A)** populated by different neuronal cell types **(Fig. 1.6B)**.

1.4.5.1 Olfactory Nerve Layer (ONL)

The outermost layer of the olfactory bulb is the ONL, which engulfs the entire bulb, and contains the incoming unmyelinated axons from the ORNs along with specialized glial cells. Interwoven bundles of axons form a dense plexus on the surface of the bulb. As mentioned previously, the specialized glial cells are olfactory ensheathing cells which surround the axon bundles within the ONL (Doucette, 1993). Sharing common features with Schwann cells and astrocytes, the ensheathing cells express neurotrophic factors (Mackay-Sim and Chuah, 2000) and show potential in promoting regeneration of injured spinal cord (Feron et al., 2005).

1.4.5.2 Glomerular Layer (GL)

Beneath the ONL lies the GL, which consists of distinctive, spherical, neuropil-rich structures called glomeruli. ORN axons form synapses within the glomeruli with the dendrites of the principal and intrinsic neurons of the olfactory bulb (Kasowski et al., 1999). The two types of principal neurons in the olfactory bulb are mitral and tufted cells. Intrinsic neurons consist of periglomerular, granular and short axon cells (Shepherd et al., 1998). Each ORN axon form synapses within a single glomeruli, however in the rat there are approximately 20 million ORNs and 2400 glomeruli (Meisami and Sendera, 1993). Therefore the convergence of ORN axons to each glomeruli is about 8000:1. Overall the glomeruli play a key role in the coding of odorant molecules transported from the ORNs to the olfactory bulb.

Figure 1.6 Anatomical organisation of the olfactory bulb and the main projection pathways in the olfactory system.

A. Layers of the main olfactory bulb. Horizontal section of rat olfactory bulb displaying the basic laminar organisation (haematoxylin and eosin stained). ONL, olfactory nerve layer; GL, glomerular layer; EPL, external plexiform layer; MCL, mitral cell layer; IPL, internal plexiform layer; GCL granular cell layer. Scale bar = 25 μm.

B. Neuronal circuitry organisation in the main olfactory bulb of the rat.

Axons from ORNs (red) enter the olfactory bulb at the ONL and form synapses in the GL with mitral cells (MC, orange) and tufted cells (external, eTC; middle, mTC; and deep, dTC; purple). These synaptic connections are located within spheroid neuropil-rich structures called glomeruli (blue). Glomeruli are surrounded by local interneurons (intrinsic neurons, grey) including: periglomerular cells (PGC) and short axon cells (SA), which form lateral connections between glomeruli. Along with mTC and dTCs the EPL also contains Van Gehuchten cells (vC). Axons from mitral and tufted cells are sent through the IPL and along the lateral olfactory tract (LOT) to the olfactory cortex. Granule cells (GC, grey) are localised in the GCL and MCL at different depths. Central afferent fibres (CFF) from various brain regions innervate most layers of the olfactory bulb.

Figure 1.6B was adapted and modified with permission from Prof. AC Puche.

A

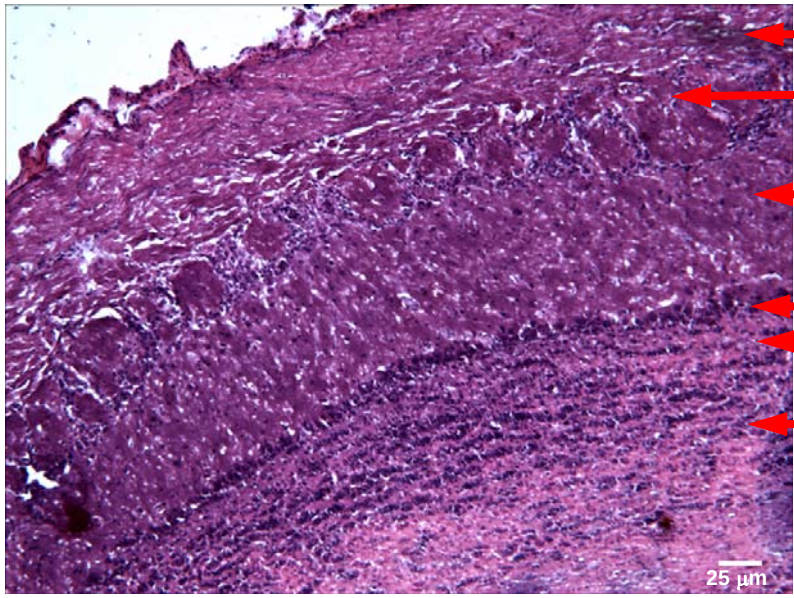
ONL
GL
EPL
MCL
IPL
GCL
25 µm

B

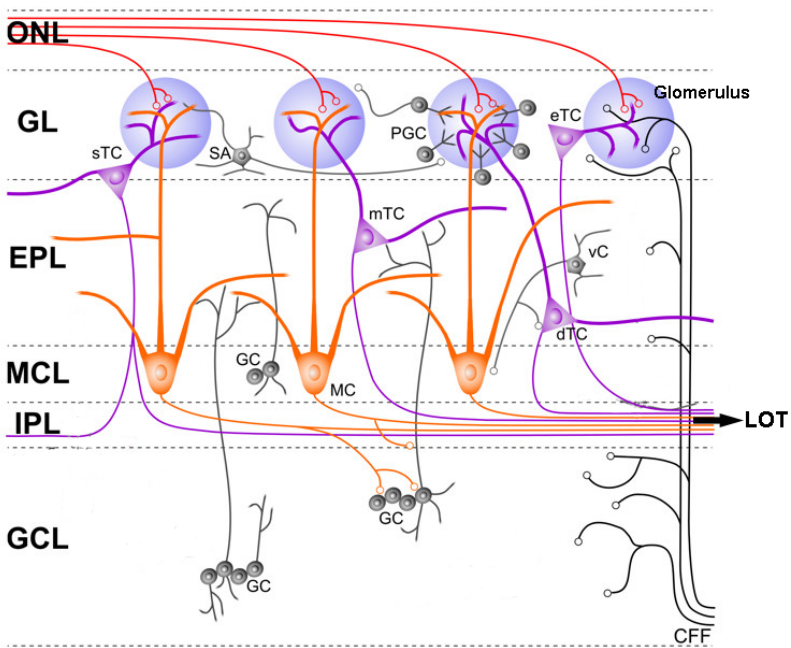
ONL
GL
EPL
MCL
IPL
GCL
sTC
SA
PGC
eTC
Glomerulus
mTC
vC
dTC
GC
MC
LOT
GC
GC
CFF

1.4.5.3 External Plexiform Layer (EPL)

Under the glomeruli lies the EPL which consists of very dense neuropil and a low density of cell bodies. The EPL contains mostly dendrites of mitral, tufted and granule cells, along with middle and deep tufted cells and Van Gehuchten cell interneurons (Shepherd et al., 1998)

1.4.5.4 Mitral Cell Layer (MCL)

The relatively thin layer below the EPL contains a monolayer of mitral cell somata and is referred to as the MCL. These principal neurons have a single primary dendrite which transverses the EPL, terminating within a single glomerulus. Mitral cells also have several secondary basal dendrites which extend laterally across the EPL (Mori et al., 1983). The major axons of mitral cells are myelinated and run caudally towards the olfactory centres of the primary olfactory cortex. These axons also give off recurrent collaterals which terminate in the internal plexiform layer and deep in the granule layer (Mori et al., 1983).

1.4.5.5 Internal Plexiform Layer (IPL)

The IPL is a thin neuropil region with a low density of cells lying subadjacent to the MCL. The IPL contains a few short axon cells but, mainly consists of granule cell peripheral dendrites and axon collaterals from mitral and tufted cells. Some basal forebrain and brainstem neuron axons terminate in the IPL (McLean and Shipley, 1987). Included in the IPL are the axons of projection neurons that will later coalesce to form the lateral olfactory tract.

1.4.5.6 Granule Cell Layer (GCL)

The deepest neuronal layer in the olfactory bulb is the GCL, which contains the most abundant neuronal cell population in the bulb (Meisami and Safari, 1981). The granule cell neurons located in this region lack axons and have peripheral and deep dendritic processes (Price and Powell, 1970). Somata of the granule cells are tightly packed and arranged in row-like aggregates or islets. Granule cells are classified into three different types based on the positioning of their somata (Mori et al., 1983; Orona et al., 1983). Type I granule cells have intermediately located cell bodies, whereas type II and III have deep and superficial positioned somata (Mori et al., 1983; Orona et al., 1983).

1.4.6 Primary Olfactory Cortex

All secondary areas of the brain to which the mitral and tufted cells of the olfactory bulb directly project are collectively called the primary olfactory cortices (de Olmos et al., 1978), or sometimes referred to as secondary olfactory structures. **Fig. 1.7** gives a summary of the main projection pathways in the olfactory system. The major regions of the primary olfactory cortex can be divided into several different areas (see **Fig. 1.8 A-C**) which include: 1) the anterior olfactory nucleus; 2) the rostromedial olfactory cortices, including the indusium griseum, anterior hippocampal continuation, tenia tecta, infralimbic cortex and olfactory tubercle; 3) the lateral olfactory cortices including the piriform cortices, the periamygdaloid cortex and the lateral entorhinal cortex (de Olmos et al., 1978; Shipley et al., 2004).

The coalescence of myelinated mitral and tufted cell axons at the ventrolateral region of the olfactory bulb forms the lateral olfactory tract which advances caudally towards the olfactory cortex regions. Most of the primary olfactory cortex structures are located along the venterolateral surface of the

Figure 1.7 Circuit diagram showing the main projection pathways in the olfactory system.

AOB, anterior olfactory bulb; AON, anterior olfactory nucleus; VNO, vomeronasal organ; PC, pyriform cortex; OT, olfactory tubercle; AMYG, amygdala; TEC, transitional entorhinal cortex; NHLDB, nucleus of horizontal limb of diagonal band; MD, mediodorsal.

Olfactory receptor neuron (orn); periglomerular cell (pg); mitral cell (mc); tufted cell (tc); granular cell (gc). Olfactory neural layer (on); glomerular layer (glom); external plexiform layer (epl); mitral call layer (mcl); granule cell layer (gcl).

Figure was extracted from Smith & Shepherd (2008).

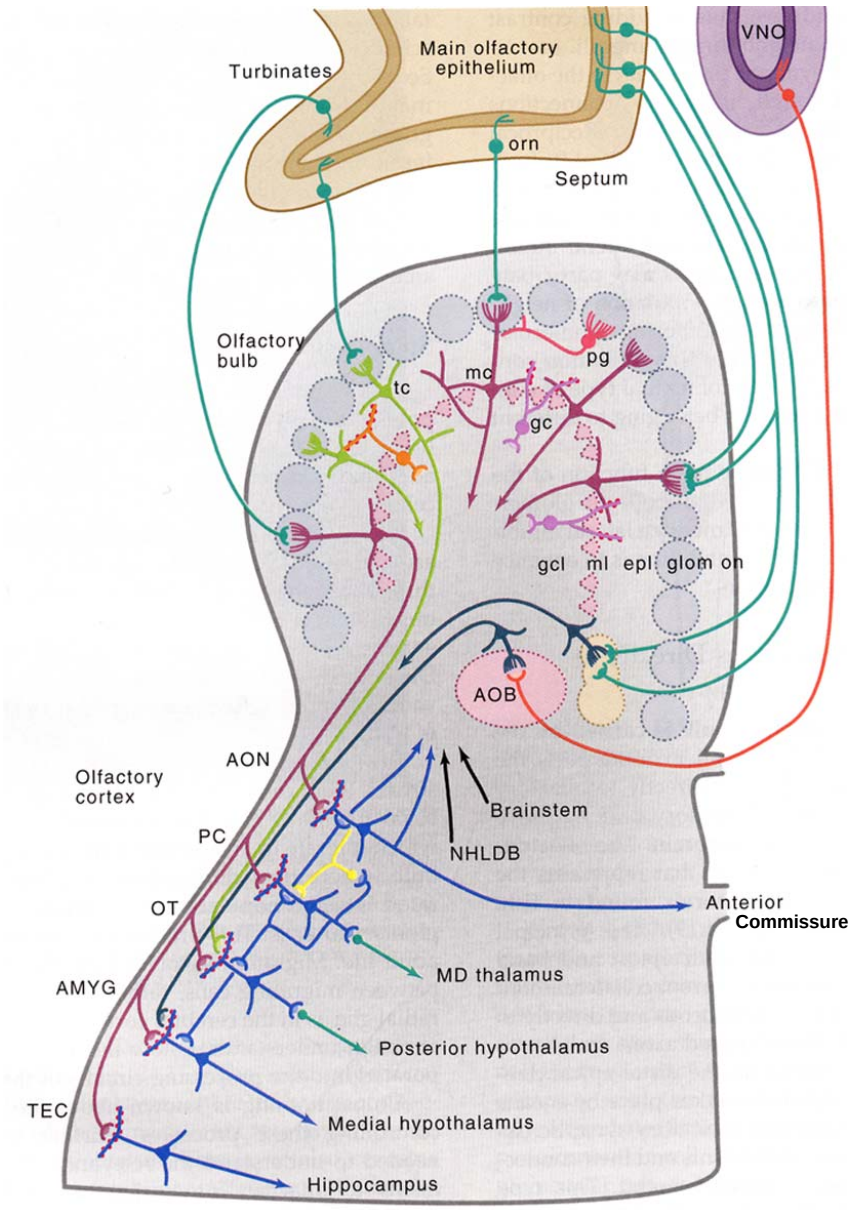
VNO
Main olfactory epithelium
Turbinates
orn
Septum
Olfactory bulb
mc
pg
tc
gc
gcl
ml
epl
glom
on
AOB
AON
Olfactory cortex
Brainstem
NHLDB
PC
OT
Anterior Commissure
AMYG
MD thalamus
Posterior hypothalamus
TEC
Medial hypothalamus
Hippocampus

Figure 1.8 Location of secondary olfactory structures or primary olfactory cortex in the rat brain.

Panels A-C display sagittal rat brain sections, adapted from Paxinos and Watson, (1998), of different levels from medial to lateral.

A. Secondary olfactory regions at lateral 0.4mm from bregma on sagittal brain map. OB, olfactory bulb; AON, anterior olfactory nucleus; IL, infralimbic cortex; AHC, anterior hippocampal continuation; IG, indusium griseum; Tu, olfactory tubercle; ac, anterior commissure; AH/DA, anterior and dorsal hypothalamic areas; VMH, ventromedial hypothalamic nucleus; MTN, medial thalamic nucleus; DG, dentate gyrus; CA1 and CA3 regions of hippocampus.

B. Secondary olfactory regions at lateral 2.4mm from bregma on sagittal brain map. AOL, lateral anterior olfactory nucleus; lo, lateral olfactory tract; Pir, piriform cortex; DEn, dorsal endopiriform nucleus; aca, anterior commissure, anterior part; HDB, horizontal limb of the diagonal band nucleus; LOT, lateral olfactory tract nucleus; VT, ventral thalamic nucleus; STh, sub-thalamic nucleus.

C. Secondary olfactory regions at lateral 3.9mm from bregma on sagittal brain map. VEn, ventral endopiriform nucleus; CxA, periamygdaloid cortex; ACo, anterior commissure; PMCo, posteriomedial cortical amygdaloid nucleus; LEnt, lateral entorhinal cortex; CA1, CA2, CA3, DG, hippocampus.

Figure adapted from Cleland and Linster (2003).

A

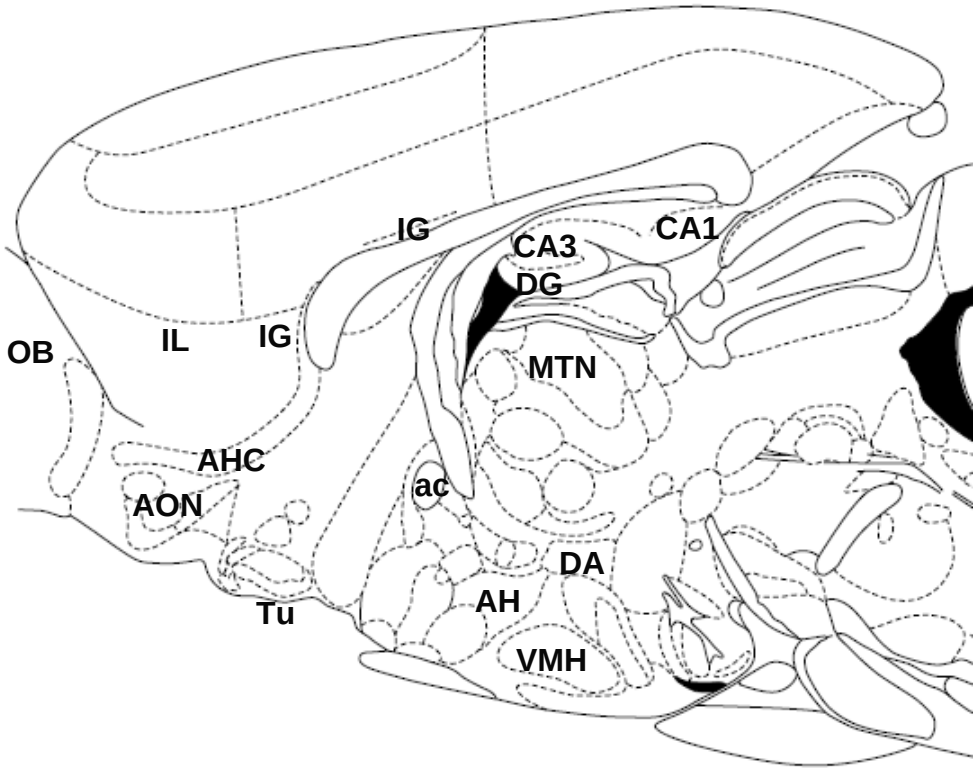
IG
CA3
CA1
DG
OB
IL
IG
MTN
AHC
ac
AON
DA
AH
Tu
VMH

B

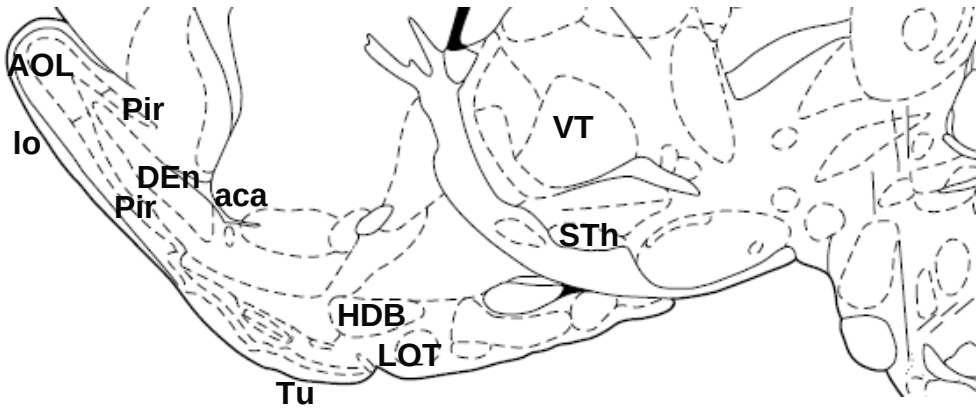
AOL
Pir
lo
VT
DEn
aca
Pir
STh
HDB
LOT
Tu

C

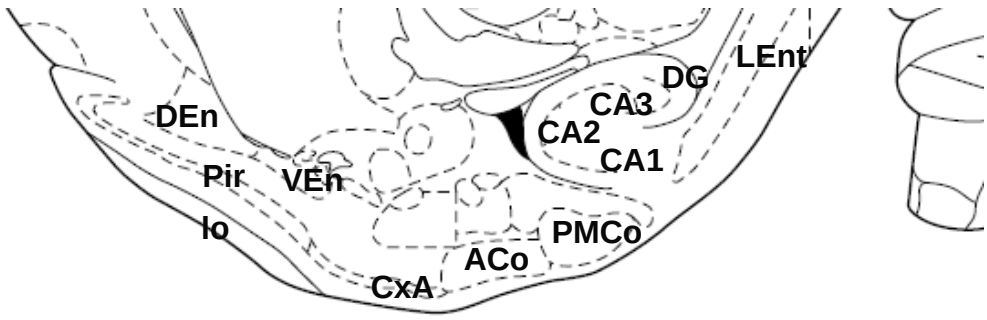
LEnt
DG
CA3
DEn
CA2
CA1
Pir
VEn
lo
PMCo
ACo
CxA

mammalian brain **(Fig. 1.8 A-C)** and, except for the inter-hemispheric commissures, are paired (Cleland and Linster, 2003). Within the olfactory peduncle, connecting the olfactory bulb to the olfactory cortex, lies the rostral migratory stream. Neuroblasts from the subventricular zone migrate via the rostral migratory stream to the olfactory bulb and undergo differentiation into MOB interneurons (Alvarez-Buylla and Garcia-Verdugo, 2002).

1.4.7 Innervation of the olfactory system

The olfactory bulb receives quite considerable centrifugal innervation or bulbopetal inputs (Shipley and Ennis, 1996). There are two major groups of axons targeting the olfactory bulb from caudal brain regions. These groups of bulbopetal inputs include those that arise from the primary olfactory cortex and those from the non-olfactory subcortical systems (Kratskin and Belluzzi, 2003).

Within the primary olfactory cortex, about 55% of mouse centrifugal neurons projecting to the olfactory bulb originate in the AON (Carson, 1984). Most AON afferents primarily terminate in the GCL, IPL and GL layers of the olfactory bulb (Haberly and Price, 1978). Containing about 36% of bulbopetal neurons projecting to the olfactory bulb in mice is the piriform cortex (Carson, 1984). Axons from this region terminate in the GCL (Haberly and Price, 1978). Originating in the lateral olfactory tract, about 2.4% of bulbopetal neurons project to the deeper parts of the GCL (Carson, 1984). Other neurons located in the entorhinal cortex, cortical amygdaloid cortices and periamygdaloid areas also project into the olfactory bulb (de Olmos et al., 1978).

Innervation of the olfactory bulb from non-olfactory structures is comprised of axons originating from three principle areas in the basal forebrain and brainstem. The major source of bulbopetal axons are located in the nucleus of the horizontal

limb of the diagonal band (HLDB) and contribute 3.5% of bulbopetal cells in mouse brain (Carson, 1984). The HLDB innervates the neocortex and hippocampus, playing an important role in learning and memory. Tracing studies have established that neurons from the HLDB project to the GL, EPL and GCL olfactory bulb layers (Price, 1968; Macrides et al., 1981)

Within the midbrain, dorsal and median raphe nuclei are a significant source of bilateral projections to the MOB, and in the rat almost 1300 raphe neurons project to the bulb (McLean and Shipley, 1987). Most of these axons terminate in the bulb glomeruli and deeper layers (McLean and Shipley, 1987).

The third principal source of non-olfactory innervation involves projections from the locus coeruleus (LC). About 40% of the 1600 neurons in the LC send axons to the rat olfactory bulb (Shipley et al., 1985). Axons from the LC terminate mainly in the IPL and GCL layers of the bulb (McLean et al., 1989).

1.5 Transport Pathways from Olfactory regions to the CNS

There have been many studies and reviews in the literature suggesting that macromolecules administered intranasally are transported to the CNS by several different pathways as summarized in **Fig. 1.9** (Mathison et al., 1998; Thorne and Frey 2nd, 2001; Illum, 2004). These reviews have broadly classified the various pathways from the olfactory mucosa in the nasal cavity to the CNS, into three main transport routes:

1) the olfactory nerve pathway or intracellular axonal transport; which involves internalisation of the substance into ORNs, intracellular transport to the olfactory bulb and further distribution to other CNS areas.

2) the olfactory epithelial pathway or extracellular transport, which requires absorption of the substance across the olfactory epithelium and further extracellular transport to the CNS via perineuronal channels.

3) the systemic pathway, which relies on the highly vascular nature of the respiratory and olfactory epithelia, allowing substances to gain access to the circulation.

Following nasal administration, certain substances which escape normal mucociliary clearance and enzymatic degradation systems, may cross the respiratory mucosa and enter the systemic circulation **(Fig. 1.9)**. If not eliminated by hepatic first- pass metabolism and are sufficiently lipophillic, the substance may cross the BBB and enter the CNS through the systemic pathway. However the studies described in this thesis will mainly focus on the intracellular and extracellular olfactory transport pathways.

Table 1.1 presents a list of substances including viral vectors, drugs and protein growth factors that are reported to gain direct access to the CNS after intranasal administration in various animal species. Also listed are the various methods of detection of the delivered substance.

Figure 1.9 A schematic diagram illustrating the proposed pathways for substances entering the nasal cavity and passage to brain tissue or CSF.

These pathways are divided into three broad groups: 1) Intracellular or transneuronal transport through the ORNs; 2) Extracellular transport through olfactory or trigeminal perineural spaces; 3) Systemic transport via the respiratory mucosa. Nasal administered substances may enter the CSF via the extracellular pathways or through systemic circulation.

Chart is adapted from Thorne *et. al.* (2004).

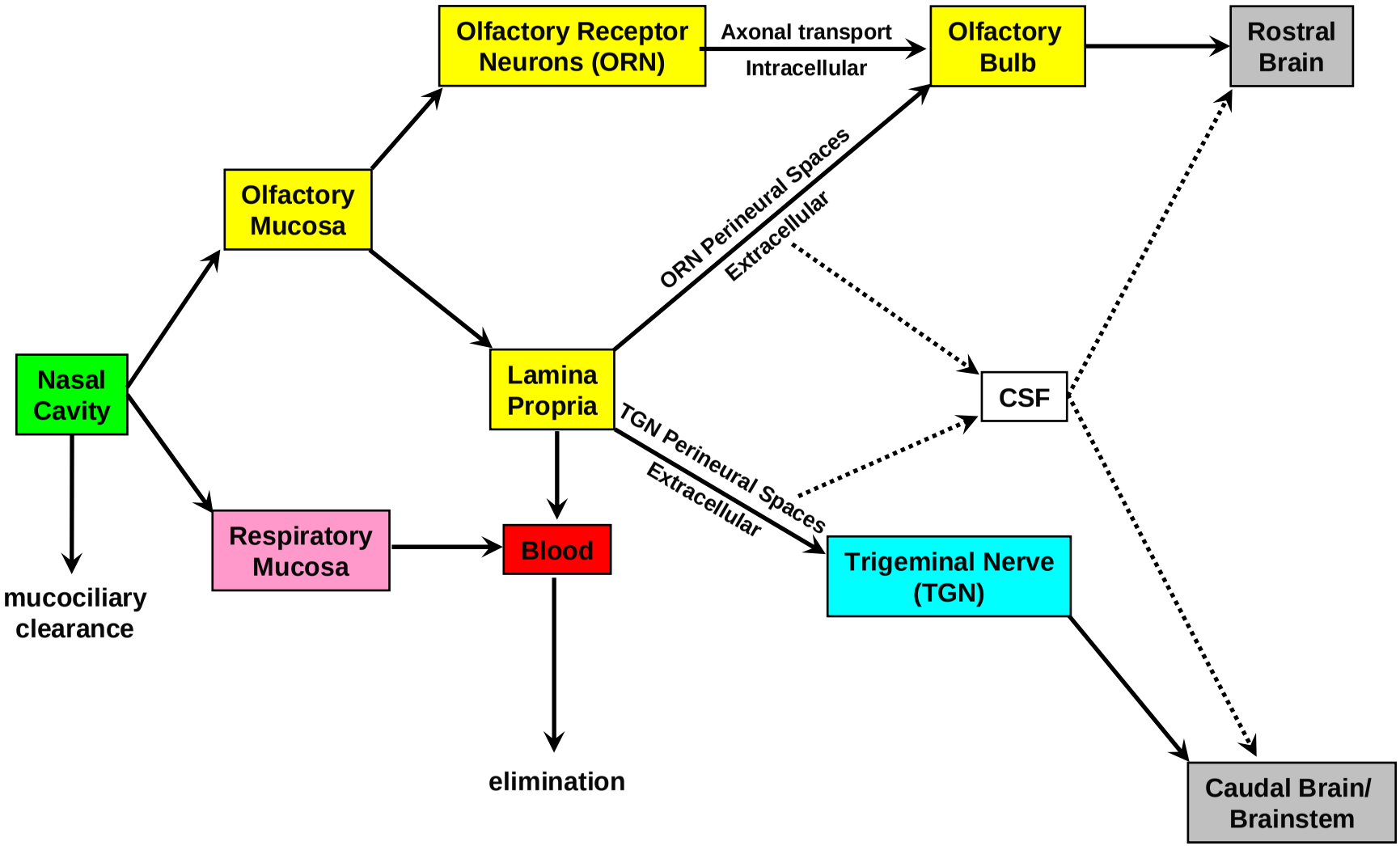
Olfactory Receptor Neurons (ORN)
Axonal transport
Intracellular
Olfactory Bulb
Rostral Brain
Olfactory Mucosa
ORN Perineural Spaces
Extracellular
Nasal Cavity
Lamina Propria
CSF
TGN Perineural Spaces
Extracellular
Respiratory Mucosa
Blood
Trigeminal Nerve (TGN)
mucociliary clearance
elimination
Caudal Brain/ Brainstem

Table 1.1 Selected studies of various macromolecular substances reported to reach the CNS following intranasal administration in different animal models.

Substance	Animal Model	Sample	Detection Method	Reference
Adenoviral lacZ vector	Rat	Brain	Histochemical	(Draghia et al., 1995)
β-Alanine (as carnosine)	Mouse	Brain	Autoradiography, Biochemical analysis Radioactivity count	(Burd et al., 1982)
Albumin (labelled with Evans blue)	Mouse	Brain	Light microscopy Fluorescence microscopy Electron microscopy	(Kristensson and Olsson, 1971)
Cephalexin	Rat	CSF	HPLC	(Sakane et al., 1991)
Cocaine	Rat	Brain	HPLC	(Chow et al., 1999)
Dextrans (FITC labelled)	Rat	CSF	HPLC	(Sakane et al., 1995)
Dopamine	Mouse	Brain	Autoradiography	(Dahlin et al., 2000)
Estradiol	Rat	CSF	Radioactivity count	(Anand Kumar et al., 1974)
Fibroblast Growth Factor	Mouse	Brain	Fluorescence microscopy	(Jin et al., 2003)
Horseradish peroxidase (HRP)	Monkey Mouse Rat	Brain	Histochemical Light microscopy Electron microscopy	(Kristensson and Olsson, 1971; Balin et al., 1986; Thorne et al., 1995)
Insulin	Mouse	Brain	Radioactivity count	(Gizurarson et al., 1997)
Insulin-like Growth Factor	Rat	Brain	Radioactivity count Autoradiography	(Thorne et al., 2004)
Interferon-β	Monkey	Brain	Radioactivity count Autoradiography	(Thorne et al., 2008)
Leptin	Rat	Brain	Radioactivity count	(Fliedner et al., 2006)
Leucine	Toad	Brain	Autoradiography	(Weiss and Holland, 1967)
Lidocaine	Rat	CSF	HPLC	(Chou and Donovan, 1998)
Midazolam	Dog	CSF	HPLC	(Henry et al., 1998)
Nerve growth factor	Rat	Brain CSF	ELISA Radioactivity count	(Frey 2nd et al., 1997; Chen et al., 1998)
Progesterone	Monkey	CSF	RIA Radioactivity count	(Anand Kumar et al., 1982)
Semliki Forest Virus-EGFP	Mouse	Brain	Fluorescence microscopy, ELISA	(Jerusalmi et al., 2003)
Sulphasomidine	Rat	CSF	HPLC	(Sakane et al., 1994)
Taurine	Mouse	Brain	Autoradiography Radioactivity count	(Brittebo and Eriksson, 1995)
Vasoactive intestinal peptide	Rat	Brain	Radioactivity count	(Gozes et al., 1996)
WGA-HRP	Mouse Rat Monkey	Brain	Histochemical Light microscopy Electron microscopy	(Broadwell and Balin, 1985; Balin et al., 1986)
WGA-HRP	Rat	Brain	Light microscopy Enzymatic assay Fluorescence microscopy Electron microscopy	(Shipley, 1985; Baker and Spencer, 1986; Thorne et al., 1995)
Zidovudine (AZT)	Rat	CSF	HPLC	(Seki et al., 1994)

ELISA, enzyme-linked immunosorbent assay; FITC, fluorescein isothiocyanate; WGA-HRP, wheat germ agglutinin-horseradish peroxidase; HPLC, high performance liquid chromatography; RIA, radioimmunoassay. Modified from (Dahlin, 2000).

1.5.1 Intracellular transport pathways

Intranasal administered substances, including macromolecules, are able to enter ORNs and gain direct access to the CNS via axonal transport to the olfactory bulb **(Fig. 1.9 & Fig. 1.10)**, followed by trans-synaptic transfer to secondary neurons which innervate the brain. These substances are thought to enter the ORN dendrites by mechanisms involving receptor mediated endocytosis or pinocytosis (De Lorenzo, 1970; Baker and Spencer, 1986). With evidence of a superfamily of different odorant receptors present on ORN dendrites (Buck and Axel, 1991), it is likely that nasal administered substances may bind to these receptors and be internalized. However, whether internalization of substances into ORNs occurs by either receptor mediated or non-receptor mediated processes, may depend upon the concentration of the delivered substance (Baker and Genter, 2003). In addition to the olfactory nerve, the trigeminal nerve, which ramifies throughout the respiratory and olfactory epithelia, may also be able to transport macromolecules and virus particles to the brain via intracellular transport (Tomlinson and Esiri, 1983; Fabian and Coulter, 1985; Perlman et al., 1990).As the trigeminal nerve innervates the olfactory and respiratory mucosae, any macromolecules penetrating these surfaces can potentially enter the trigeminal nerve.

The internalized substance is transported axonally along the fila olfactoria, traversing the cribriform plate and reaching the olfactory bulb GCL. Within the glomerulus, the endogenous substance may undergo trans-synaptic transfer between ORN and mitral or tufted cell axo-dendritic contacts. Further transneuronal transport from the olfactory bulb to different brain areas has been observed in second-order neurons and reported in both anterograde and retrograde directions (Shipley, 1985; Itaya, 1987). It is a commonly known phenomenon that macromolecules are axonally transported in either an anterograde or retrograde direction (Schwab and Thoenen,

Figure 1.10 The intracellular and extracellular pathways of olfactory transport into the rat CNS.

Intranasal administered substances gain access to the rat olfactory bulb and rostral brain regions by the intracellular axonal pathway (displayed in red). Extracellular pathways (displayed in blue) allow rapid transport of intranasal administered substances and can be subdivided into two routes: A) transport via peripheral olfactory perineural spaces connecting the nasal cavity with olfactory bulb and rostral brain regions; B) transport via perineural spaces associated with the trigeminal nerve complex connecting the nasal cavity with the caudal brain regions and brainstem.

Figure is adapted from Thorne *et. al.* (2004).

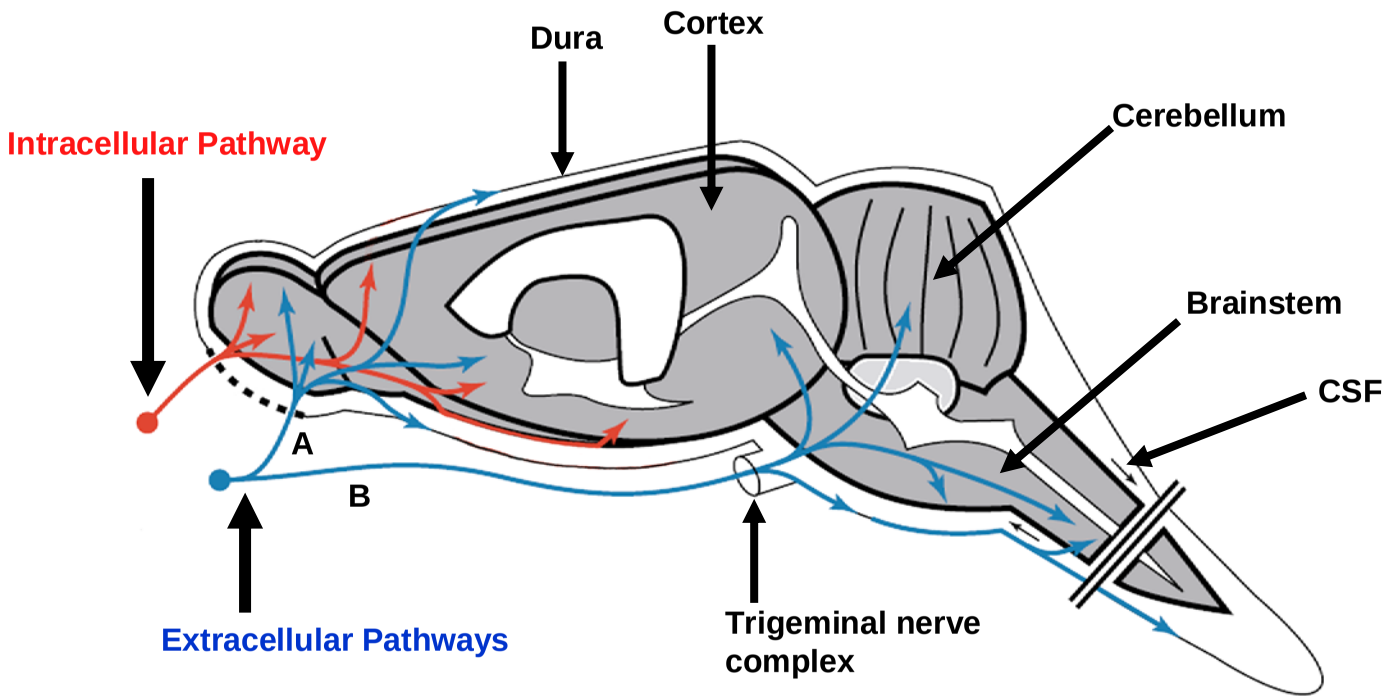
Dura
Cortex
Cerebellum
Intracellular Pathway
Brainstem
CSF
A
B
Extracellular Pathways
Trigeminal nerve complex

1977), and that these transport mechanisms occur in ORNs (Broadwell and Balin, 1985; Shipley, 1985; Baker and Spencer, 1986). In these studies, anterograde labelling has been observed in mitral cells terminating in the olfactory tubercle, piriform cortex and lateral olfactory tract (Baker and Spencer, 1986). Retrograde transport was observed in brain regions projecting to the olfactory bulb including the locus coeruleus, dorsal raphe nucleus and the horizontal limb of the diagonal band (Shipley, 1985).

Axonal transport of internalized substances within the ORNs may occur by either fast or slow transport systems (Weiss and Buchner, 1988). The nature of the internalization and the intracellular organelles involved may determine whether the transported substance travels transneuronally or only to the olfactory bulb (Baker and Genter, 2003). Several studies have compared the mechanisms of intracellular transport of WGA-HRP and HRP within the ORN, and found that different endocytic mechanisms are involved. Unconjugated HRP enters ORNs by a fluid-phase endocytosis because the protein lacks binding sites on the ORN plasmalemma (Broadwell and Balin, 1985). However, the 62kDa lectin conjugate, WGA-HRP, binds ORN cell surface glycoproteins and undergoes receptor-mediated endocytosis followed by transneuronal transport after processing in the trans Golgi saccule (Broadwell and Balin, 1985; Shipley, 1985; Baker and Spencer, 1986). Where WGA-HRP is processed and transported in vesicles destined for synaptic terminals, HRP is primarily endocytosed into lysosomes and not processed through the Golgi saccule (Broadwell and Balin, 1985). The above studies and others have shown that the intracellular axonal route of transport is particularly slow and may take up to 24hrs or longer to reach the CNS (Kristensson and Olsson, 1971).

Some examples of intracellular transport through ORNs are listed in **Table 1** and include: adenoviral lacZ vector, Evans blue labelled albumin, Semliki forest

virus and WGA-HRP. Other examples of intracellular transport through ORNs include gold particles, which are thought to undergo pinocytosis and are transneuronally transported (De Lorenzo, 1970). Several types of viruses have been reported to utilize axonal vacuoles within the ORNs and, through transsynaptic movement, gain access to brain areas synaptically connected to the olfactory bulb(Monath et al., 1983; Esiri and Tomlinson, 1984). Neurotropic viruses utilizing this route of entry have included: poliomyelitis virus (Landsteiner and Levaditi, 1910), which was found to travel within olfactory axons following intranasal application in primates (Bodian and Howe, 1941), rabies (Rake, 1937; Lafay et al., 1991), herpes simplex (Esiri and Tomlinson, 1984), vesicular stomatitis virus (Ozduman et al., 2008), hepatitis (Barnett and Perlman, 1993) and semliki forest virus (Oliver and Fazakerley, 1997).

Overall, most of these studies suggest that nose to brain transport via the ORN transneuronal pathway occurs through receptor-mediated endocytosis, vesicular axonal transport within ORNs and transsynaptic transfer to second order neurons.

1.5.2 Extracellular transport pathways

An alternative pathway which provides direct and rapid transportation of macromolecules from the nasal cavity to the CNS is known as the olfactory epithelial pathway or extracellular transport route (Balin et al., 1986; Thorne et al., 1995; Mathison et al., 1998; Illum, 2000) **(Fig. 1.9 & Fig. 1.10)**. In the extracellular transport pathway, substances enter the olfactory epithelium from the nasal cavity through the olfactory sustentacular cells or the Bowman's gland cells. The delivered substance may enter the sustentacular and Bowman's gland cells by either receptor-mediated endocytosis, fluid-phase endocytosis or by passive diffusion. Alternatively

the substance may cross the tight junctions between the supporting cells by paracellular mechanisms, or flow through open intracellular clefts between the supporting cells. After crossing the olfactory basal membrane, the substance may enter the lamina propria, thereby gaining access to the perineural spaces surrounding the olfactory nerve fascicles. Perineural spaces around the olfactory and trigeminal nerves are considered to be extensions of the subarachnoid space, allowing CSF in the subarachnoid space to be continuous with the perineural fluid (Yoffey, 1958; Jackson et al., 1979)(see **Fig. 1.5B**). Therefore, the delivered substance could rapidly travel through perineural spaces reaching the CSF and CNS.

Recent studies by Thorne *et. al.* have provided experimental evidence supporting the presence of a newly identified extracellular trigeminal pathway between the nasal cavity and the CNS (Thorne et al., 2004; Thorne et al., 2008). Therefore it is suggested that the extracellular transport pathway can be subdivided into at least two routes: A) rapid transport into the parenchymal CNS via peripheral olfactory perineural spaces; B) rapid transport into the parenchymal CNS via perineural spaces associated with the peripheral trigeminal complex (see **Fig. 1.9** and **Fig. 1.10 A&B**) (Thorne et al., 2004).

1.5.2.1 Transport via olfactory nerve perineural spaces

As outlined previously, olfactory neuron fascicles exiting the lamina propria are surrounded by perineural epithelium (Shantha and Bourne, 1968), which is either loosely or tightly adhered to the axons. Extracellular transport from the nasal cavity, through the olfactory epithelium, into the CSF relies on a direct anatomical connection between the nasal submucosa, the sub-arachnoid extensions and perineural spaces around the olfactory nerve fascicles which traverse the cribriform plate. Substances are able to enter the perineural space either through an “open-cuff

model" **(Fig. 1.11A)**, where the perineural epithelium is loosely attached to the olfactory axons, or through epithelial cell junctions and pinocytosis if the perineural epithelium is closely attached to the axons ("closed-cuff model") **(Fig. 1.11B)** (Jackson et al., 1979).

This transport pathway to the CNS through olfactory perineural spaces appears to be much faster than transport via the intracellular ORN axonal pathway. Smaller molecular weight substances appear rapidly in the CNS following delivery and are thought to be transported via this pathway (Frey 2nd et al., 1997).

1.5.2.2 Transport via trigeminal nerve perineural spaces

Rapid extracellular transport from the nasal cavity to caudal brain regions, including the brainstem and spinal cord, using a trigeminal nerve pathway has been recently identified by Thorne *et. al.* (2004) (**Fig. 1.9 & 1.10B**). This study suggested that an extracellular pathway may exist from the respiratory epithelium of the nasal passages, where the nasal (V2, maxillary) branch of the trigeminal nerve provides sensory innervation (Thorne et al., 2004). It is known that the trigeminal nerve conveys somatosensory information from the nasal cavity which includes mechanical sensation, thermal sensation and nociception (i.e. stinging, burning and strongly pungent sensations evoked from inhaled substances)(Silver, 1991). Several studies have suggested that viruses and bacteria are able to utilize the trigeminal nerve pathway to gain direct access to the CNS from the nasal cavity (Esiri and Tomlinson, 1984; Perlman et al., 1989; Jin et al., 2001) Using the lectin conjugate, WGA-HRP, intracellular transport can be shown in the trigeminal ganglion and brainstem, 48hrs after nasal delivery (Anton and Peppel, 1991). Some trigeminal ganglion cells, which project to the olfactory epithelium, have also been found to send collaterals to the olfactory bulb (Schaefer et al., 2002). Therefore the perineural and other supporting

Figure 1.11 Schematic cellular diagrams showing the two models used to describe the transport of nasal delivered substances, including tracers, within perineural spaces.

A. Open cuff-model. The perineural epithelium is loosely adherent to the olfactory axon and substances are able to freely enter the perineural space or lymphatic vessels.

B. Closed-cuff model. The perineural epithelium is closely adherent to the olfactory axon, restricting movement of substances.

Figure was adapted from Jackson *et al.* (1979).

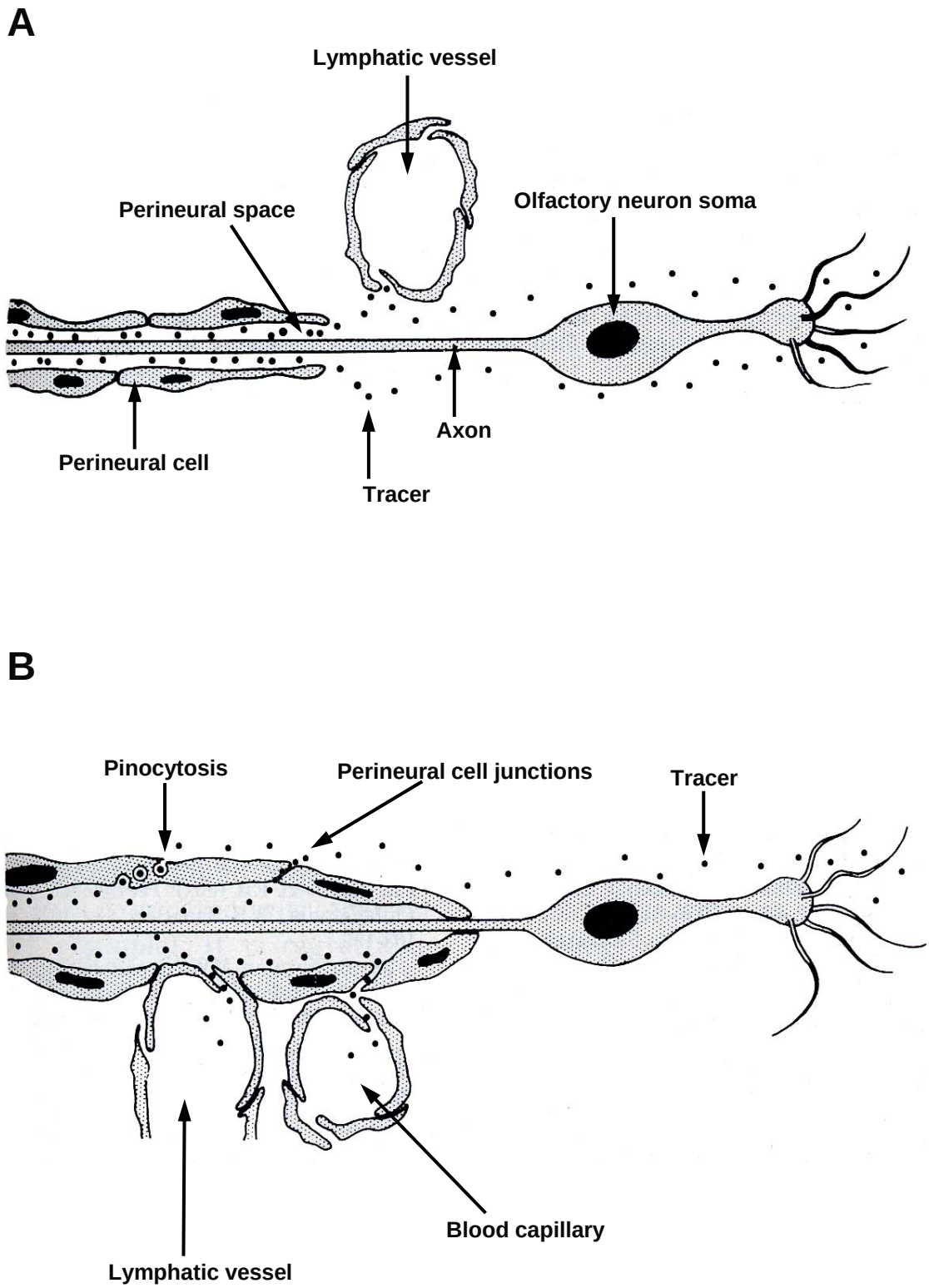
A
Lymphatic vessel
Perineural space
Olfactory neuron soma
Axon
Perineural cell
Tracer
B
Pinocytosis
Perineural cell junctions
Tracer
Blood capillary
Lymphatic vessel

cells associated with the trigeminal and olfactory nerve complexes may provide compartments and channels for rapid extracellular transport to the CNS.

1.5.3 Systemic and Lymphatic pathways

A third major route of entry of substances from the nasal cavity into the circulation and possibly the CNS is termed the systemic pathway, and generally results from the high vascularity of the respiratory and olfactory mucosa. Also described in this section is an alternate pathway through the lymphatic vessels located in the olfactory lamina propria. In the previous sections, the intracellular and extracellular olfactory pathways constitute direct transport pathways of substance delivery into the brain. However, the systemic and lymphatic pathways are indirect transport pathways to the brain and substances are still required to cross the BBB or blood-CSF barriers.

1.5.3.1 Nasal systemic pathway

Nasal delivered substances, which cross either the olfactory or respiratory epithelia, may enter the systemic circulation through capillaries present in the olfactory lamina propria and in the respiratory subepithelium. The nasal systemic route of drug delivery has been well documented as a method of avoiding loss of drug by hepatic first-pass metabolism (Hussain, 1998). While in the circulation only specific substances, which are either suitably lipophilic or have specialized uptake mechanisms, are able to cross the BBB and access the CNS. Due to the unique properties of the BBB, as described in the previous section 1.2, circulating molecules may gain access to the brain interstitial space by one of two general mechanisms: 1) lipid mediated free diffusion; 2) catalysed transport by either carrier-mediated or receptor-mediated mechanisms (Pardridge, 2002). Generally, lipophilic molecules

are absorbed across the nasal mucosa very rapidly into systemic circulation with a bioavailability of close to 100%, resembling that of intravenous injection (Illum, 2003). Polar molecules, including low molecular weight and high molecular weight molecules, encounter a nasal mucosa of low permeability. These have bioavailabilities of less than 10% for low molecular weight and less than 1% for high molecular weight molecules including peptide drugs (Illum, 2000). Nasal delivered drugs may cross the epithelial cell membrane by either transcellular routes through the epithelial cells or paracellular routes through the tight junctions between the epithelial cells (Illum, 2003).

1.5.3.2 Nasal lymphatic pathway

The lymphatic vessels in the olfactory and respiratory lamina propria are believed to have direct connection with the subarachnoid space CSF. Considerable evidence points towards a pathway connecting the olfactory subarachnoid space CSF with lymphatics of the nasal mucosa and this connection is thought to be the main pathway through which CSF material flows into the lymphatic system (Bradbury et al., 1981; Bradbury and Westrop, 1983). Another study shows how this pathway can facilitate rapid transport as demonstrated by X-ray contrast media leakage into the nasal cavities not long after the start of infusion into the cisterna magna (Brinker et al., 1997). Pathways connecting the CNS with nasal lymphatics may involve transport within the perivascular spaces of cerebral blood vessels (Ichimura et al., 1991). Therefore it is possible that intranasal administered substances which are able to cross the olfactory epithelium and enter the lamina propria, could enter lymphatic vessels at the site where circulating CSF drains from the subarachnoid sleeves. Eventually the substance would appear in systemic circulation after travelling through the lymphatic flow.

1.6 Intranasal Delivery of Therapeutic Macromolecules

Many therapeutic drugs are often polar and large molecular weight macromolecules which are inhibited from entering the CNS by the BBB. These include proteins and polypeptides, such as neurotrophic factors and different anti-inflammatory cytokines; RNAi or plasmid DNA vectors containing therapeutic genes; therapeutic viral vectors and other therapeutic agents of varying sizes. Many of these types of therapeutic drugs are considered suitable for the treatment of different neurodegenerative disorders such as Alzheimer's and Parkinson's disease, ischemic stroke, neuroAIDS, multiple sclerosis, Huntington's disease and even brain tumors (Hanson and Frey, 2007).

Intranasal delivery of therapeutic agents to the CNS offers a method of directly targeting drugs to critical areas of the brain, regardless of whether the drug can cross the BBB or not. Using this method of delivery, regions of the CNS along with nasal associated lymphatic tissue (NALT), cervical lymph nodes, cerebrovascular and perivascular spaces can be targeted. Many studies have demonstrated intranasal delivery of therapeutic macromolecules to the CNS in rats, mice, primates and humans (Thorne and Frey 2nd, 2001; Born et al., 2002; De Rosa et al., 2005; Thorne et al., 2008). A major advantage of intranasal delivery is that it enables a reduction of systemic exposure of a drug, thus avoiding hormone-like side effects. However, this benefit would depend on size, charge and lipophilicity of the delivered drug. This effect has been demonstrated with insulin, a charged molecule which reaches the brain without changing the blood glucose levels (Born et al., 2002).

As introduced in the section 1.5.1, macromolecules entering the CNS via the olfactory nerve pathway have been found to be distributed within rostral brain regions, such as olfactory bulb, anterior olfactory nucleus, forebrain and

hippocampus. Additionally, macromolecules utilising extracellular transport pathways, such as along the trigeminal nerve complex, are distributed within caudal brain regions including the brainstem, cerebellum and hypothalamus (Thorne et al., 2004). Most studies involving drug distribution following intranasal delivery include initial removal of blood from the cerebrovasculature and fixation by cardiac perfusion before measurement of tissue concentration.

1.6.1 Intranasal administration of neuroprotective agents

Considerable evidence has begun to emerge supporting the role of neurotrophic factors as neuroprotective agents in neurodegenerative diseases and brain injuries (Mufson et al., 1999). Many preclinical studies have shown that some neurotrophic factors and neuroactive peptides such as NGF, IGF-1, FGF-2 VEGF and TGF-β when administered intranasally are successfully targeted to regions of the CNS and may be beneficial in treatment of neurodegenerative diseases.

CNS delivery of a neurotrophic factor from the nasal cavity was first demonstrated by Frey et. al., who successfully showed delivery of NGF, a 26.5kDa protein, to the rat CNS bypassing the BBB (Frey 2nd et al., 1997; Chen et al., 1998). Further studies utilising intranasal NGF found that this procedure effectively protected against neurodegeneration and rescued recognition memory deficits in an Alzheimer's disease transgenic mouse model (Capsoni et al., 2002; De Rosa et al., 2005).

In a study by Thorne *et. al*., the 7.6kDa protein IGF-1 was shown to be transported to rostral and caudal brain regions, spinal cord, lymphatics and cerebrovasculature walls following nasal delivery (Thorne et al., 2004). IGF-1 has also been successfully used to reduce infarct volume and improve neurological function in a rodent model of stroke using intranasal delivery within a therapeutic

window of opportunity of up to 6 hours after the onset of ischemia (Liu et al., 2001; Liu et al., 2004) Using an alternative macromolecule, the 30.4kDa glycoprotein erythropoietin, Yu *et. al*. demonstrated protection against focal cerebral ischemia (Yu et al., 2005). More recently, intranasal IGF-1 has been used to suppress the toxic effects of ataxin-1 in a mouse model of the neurodegenerative disease spinocerebellar ataxia type-1 (SCA-1) (Vig et al., 2006). This involves the suppression of degenerative effects that mutant ataxin-1 exerts on Purkinje cells of SCA-1 mice (Vig et al., 2006).

Some intranasal neurotrophic factors, such as fibroblast growth factor-2 (FGF-2) and heparin-binding epidermal growth factor (HB-EGF), have been shown to induce cerebral neurogenesis in mice and may play a role in brain repair and associated functional recovery (Jin et al., 2003). Other studies have found that the growth factors, transforming growth factor-β (TGF-β) and vascular endothelial growth factor (VEGF) are also rapidly transported to the brain from the nasal cavity (Ma et al., 2007; Yang et al., 2008). The 25kDa TGF-β could be transported to the CNS via olfactory and trigeminal pathways, and consequently exert its biological effects by regulating gene expression of its receptors (Ma et al., 2007). VEGF, a 38.2kDa recombinant human protein, was also able to bypass the BBB via olfactory- and trigeminal-associated extracellular pathways to directly enter the CNS (Yang et al., 2008).

1.6.2 Intranasal administration of neuroimmune modulatory factors and metabolic regulatory factors

In addition to CNS delivery, intranasal administration can target therapeutic macromolecules to the perivascular spaces and lymphatics, allowing modulation of neuroimmune functions. This could occur through either: prevention of monocyte

and lymphocyte activation by targeting the nasal lymphatic system; prevention of monocyte infiltration across the BBB and blocking pro-inflammatory cytokine release by targeting the perivascular spaces; or blocking neurodegenerative associated neuroinflammation by targeting the brain parenchyma.

Interferons are anti-inflammatory cytokines which possess immune regulatory, antitumor and antiviral properties (Isaacs and Lindenmann, 1987). The 20kDa protein IFN-β1b has been used for the treatment of multiple sclerosis but with poor CNS delivery and negative side effects after intramuscular and subcutaneous injection (IFNB, 1995). It has been established that intranasally delivered IFN-β1b is rapidly transported to the brain, spinal cord and lymphatics in rats (Ross et al., 2004). Significant distribution of biologically active IFN-β1b occurred throughout the CNS and cervical lymph nodes, offering a non-invasive method of drug delivery for multiple sclerosis (Ross et al., 2004). Further studies have been performed in cynomolgus monkeys and also demonstrate rapid delivery of IFN-β1b to the CNS, lymphatics and cerebrovascular blood vessel walls (Thorne et al., 2008).

Several studies have shown a central role of the appetite control hormone leptin in the regulation of body weight. Although leptin is able to cross the BBB, in obese subjects, resistance of the leptin receptors occurs at the BBB, thus reducing transport into the CNS. Utilizing intranasal leptin delivery as a means of bypassing the BBB (Kastin and Pan, 2006), several groups have demonstrated that reduced body weight and food consumption occurs in the treated rodents (Schulz et al., 2004)and an overall reduced appetite was observed (Shimizu et al., 2005). Fliedner *et. al.* provide evidence that intranasal leptin rapidly enters the brain even in the presence of excess leptin in peripheral blood (Fliedner et al., 2006). Their study seems to favour a direct extracellular transportation route of leptin from nose to brain, as supported by the work of Frey's group (Thorne et al., 2004).

1.6.3 Intranasal administration of viral vectors for gene therapy

In exploring the feasibility of gene therapy to treat CNS diseases, it is evident that viral vectors are becoming vital tools in delivering therapeutic genes to specific targets in the CNS (Hermens and Verhaagen, 1998). Three types of viral vectors commonly used to transport therapeutic genes to the CNS are the retrovirus, adenovirus and adeno-associated virus (AAV).

Most retrovirus derived vectors have been based on the murine leukemia virus (MLV). Although these vectors can integrate into the host chromosome, ensuring long term stable expression, they are only able to insert their DNA into dividing cell genomes (Hermens and Verhaagen, 1998). However retroviral vectors based on the lentivirus (e.g. Human Immunodeficiency Virus) are able to integrate into the genome of non-proliferating neural cells in the brain (Naldini et al., 1996). Currently the adenovirus is one of the most popular vectors for neuronal gene therapy because of its low pathogenicity, ability to infect post-mitotic cells and high efficiency of cell transduction (Barkats et al., 1998). In addition, adenovirus vectors can be transported in a retrograde fashion from injection site to projection cell bodies after uptake at the nerve terminals (Akli et al., 1993). An application of this ability of adenovirus to be retrograde transported to specific CNS regions is the targeting of specific neuronal populations and avoiding the deleterious side effects encountered with systemic administration (Finiels et al., 1995). Recombinant AAV continues to attract increasing interest as a gene delivery system due to its unique features including safety, broad host range, high titres, transduction of quiescent cells and vector integration (Xiao et al., 1997).

There have been several studies examining intranasal administration of adenoviral and other viral vectors for the purpose of noninvasively targeting gene therapy to the CNS. A study by Draghia *et al*. demonstrated that following nasal

delivery of AdRSV-lacZ, olfactory bulb mitral cells, neurons in the anterior olfactory nucleus, locus coeruleus and area postrema all expressed β-galactosidase (Draghia et al., 1995). Their results suggest transport of adenovirus to the olfactory nucleus via a retrograde mechanism, followed by transneuronal transport to other brain regions. Other studies by Holtmaat *et al*., Zhao *et al*. and Hermens *et al*. have shown the usefulness of replication-deficient recombinant adenovirus in studying olfactory systems (Holtmaat et al., 1996; Zhao et al., 1996; Hermens et al., 1997). Using nasal delivered adenoviral vector containing lacZ reporter gene and cytomegalovirus (CMV) promoter, transgene expression was shown predominantly in ORN's compared to olfactory sustentacular cells and basal cells (Holtmaat et al., 1996; Zhao et al., 1996). Development of a WGA-expressing recombinant adenoviral vector system allowed Kinoshita *et al*. to visualize mouse olfactory pathways from the olfactory epithelium to the olfactory cortex brain regions (Kinoshita et al., 2002). Transsynaptic anterograde labelling appeared to be observed in the anterior olfactory nucleus, olfactory tubercle, piriform cortex and lateral entorhinal cortex; whereas transsynaptic retrograde transport was observed in the horizontal limb of diagonal band, median raphae nucleus and locus coeruleus (Kinoshita et al., 2002).

In an alternative study to those using adenoviral vectors, one group examined the intranasal delivery of Semliki Forest Virus (SFV) expressing either an enhanced GFP (EGFP) reporter gene or IL-10 therapeutic gene (Jerusalmi et al., 2003). In an experimental mouse model of autoimmune encephalomyelitis, intranasal delivered SFV expressing IL-10 was found to ameliorate the encephalomyelitis.(Jerusalmi et al., 2003). Intranasal delivery has also been used to noninvasively target gene therapy to the CNS using either mammalian viral vectors such as HSV (Laing et al., 2006) or filamentous phage vectors (Frenkel and Solomon, 2002). Using a replication-competant, glioma-adapted vesicular stomatis virus, one group has been able to

selectively infect and destroy olfactory bulb tumors following intranasal inoculation (Ozduman et al., 2008)

1.7 Project Rationale, Hypothesis and Aims

1.7.1 Project Rationale and Overview

Although some of the intracellular and extracellular pathways for nose to brain transport bypassing the BBB have been previously identified and characterized (as described in section 1.5), it is currently unclear exactly which pathways are used by particular macromolecules, including certain neurotrophic factors, growth factors and viral vectors **(Fig. 1.12)**. One such therapeutic neurotrophic factor which holds great potential for treatment of several neurological diseases is CNTF.

The 23kDa pluripotent neurocytokine, CNTF, is a member of the IL-6 cytokine family and is expressed by glial cells in the peripheral nerve and CNS (Manthorpe M. et al., 1993; Sleeman et al., 2000). Originally described as a trophic factor for motor neurons in the ciliary ganglion (Adler et al., 1979; Lin et al., 1990), CNTF also promotes differentiation of sympathetic neurons and glial progenitors into astrocytes (Sleeman et al., 2003). CNTF mediates its effects through binding to a heterotrimeric receptor complex consisting of CNTF-receptor α (CNTFR α), gp130Rβ, and leukaemia inhibitory factor (LIF) β receptor (Ip and Yancopoulos, 1996). It is believed that CNTF is a cytoplasmic protein which lacks a signal sequence peptide and is not secreted from neuronal cells (Sleeman et al., 2000), however CNTF is released upon nerve injury and acts on injured neurons. CNTF is a survival factor for a wide spectrum of neurons including motor neurons, sensory neurons, dopaminergic neurons in substantia nigra, cholinergic neurons in the basal forebrain and corticostriatal neurons. Thus CNTF has potential for the treatment of a number of neurological diseases such as demyelinating diseases, spinal cord injury, amyotrophic lateral sclerosis and motor neuron disease. Since CNTF activates the Janus kinase/ signal transducer and activator of transcription (JAK/STAT) signalling

Figure 1.12 Suggested pathways for the entry of the neurotrophic factor rhCNTF or viral vectors adenovirus and AAV into the CNS from the nasal cavity.

It is currently not fully known which mechanisms of transport are used by protein neurotrophic factors and viral vectors.

Recombinant human Ciliary Neurotrophic Factor (rhCNTF); Adeno-associated virus (AAV); blood brain barrier (BBB); cerebrospinal fluid (CSF).

Figure was adapted from Illum (2004).

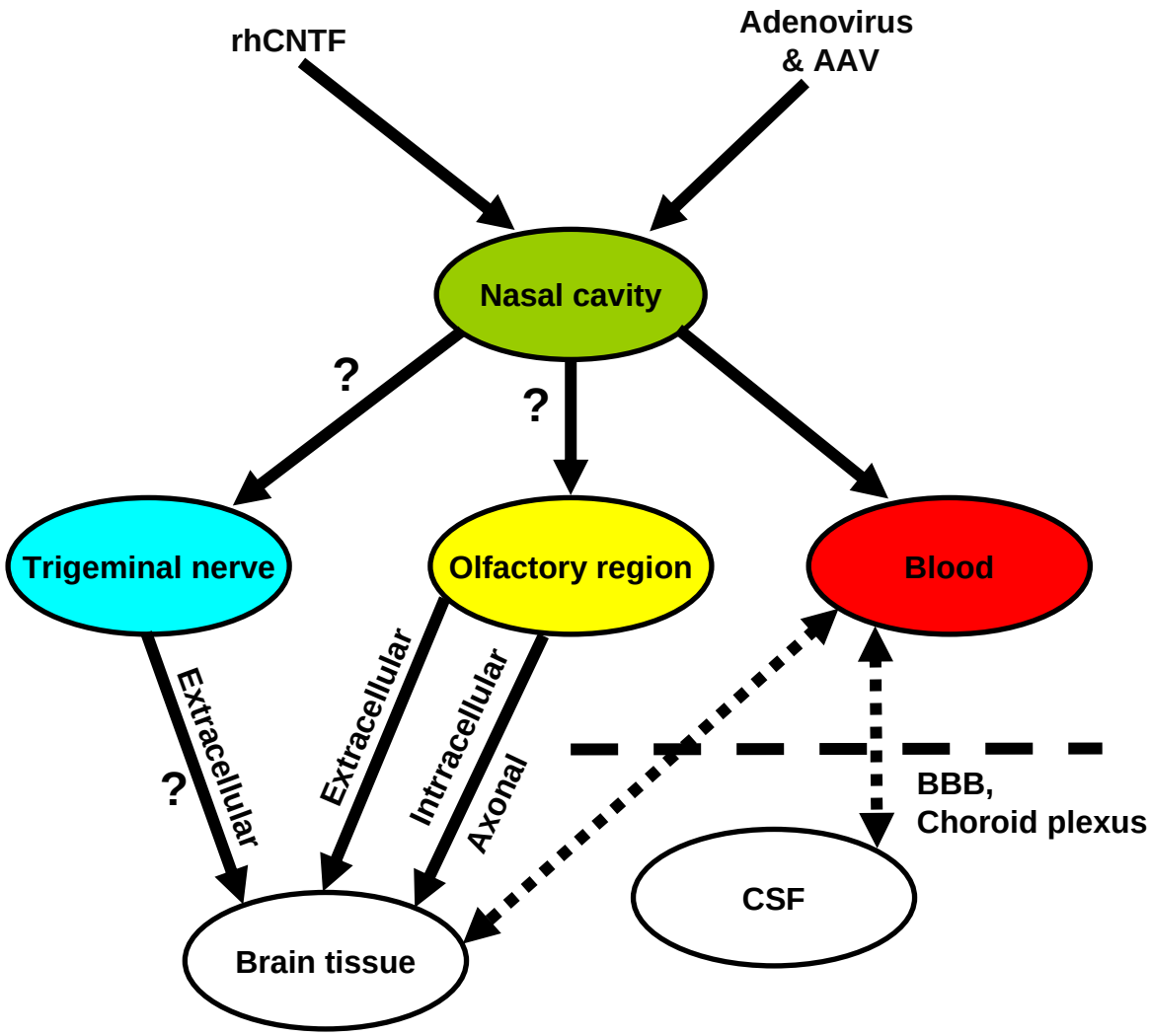
rhCNTF
Adenovirus
& AAV
Nasal cavity
?
?
Trigeminal nerve
Olfactory region
Blood
?
Extracellular
Extracellular
Intracellular
Axonal
BBB,
Choroid plexus
CSF
Brain tissue

pathways of satiety neurons in hypothalamic nuclei (Ip and Yancopoulos, 1996) and shares the signalling pathway of leptin, the obesity gene controlling energy metabolism, it is an important drug target for obesity (Gloaguen et al., 1997; Lambert et al., 2001). In fact, modified CNTF has been used in a phase II clinical trial for obesity (Ettinger et al., 2003).

The first part of this research project will focus on the transport of CNTF from the olfactory region to the CNS for the following reasons: i) ORNs express CNTF (Langenhan et al., 2005) and a gene which regulates CNTFR α (Young et al., 1997); ii) the CNTF receptor is expressed in the olfactory bulb(Lee et al., 1997); iii) little is known about the transport of CNTF to the brain either through ORNs or directly through the olfactory epithelium ; iv) CNTF has a protective role in a wide spectrum of different groups of neurons and is a drug target for different neurological diseases; v) CNTF has a unique role in regulation of food consumption and energy metabolism via central control and vi) there is a strong relationship between the olfactory nerve pathway and hypothalamic energy control centres, thus nasal CNTF administration may target hypothalamic nuclei.

The second part of this research study will examine the feasibility of using viral vectors to transfer a traceable gene product directly into the brain via the ORN's. Substantial clinical evidence shows that many viruses can infect brain via nasal route. The human encephalitis caused by herpes simplex virus is most likely caused through infection via the nasal route (Kennedy and Chaudhuri, 2002). In animal models, Montana Myotis leukoencephalitis virus inoculated via nasal route also cause flavivirus encephalitis with pathological changes along the nasal route to the brain regions (Charlier et al., 2002). Despite the clear concept and potential application, few studies attempt to use olfactory neurons as an avenue to transport therapeutic gene vectors into the brain. Using adenoviral vector, Draghia *et. al*.

showed that the LacZ gene can be expressed in olfactory mitral cells, anterior olfactory nuclei, locus coeruleus and area postrema for a short of period of time (Draghia et al., 1995). A more recent study using Semliki forest virus particles in nasal cavity showed that EGFP was detected only in olfactory bulb (Jerusalmi et al., 2003) also in a short period of time in some but not all animals. While these studies are encouraging, the expression of transgene at a lower level for a short period of time makes the use impractical for chronic neurological diseases. In consideration of the low titres of viral particle preparations used by these authors, their studies may be far from optimal and much more room for improvement is required. In addition, since different viruses have different neurotropisms, the choice of viral vector may also be crucial. Optimal delivery of viral vectors with a property of chromosomal integration such as AAV may increase the extent of gene expression in the brain.

1.7.2 Project Hypothesis

- The neurotrophic factor CNTF is transported from the olfactory mucosa directly to the brain through both intracellular olfactory nerve and extracellular trigeminal routes, similar to other neurotrophic factors.
- In addition, nasal delivered CNTF which is transported to the brain is biologically active and able to activate satiety pathways in a leptin-like manner.
- Therapeutic viral vector gene products can be transported to the brain via peripheral neurons that have connections with neurons in the CNS. Specifically, ORNs can internalize viral vectors, such as adenovirus and AAV, via a receptor-mediated mechanism and transport these vectors or their expressed transgene products anterogradely within axons to the olfactory bulb and further to other brain regions.

There are several lines of evidence supporting these hypotheses. First, many neurotrophic factors are expressed in the olfactory bulb and neuroepithelium (Buckland and Cunningham, 1999) and may play a role in the proliferation, differentiation and regeneration of ORNs in the olfactory neuroepithelium (Carter and Roskams, 2002; Bauer et al., 2003). Secondly, these neurons, like other neurons in the PNS and CNS, have machinery for transport of molecules and respond to ligand binding by internalization and anterogradely transport ligands such as wheat germ agglutinin (Itaya, 1987; von Bartheld, 2004). Thirdly these neurons not only transport proteins but also transport mRNA to the olfactory bulb which is necessary for the maintenance of the stereotypic projection of olfactory receptor neurons to the bulb (Vassar et al., 1994). Finally, mounting evidence suggests that large molecules can get into the brain via nasal delivery and the rate of the transfer cannot be explained by their absorption into blood route (Illum, 2002; Illum, 2004).

1.7.3 Project Aims

Chapter 2 Aims:

1. To determine whether intranasal delivered CNTF-biotin is transported directly to the CNS, and examine the temporal and spatial localisation of transported CNTF-biotin.
2. To quantitatively determine the temporal and spatial localisation of intranasal administered I^{125}-CNTF in CNS and peripheral tissues.
3. To establish the pathways involved in CNTF transport from nasal cavity to brain using unlabelled CNTF and $ZnSO_4$ denervation.
4. To examine the biological activity of nasal delivered CNTF through pSTAT activation pathways.
5. To determine whether intranasal administered CNTF can influence physiological functions such as regulation of energy metabolism by causing body weight loss in an obese rat model.

Chapter 3 Aims:

1. To examine the feasibility of using intranasal administration of viral vectors, adenovirus and AAV, to target different brain regions.
2. To characterise the temporal and spatial localisation patterns of EGFP expression following intranasal delivery of Ad5CMV-EGFP and AAV-EGFP into rats.

CHAPTER 2

INTRANASAL DELIVERY OF CILIARY NEUROTROPHIC FACTOR TO THE RAT BRAIN ALONG OLFACTORY PATHWAYS.

2.1 Summary

One of the major hurdles in drug development for brain diseases is the natural defensive structure called the blood brain barrier (BBB), which prevents therapeutic polypeptide drugs from entering the brain. From recent studies involving axonal transport, it is tempting to speculate that macromolecules such as neurotrophic factors can be delivered into the brain by peripheral neurons spanning the BBB. Specifically, therapeutic neurotrophins can be transported into the brain via the olfactory receptor neurons (ORNs).

In this study I firstly investigated the temporal and spatial localization pattern of both biotinylated and I^{125} labelled ciliary neurotrophic factor (CNTF) following a single dose nasal delivery into Sprague-Dawley rats. Two hours after nasal delivery, biotinylated CNTF was localized in the anterior olfactory nucleus and several brain regions including the hypothalamic arcuate nucleus, lateral entorhinal cortex, trigeminal nucleus and cerebellum. Intranasally delivered CNTF stimulated pSTAT3 signalling in regions of the hypothalamus and thalamus. Anaesthetized adult rats were intranasally given I^{125}-CNTF with or without unlabelled CNTF and sacrificed after 30 min, 3, 6 and 24 hours for brain tissue, blood and CSF collection. Quantitation of radioactivity in microdissected brain tissue revealed higher levels of CNTF distributed within the olfactory bulb, forebrain and trigeminal nerve which is consistent with a rapid extracellular transportation pathway from the olfactory mucosa via the peripheral trigeminal system. A separate group of rats were given zinc sulphate intranasally to produce olfactory epithelium denervation prior to nasal delivery of I^{125}-CNTF. Reduction of I^{125}CNTF radioactivity observed in the olfactory bulb and other brain regions after olfactory epithelium denervation, suggests involvement of ORN's in axonal transport of CNTF from the olfactory mucosa to the

brain. Finally I conducted a weight loss trial using an obese Zucker rat (OZR) model to test whether intranasally delivered CNTF caused weight loss, via a leptin-like mechanism, when compared to a control group of rats during a 12 day trial period. Intranasal administration of CNTF resulted in reduced body weight in the CNTF treated OZR group compared to the vehicle treated group during the 12 day trial and for three days after.

This study demonstrates that nasal delivered CNTF may be transported to the brain by either an axonal pathway through ORNs or via an extracellular route through the trigeminal system. Intranasal delivery of CNTF may be a valuable method for the treatment of obesity.

2.2 Introduction

Nasal drug administration has recently gained interest as a strategy for delivering therapeutic macromolecules to the mammalian brain and CNS for the treatment of brain diseases. One of the major hurdles facing drug development for brain diseases is the blood brain barrier (BBB) which restricts the passage of all but small (<500 Da) lipid soluble molecules from the bloodstream to the CNS (Pardridge, 2002). Intranasal drug administration provides a non-invasive alternative to established central administration routes (e.g. intracerebroventricular, intraparenchymal and intrathecal) for the direct CNS delivery of therapeutic molecules such as neurotrophic factors. Through both intracellular and extracellular pathways into the CNS, the BBB may be bypassed via the physiologically unique olfactory region of the nasal passages (Balin et al., 1986; Illum, 2000; Thorne and Frey 2nd, 2001; Thorne et al., 2004). The intracellular or intraneuronal pathway involves anterograde axonal transport within olfactory receptor neurons (ORNs) followed by transsynaptic transfer to second order mitral and tufted cells in the olfactory bulb glomeruli (Thorne et al., 2004). Several studies have clearly verified the intraneuronal pathway using nasal delivery of the wheat germ agglutinin-horseradish peroxidase (WGA-HRP) conjugate (Broadwell and Balin, 1985; Shipley, 1985; Baker and Spencer, 1986; Balin et al., 1986; Thorne et al., 1995). An extracellular or extraneuronal pathway which mediates rapid transport of macromolecules from the nasal passages to the brain has been demonstrated in studies using horseradish peroxidase (HRP) (Balin et al., 1986), nerve growth factor (NGF) (Frey 2nd et al., 1997; Chen et al., 1998) and insulin-like growth factor (IGF-1) (Thorne et al., 2004).

ORNs are the easiest accessible bipolar neurons that closely link the outside environment to the brain, and are the shortest linking neurons between the periphery and CNS. Their cell bodies and ciliated dendrites are located in the upper rear part of the nasal cavity and line the nasal septum and turbinates. The function of ORNs is to transmit signals of evaporative odorant from air to the brain (Buck and Axel, 1991). These neurons send their axons through holes in the cribiform plate of the ethmoid bone and enter the olfactory bulb forming synapses with mitral and tufted cells within a glomerular structure in the olfactory bulb **(Fig. 2.1)**. It is known that over 1000 odorant receptor genes are expressed by different types of ORNs (Buck and Axel, 1991; Chess et al., 1992; Malnic et al., 1999) and an odorant activates thousands of neurons which send converged signals to discrete glomeruli and then to the olfactory cortex (Vassar et al., 1994). The olfactory cilia of ORNs provide a large surface area contacting with the air environment, which is useful for the application of gene vectors or drugs. Due to their unique geometric localization, close linkage with the brain, a large contact surface area of cilia and the diversity of odorant receptors, it may be possible to deliver therapeutic proteins such as neurotrophic factors into the brain via axonal transport within ORNs.

Recent studies have demonstrated that nasal application of nerve growth factor (NGF) (Frey 2nd et al., 1997; Chen et al., 1998; De Rosa et al., 2005), vasopressin (Pietrowsky et al., 1996), insulin-like growth factor (IGF-1) (Thorne et al., 2004) and leptin (Schulz et al., 2004; Shimizu et al., 2005; Fliedner et al., 2006)result in significant levels of these factors in CSF and brain tissues. However, the mechanisms underlying the transport of these factors into enter the brain via the olfactory pathway are not fully understood.

Ciliary Neurotrophic Factor (CNTF) is a 22 kDa, 200 amino-acid pluripotent neurocytokine member of the IL-6 or gp130 family of cytokines which is expressed

by glial cells in peripheral nerve and in the CNS (Sleeman et al., 2000). It is believed that CNTF itself lacks a classical signal peptide sequence of a secreted protein, but is thought to convey its cytoprotective effects after release from adult glial cells by some mechanism induced by injury (Davis et al., 1993; Sleeman et al., 2000).. As a neurotrophic factor it stimulates cell survival or differentiation and gene expression in several neuronal and non-neuronal cell populations (Manthorpe M. et al., 1993; Ip and Yancopoulos, 1996). CNTF binds signal transducing subunits gp130, leukemia inhibitory factor receptor (LIFR), and CNTF receptor alpha which lead to activation of Janus Activated Kinases (JAK) and Signal Transduction and Activation of Transcription (STAT) pathways (Kishimoto et al., 1995; Ip and Yancopoulos, 1996). Since CNTF activates the JAK/STAT signaling pathways of satiety neurons in hypothalamic nuclei and shares the signaling pathway of leptin, the obesity gene controlling energy metabolism, it is a promising drug target for the treatment of obesity associated with leptin resistance (Febbraio, 2007). CNTF was first found to possess anti-obesogenic properties during a study of amyotrophic lateral sclerosis (ALS) patients (Als et al., 1996). Gloaguen *et al*. demonstrated that CNTF administration in leptin-resistant models of obesity resulted in reduced body weight, hypophagia and attenuated hyperinsulinemia (Gloaguen et al., 1997). This study was confirmed by Lambert *et al*. using $CNTF_{AX15}$ (recombinant human CNTF or Axokine) (Lambert et al., 2001).

The aim of the experiments described in this chapter was:

1. To determine whether intranasal delivered CNTF-biotin is transported directly to the CNS, and examine the temporal and spatial localisation of transported CNTF-biotin.
2. To quantitatively determine the temporal and spatial localisation of intranasal administered I^{125}-CNTF in CNS and peripheral tissues.

3. To establish the pathways involved in CNTF transport from nasal cavity to brain using unlabelled CNTF and $ZnSO_4$ denervation.
4. To examine the biological activity of nasal delivered CNTF through pSTAT activation pathways.
5. To determine whether intranasal administered CNTF can influence physiological functions such as regulation of energy metabolism by causing body weight loss in an obese rat model.

2.3 Materials and Methods

2.3.1 Animals

Male Sprague-Dawley rats were obtained at 6-8 weeks of age and used for I^{125} and biotinylated-CNTF tracing experiments. Male obese (*fa/fa*) Zucker rats (OZR) (Zucker and Zucker, 1961; Zucker and Zucker, 1963) were obtained at 16 weeks of age and allocated into two groups (n=5). All animals were individually caged and housed in a temperature controlled room with a 12 hour / 12 hour light / dark cycle, with unlimited access to normal laboratory chow and water. All animals were used in this study under the guidelines of the National Health and Medical Research Council of Australia and with approval from the Animal Welfare Committee of Flinders University, Adelaide, in compliance with approval number 577/04.

2.3.2 CNTF solutions

Recombinant human CNTF which shares about 80% sequence homology with rat CNTF and has biological activity comparable to that of native rat CNTF (Masiakowski et al., 1991) was used in this study. Recombinant human CNTF (Regeneron, Tarrytown, NY) was labelled with biotin using EZ-link Biotin-BMCC according to the protocol provided by the manufacturer (Pierce, Rockford, IL).

Radioiodinated CNTF (specific activity $4X10^5$cpm/ng protein) was prepared using von Bartheld's modified enzymatic lactoperoxidase method from an initial 10μg CNTF and 0.8mCi I^{125}-Na (100mCi/mL, GE Healthcare, Rydalmere, NSW)(von Bartheld, 1998; von Bartheld, 2000). Unincorporated I^{125} was separated from the I^{125}-CNTF by 2 cycles of ultrafiltration using Millipore Ultrafree-MC centrifugal filter units (Millipore, North Ryde, NSW), until 94.4% incorporation of

I^{125} was achieved, as determined by trichloroacetic acid (TCA) precipitation. After completing the radio-tracing experiments, TCA precipitation was performed on the remaining aliquot confirming greater than 90% integrity of I^{125}-CNTF.

2.3.3 Immunofluorescence

Adult Sprague-Dawley rats (n=4 each group) were anaesthetized by an intraperitoneal injection of a Ketamine (80mg/kg): Xylazil (15mg/kg), placed in the prone position and biotinylated human CNTF (1.5mg/mL) was administered to the rat's nasal cavities by micropipette with 5μL droplet solution delivered to each nostril for a total of 50μL delivered over a 30 min period. Rats were allowed to naturally inhale the solution during nasal inoculation before regaining consciousness. Control animals (n=2) received 50μL intranasal inoculations of biotinylated BSA (Pierce, Rockford, IL). Rats were re- anaesthetized either 30 mins or 2 hours after the commencement of nasal delivery and transcardially perfused with 100mL cold $NaNO_3$ solution immediately followed by a solution of cold 4% paraformaldehyde (200mL), buffered to pH 7 with 0.1M phosphate buffer. After perfusion, the brain and olfactory bulbs were dissected out and postfixed in the same fixative for 24 hours at 4^0C. The olfactory bulbs and brains were cryoprotected in 30% sucrose, for 48 hours before freezing in Tissue Tek OCT tissue protection medium (ProSciTech, Thuringowa Qld) and sectioning on a Leica cryostat (Leica-Microsystems, North Ryde, NSW). Frozen coronal and sagittal sections (15-20μm, 10 sections per animal) were collected on gelatin-coated slides and stored at -70^0C until required. Sections were washed three times in phosphate buffered saline (PBS) containing 0.2% Triton-X100 (PBST) for 10min each and incubated with a 1:500 dilution of streptavidin-Cy3 conjugate (Sigma-Aldrich, Castle Hill, NSW) for 2 hours at room temperature. Sections were washed three times in PBST, mounted with VECTASHIELD®

containing DAPI nuclear stain (Vector Laboratories, Burlingame, CA) and cover-slipped. Slides were examined with a 548nm filter using an Olympus BX-50 epifluorescent microscope (Olympus, Vic, Australia) equipped with a CoolSNAP CCD camera (Roper Scientific, Ottobrunn, Germany).

2.3.4 Immunofluorescence double-labelling

For the double-labelling experiments, coronal brain sections, collected and washed with PBST as described above, were firstly incubated in 5% normal donkey serum diluted in PBST for 1 hr at room temperature before overnight 4^0C incubation in either anti-neurofilament (N52) monoclonal antibody (Sigma-Aldrich, Castle Hill, NSW), or anti-glial fibrillary acidic protein (GFAP) polyclonal antibody (DAKO, Vic, Australia) both diluted 1:500 in the blocking buffer. Sections were then incubated for 1hr in anti-mouse-488 conjugated secondary antibody (Sigma-Aldrich, Castle Hill, NSW).

2.3.5 Haematoxylin and Eosin staining method for frozen sections

Frozen sections (20μm, 10 sections per animal), cut horizontally from perfused rat olfactory mucosa and olfactory bulb as previously described. Sections were routinely haematoxylin and eosin stained (Bancroft and Stevens, 1982) using a modified Harris type haematoxylin (see Appendix) and alcoholic eosin staining method developed in the Department of Anatomy and Histology, Flinders University.

2.3.6 Zinc Sulphate application

An aqueous solution of 5% zinc sulphate was applied to the nasal cavities of rats to cause extensive destruction of the olfactory neuroepithelium by coagulation

necrosis. Groups of rats (n=4) were anaesthetized as described previously and received 50μL 5% $ZnSO_4$ by intranasal irrigation with alternating 5μL droplets between nares. The procedure was repeated on the following day to ensure total destruction of the olfactory neuroepithelium. Rats were allowed to recover for 24 hrs before use in subsequent CNTF nasal delivery experiments. To assess the extent of olfactory neuroepithelial damage, n=2 rats were sacrificed 2 days after intranasal zinc sulphate treatment. Olfactory tissues were isolated and collected as described previously and processed for Haematoxylin/Eosin staining. The extent of olfactory neuroepithelium and olfactory bulb damage is illustrated in **Fig 2.1B & 2.1D.** Markedly reduced olfactory neuroepithelium, destruction of the olfactory nerve layer (ONL) and damaged glomerular layer (GL) in the olfactory bulb was observed. However the tissue sections shown in **Fig 2.1** are very over-stained and better sections would be required to fully confirm the effectiveness of the $ZnSO_4$ treatment.

2.3.7 Phosphorylated STAT3 Immunohistochemistry

Recombinant human CNTF (1.6 mg/ml) was administered by intranasal delivery to Sprague-Dawley rats (n=4) before the rats were sacrificed and perfused 30 mins after delivery, as described in the previous section. Control animals (n=2) received an equivalent intranasal volume of 1% BSA in PBS. Coronal 20μm brain sections (10 sections per animal) were collected, free floating, in PBST. Antigen retrieval was performed on the sections by heating in boiling 1mM EDTA, pH 8 and cooling to room temperature two times. Sections were washed in PBST and treated with a solution of 1% hydrogen peroxide/50% methanol in distilled water for 10 mins before washing three times in PBST. After 2 hr blocking in 5% normal horse serum in PBST, sections were incubated overnight at 4^0 C with rabbit anti-pSTAT3 (Cell Signaling Technology, Danvers, MA) diluted 1:50 in blocking reagent.

Figure 2.1

Olfactory neuron degeneration in olfactory epithelium (OE) and olfactory bulb (OB) following intranasal irrigation with 5% $ZnSO_4$ compared to a control OE receiving intranasal saline irrigation.

In the $ZnSO_4$ treated tissue, there is a reduction in the thickness of the OE **(B)** compared to the normal tissue **(A)**. In the OB, $ZnSO_4$ treatment resulted in a degenerated ONL and shrunken GL **(D)** compared to normal OB layers **(C)**.

(1) A schematic diagram adapted from Oberto *et.al*. (2001), showing the effects of $ZnSO_4$ (left side) on the OE and OB.

(2) Light photomicrograph images of haematoxylin and eosin stained olfactory mucosa and OB; **(A)** olfactory mucosa. saline treated, **(B)** olfactory mucosa. $ZnSO_4$ treated, **(C)** OB saline treated, **(D)** OB $ZnSO_4$ treated; dashed line shows position of ONL. **LP**, lamina propria; **OE**, olfactory epithelium; **ONL**, olfactory nerve layer; **GL**, glomerular layer; **EPL**, external plexiform layer; **MCL**, mitral cell layer; **GRL**, granule cell layer. The olfactory tissue sections shown here are heavily over-stained and better stained higher power sections would be required to fully confirm the effectiveness of the $ZnSO_4$ treatment on the olfactory epithelium. .Scale bar = 25μm.

1

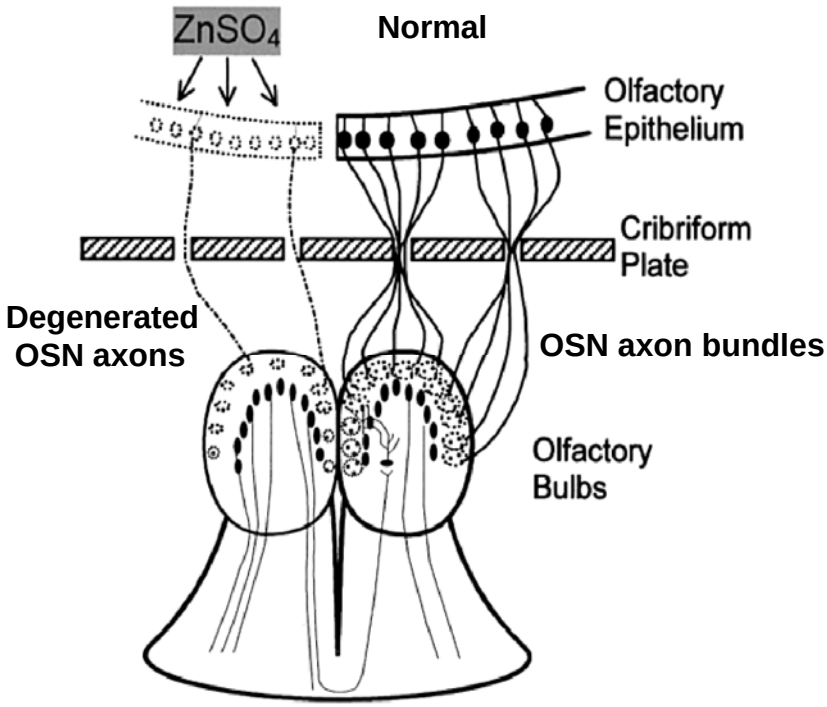
ZnSO4
Normal
Olfactory
Epithelium
Cribriform
Plate
Degenerated
OSN axons
OSN axon bundles
Olfactory
Bulbs

2

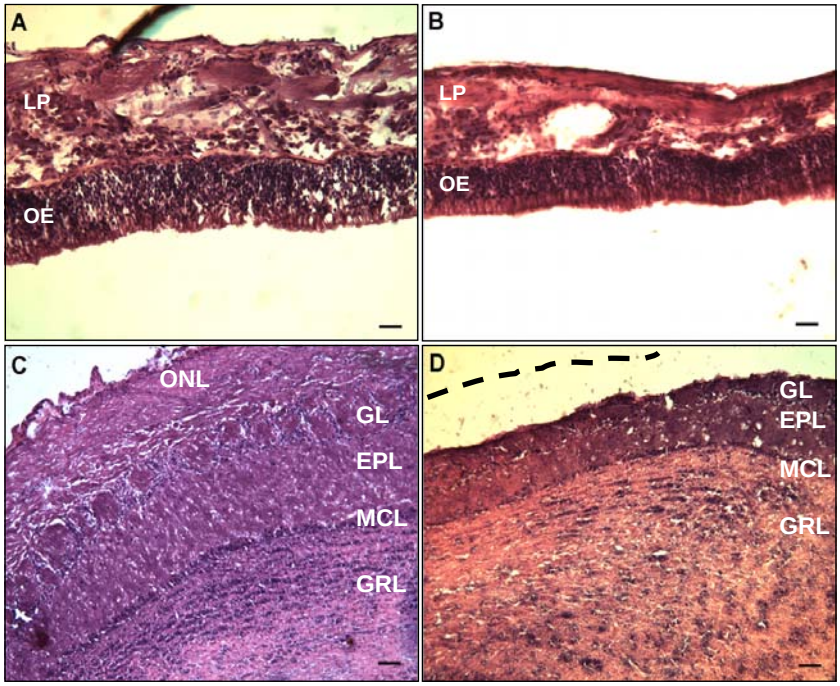
A
LP
OE
B
LP
OE
C
ONL
GL
EPL
MCL
GRL
D
GL
EPL
MCL
GRL

Sections were then washed in PBST and incubated for 2 hrs at room temperature with donkey anti-rabbit Alexa 488 (Invitrogen Molecular Probes, Carlsbad, CA) diluted 1:500 in PBST. Control sections were incubated in pre-immune serum overnight at 4^0C instead of the primary antibody at the same dilution. Sections were washed three times as described previously, cover-slipped and mounted using VECTASHIELD® (Vector Laboratories, Burlingame, CA). Slides were examined at 488nm using an Olympus BX-50 epifluorescent microscope (Olympus, Vic, Australia) equipped with a CoolSNAP CCD camera (Roper Scientific, Ottobrunn, Germany) and images acquired.

2.3.8 Intranasal delivery of I^{125}-CNTF into Sprague-Dawley rats

Adult male Sprague-Dawley rats were separated into 4 groups (n=4), anaesthetized as described previously and placed in prone position. A total of 40μL I^{125}-CNTF (29ng, $8X10^6$cpm) was intranasally administered by micropipette in alternating 5μL droplets between nares, as described previously. At 30 min, 3, 6 and 24 hours after initial nasal delivery (n=4 per timepoint), 1 mL blood samples were taken by cardiac puncture, and all animals were sacrificed by transcardial perfusion firstly with 100mL 1% $NaNO_3$ solution, followed by 200mL 1% paraformaldehyde/1.25% glutaraldehyde in 0.1M Sorenson's phosphate buffer. Brains, olfactory tissues and peripheral tissues were carefully removed from each animal.

In a separate group of rats (n=4), 500 fold excess unlabelled huCNTF (10.7μg) was mixed with I^{125}-CNTF (21.43ng) and nasally delivered to these rats as described above. Control rats (n=4) received I^{125}-CNTF with no unlabelled CNTF. Brain and peripheral tissue samples were collected 30 min after the start of delivery.

Primary olfactory neurons were destroyed in the olfactory mucosa by nasal delivery of 100μL of an aqueous solution of 5% $ZnSO_4$ in a separate group of rats

(n=4) 2 days prior to intranasal delivery of I^{125}-CNTF. A control groups of rats (n=4) received 100μL sterile saline 2 days before intranasal delivery of I^{125}-CNTF. All animals were transcardially perfused after 30 mins and brain, blood, CSF and peripheral tissue samples were collected.

2.3.9 Harvest of central and peripheral tissues and measurement of I^{125}-CNTF content.

Following perfusion, detailed microdissection was performed on each animal, with care taken to avoid cross-contamination of tissues. Thirteen discrete brain **(Table 2.1)** and olfactory regions were further microdissected with a scalpel and collected in 5mL tubes for gamma counting. The trigeminal nerve opthalamic (V_1) and maxillary (V_2) segments, extending from the point where the nerve root connects the brainstem posteriorly, was carefully dissected away from the surrounding cranial cavity. Each tissue sample was wet-weighed and then analysed in a Packard Cobra gamma counter (GMI, Ramsey, MN). Cisternal samples (100-200 μL) of CSF were collected immediately after transcardiac perfusion using an insulin syringe from the cisterna magna. Data is presented as counts per minute (CPM) per mg wet weight of brain or peripheral tissue, assuming negligible metabolism of I^{125}-CNTF. The average total brain cpm/mg values for each animal were calculated by dividing the sum of the CPM of each brain samples by the sum of the wet-weight (g) of these samples.

2.3.10 Intranasal delivery of huCNTF into OZR (*fa/fa*)

Male homozygous OZR (*fa/fa*) were kindly provided by Prof. Greg Barritt (Flinders University) and were allocated into 2 groups, obese treatment and obese control (n=5) based on the type of nasal treatment received. Body weight and food consumption were monitored daily over 15 days. The rats received daily doses of either huCNTF (0.06mg/kg, treatment group) or BSA in PBS vehicle (1mg/ml,

Table 2.1 Brain regions and peripheral tissue samples collected during radiotracing experiments using I^{125}-CNTF.

Tissue region	**Abbreviation**
Olfactory bulb	Ob
Forebrain	Fb
Frontal cortex	FCt
Parietal cortex	PCt
Hypothalamus	Hy
Thalamus	Th
Hippocampus	Hc
Midbrain	Mb
Cerebellum	Cb
Pons	Pn
Medulla	Md
Cervical spinal cord	CSc
Trigeminal nerve	Tg
Blood	Bl
Heart	H
Lung	L
Liver	Liv
Hind limb Muscle	Mus
Cerebral spinal fluid	CSF

control group) for a 12 day treatment period. For one week before the start of nasal delivery, the rats were handled and weighed so that they became accustomed to the procedure. During the treatment period, the rats were anaesthetized by isoflurane inhalation, placed in a supine position and received nasal instillation of either huCNTF (0.06mg/kg, 30μL) or vehicle control (0.03mg, 30μL). After nasal delivery the rats were allowed to recover and returned to their individual cages. Food intake was determined by weighing the amount of chow remaining in the food dishes over a 24hr period.

2.3.11 Statistical analysis

All data are expressed as mean ±SEM. The effects of different treatments applied were studied as a function of time for the OZR obesity trial and radio-tracing time-course, or a function of brain tissue region in the $ZnSO_4$ denervation and competitive binding experiment. Therefore statistical analysis of the data was by ANOVA for repeated measures. If there was a significant difference between brain areas or different types of treatment groups, a *post hoc* Bonferroni test would be performed. $P < 0.05$ was accepted as the level of statistical significance.

2.4 Results

2.4.1 Localization of biotinylated CNTF in brain regions 30mins-2hrs after intranasal delivery

Two hours after CNTF-biotin intranasal inoculation, CNTF-biotin streptavidin-CY3 fluorescence was detected in neuronal cells of several brain regions **(Fig.2.2 A-F)**. Higher magnifications of sagittal rat brain sections revealed strong specific fluorescence localized within the cytoplasm of neuronal cells in the anterior olfactory nucleus (AOV) and in the lateral hypothalamus (LH) **(Fig.2.2 A and B)**. Specific fluorescence was also localized within cells of the cerebellum **(Fig.2.2 C)**, including the Purkinje cell layer (**Fig.2.2 D)**. As shown in **Fig.2.2 E**, several neuronal cells in the inferior colliculus displayed localized fluorescence. Control brain sections showed no specific fluorescence 30min-2hrs after intranasal inoculation of separate rats with biotinylated BSA, followed by treatment of sections with streptavidin-CY3 **(Fig.2.2 F)**. In all cells observed, CNTF-biotin/avidin-Cy3 fluorescence appeared to be granular and localized within the cellular cytoplasm.

In a separate group of rats, olfactory, cortical and forebrain sections were collected 30mins after intranasal delivery of biotinylated CNTF into the rats. CNTF-biotin Cy3 fluorescence was detected in neuronal cells (arrows) of the lateral entorhinal cortex region (LEnt) **(Fig.2.3 A-B)**. The dorsal endopiriform cortex (DEn) of the forebrain **(Fig.2.3 C-D)** contained several positive neuronal cells (arrows) with localised CNTF-biotin. **(Fig.2.3 E-F)** Positive cells (arrows) were also detected in the olfactory bulb neural and glomerular layers. Cellular nuclei were counterstained with DAPI for better visualization of neurons.

Figure 2.2

Localization of CNTF-biotin in rat brain regions 2 hours after intranasal inoculation.

(A-F) High magnification images of sagittal rat brain sections displaying CNTF-biotin streptavidin-CY3 fluorescence localized within the cytoplasm of various neuronal cell populations. These include: **(A)** neuronal cells of the anterior olfactory nucleus, ventral part (arrowheads), **(B)** cells in the lateral hypothalamus (arrows) **(C)** cells in the cerebellum (arrowheads), **(D)** purkinje cells in the cerebellum (arrows), **(E)** cells in the inferior colliculus (arrowheads). **(F)** No biotinylated CNTF was observed in brain tissues after intranasal inoculation with BSA-biotin and incubation with streptavidin-CY3. Scale bar = 25μm. Images A-F correspond to the regions marked on Paxinos' sagittal rat brain map (Paxinos and Watson, 1998).

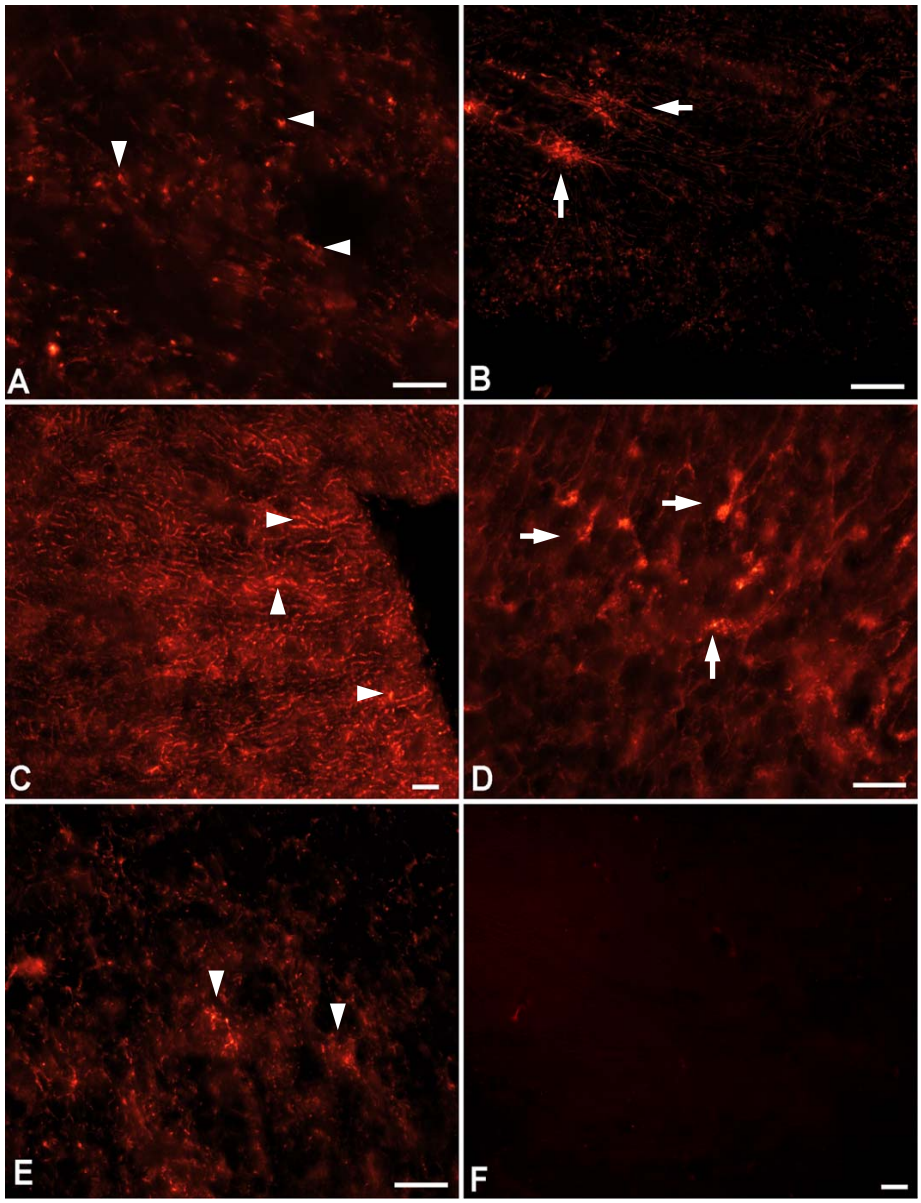

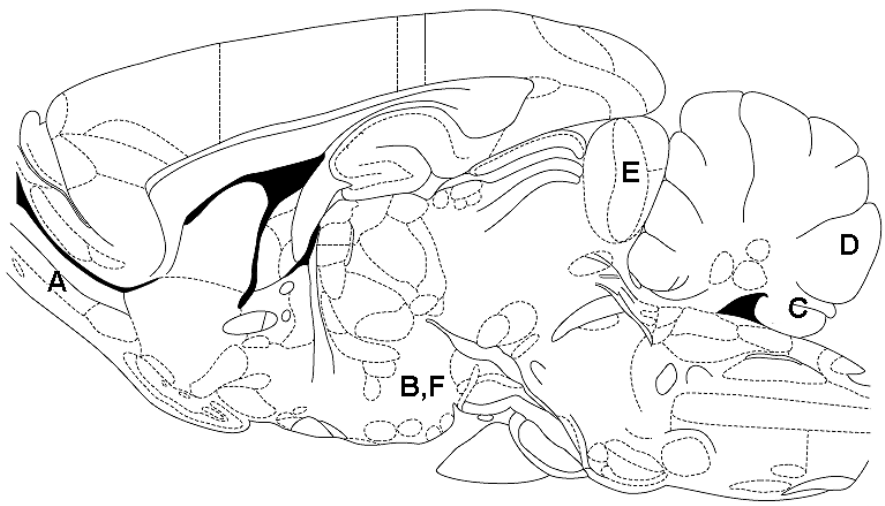

Lateral 1.40 mm, Paxinos and Watson, 1998

Figure 2.3

Biotinylated CNTF CY3-fluorescence in olfactory, cortical and forebrain coronal sections (A-F), 30mins after intranasal delivery of CNTF into Sprague-Dawley rats.

(A-B) Fluorescent neuronal cells (arrows) were observed in the lateral entorhinal cortex (LEnt). **(C-D)** Neuronal cells within the dorsal endopiriform cortex (DEn)(arrows) contained CNTF-biotin. **(E-F)** Positive cells (arrows) within the olfactory bulb neural (ON) and glomerular layers (GL). Cellular nuclei (blue) in these sections were counterstained with DAPI. Scale bars = 25μm. Images A-F correspond to the regions marked on Paxinos' coronal rat brain maps (Paxinos and Watson, 1998).

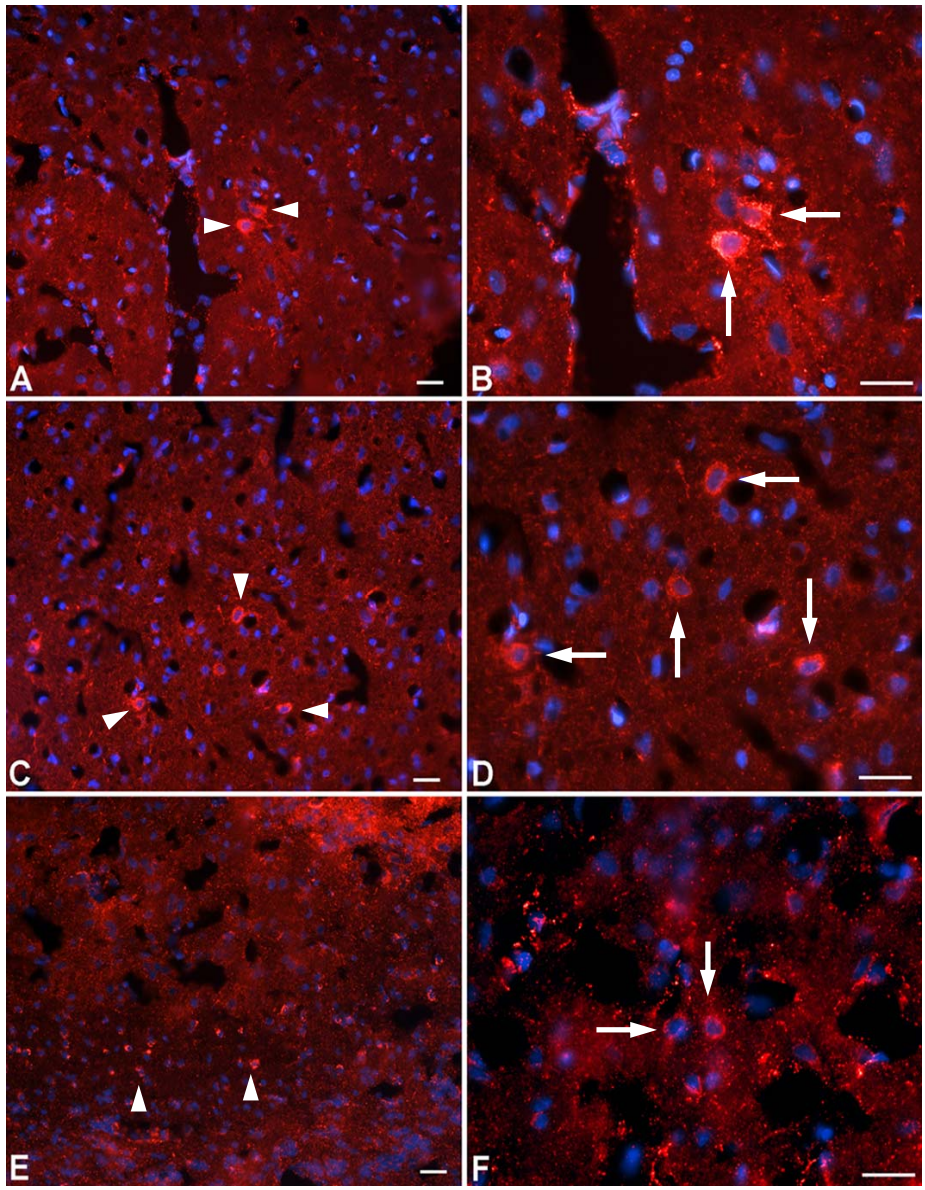

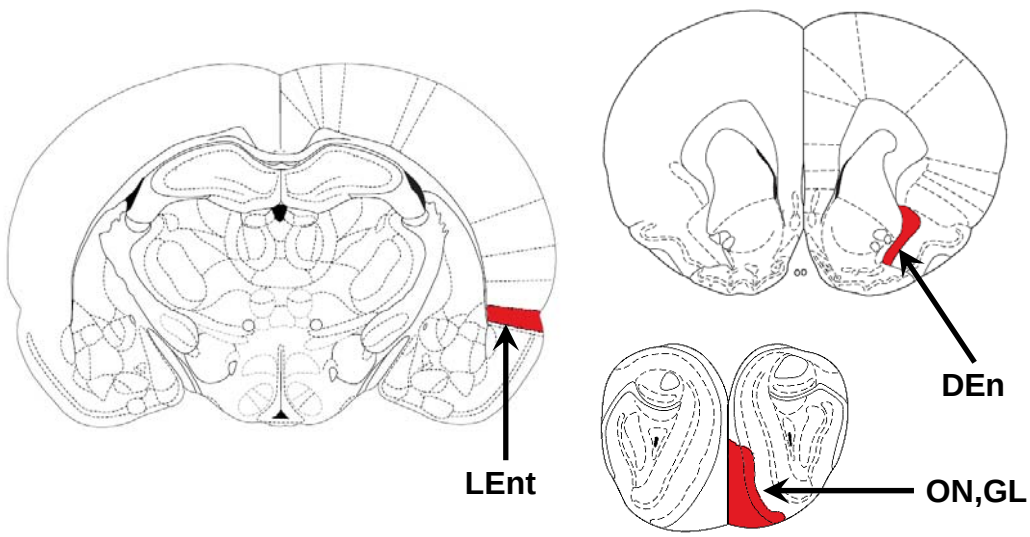

Bregma -3.14 mm, 2.20 mm, 5.70 mm, Paxinos and Watson, 1998

2.4.2 Intranasal administered CNTF co-localizes with neurofilament marker (N52) and cytoskeletal marker GFAP

Coronal brain sections were taken from rats which received intranasal administration of CNTF-biotin (n=4) and incubated in anti-neurofilament antibody N52. Within the OB **(Fig.2.4 A-D)**, Hyp **(Fig.2.4 E-H)** and LEnt **(Fig.2.4 I-L)** CNTF-biotin (red) co-localized with neurofilament N52 (green) as shown in merged images **Fig.2.4 D, H & L** by yellow neuronal cells marked by arrows. In the OB, CNTF-biotin appeared to co-localize with N52 in neuronal cells within the OB glomerular layer only. No cells in the OB neural layer were positive for N52 **(Fig.2.4 B)**, indicating that only the un-myelinated axons of ORNs are present in this layer.

Another set of coronal brain sections, taken from rats which received intranasal administration of CNTF-biotin (n=4), were incubated in anti-GFAP antibody. In some of these sections, within the Hyp **(Fig.2.5 A-D)** and LEnt **(Fig.2.5 E-H)**, CNTF-biotin (red) co-localized with GFAP positive (green) astrocytes as shown in merged images **Fig.2.5 D & H** by arrowed cells. In both figures **2.4** and **2.5**, cellular nuclei were counterstained with DAPI for better visualization of nuclei.

2.4.3 Effect of $ZnSO_4$ denervation of olfactory mucosa prior to biotinylated CNTF intranasal application.

In this experiment, the distribution of biotinylated CNTF was examined in the rat brain following $ZnSO_4$ mediated disruption of the olfactory epithelium. Rats received nasal irrigation with 5% $ZnSO_4$ 2 days prior to intranasal delivery of CNTF-biotin. CNTF-biotin was localized within the trigeminal nucleus and the ventral cochlear region of the cerebellum **(Fig.2.6 A-F)**, 30 mins after intranasal delivery. In control sections from $ZnSO_4$ treated animals which received intranasal biotinylated BSA, no specific fluorescence was observed **(Fig.2.6 B)**. Neuronal cells from the

Figure 2.4

CNTF-biotin co-localizes with neurofilament N52 in the olfactory bulb (OB; A-D), hypothalamus (Hyp; E-H) and lateral entorhinal cortex (LEnt; I-J).

(A-D) CNTF-biotin (red) co-localized (yellow) with N52 (green) within neuronal cells of the olfactory glomeruli (as shown by arrows in panels A, B and D). **(E-H)** Neurons in the hypothalamus (arrows in panels E, F and H) showed co-localization (yellow) of CNTF-biotin (red) with N52 (green). A neuron (arrowed cell in panels I, J and L) in the LEnt displaying co-localization (yellow) of CNTF-biotin with N52. Cellular nuclei (shown in panels C, G and K) were counterstained with DAPI (blue). Scale bars= 25μm

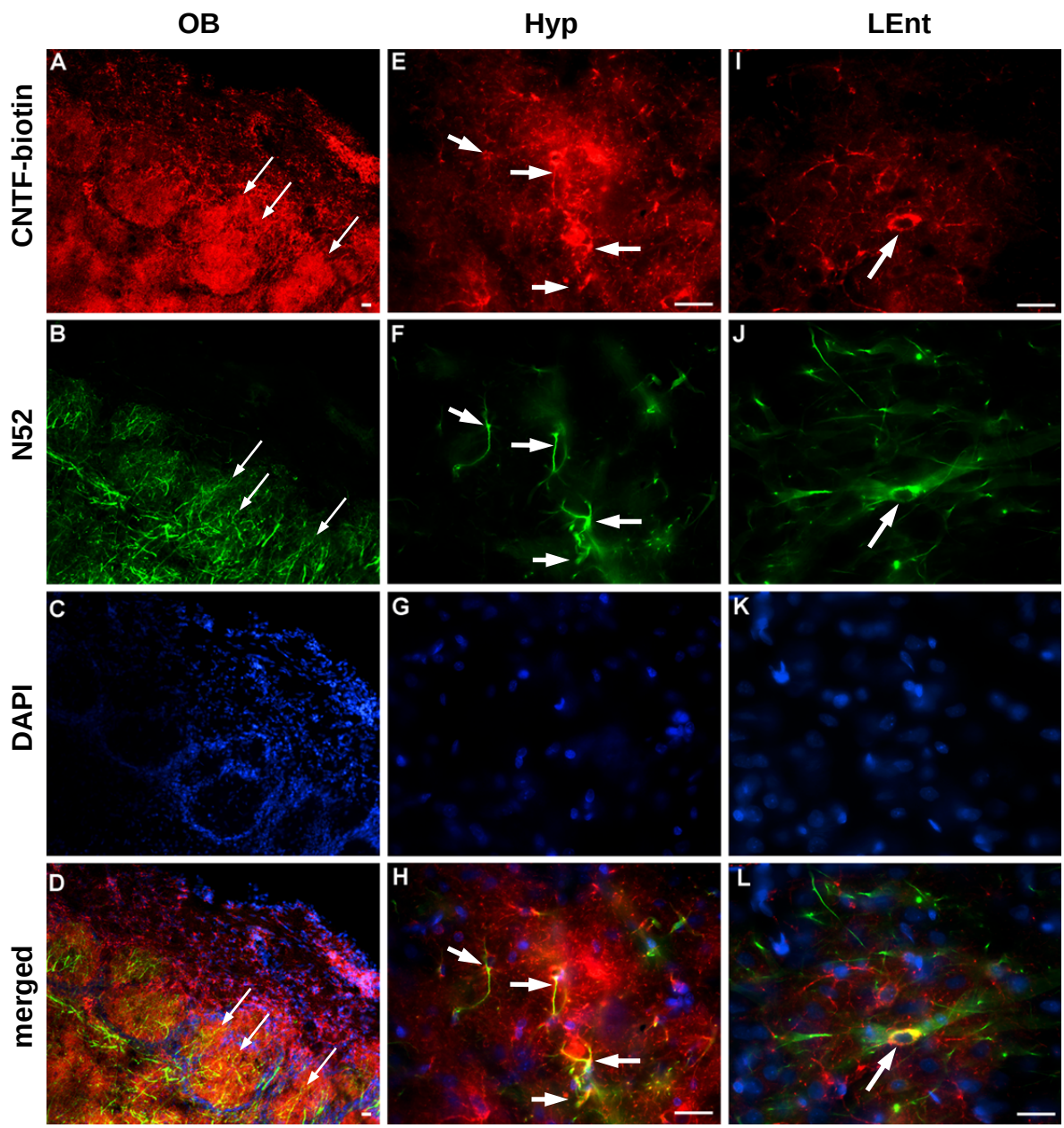
OB
Hyp
LEnt
CNTF-biotin
N52
DAPI
merged
A
B
C
D
E
F
G
H
I
J
K
L

Figure 2.5

Some intranasal delivered CNTF-biotin is localized within astrocytes of the Hyp (A-D) and LEnt (E-H) regions.

(A-D) CNTF-biotin (red) co-localized (yellow) with GFAP (green) within astrocytes (as shown by arrows in panels A, B and D) of the hypothalamus. **(E-H)** An astrocyte in the LEnt (arrowed cell in panels E, F and H) displayed co-localization (yellow) of CNTF-biotin (red) with GFAP (green). Cellular nuclei (shown in panels C and G) were counterstained with DAPI (blue). Scale bars= 25μm

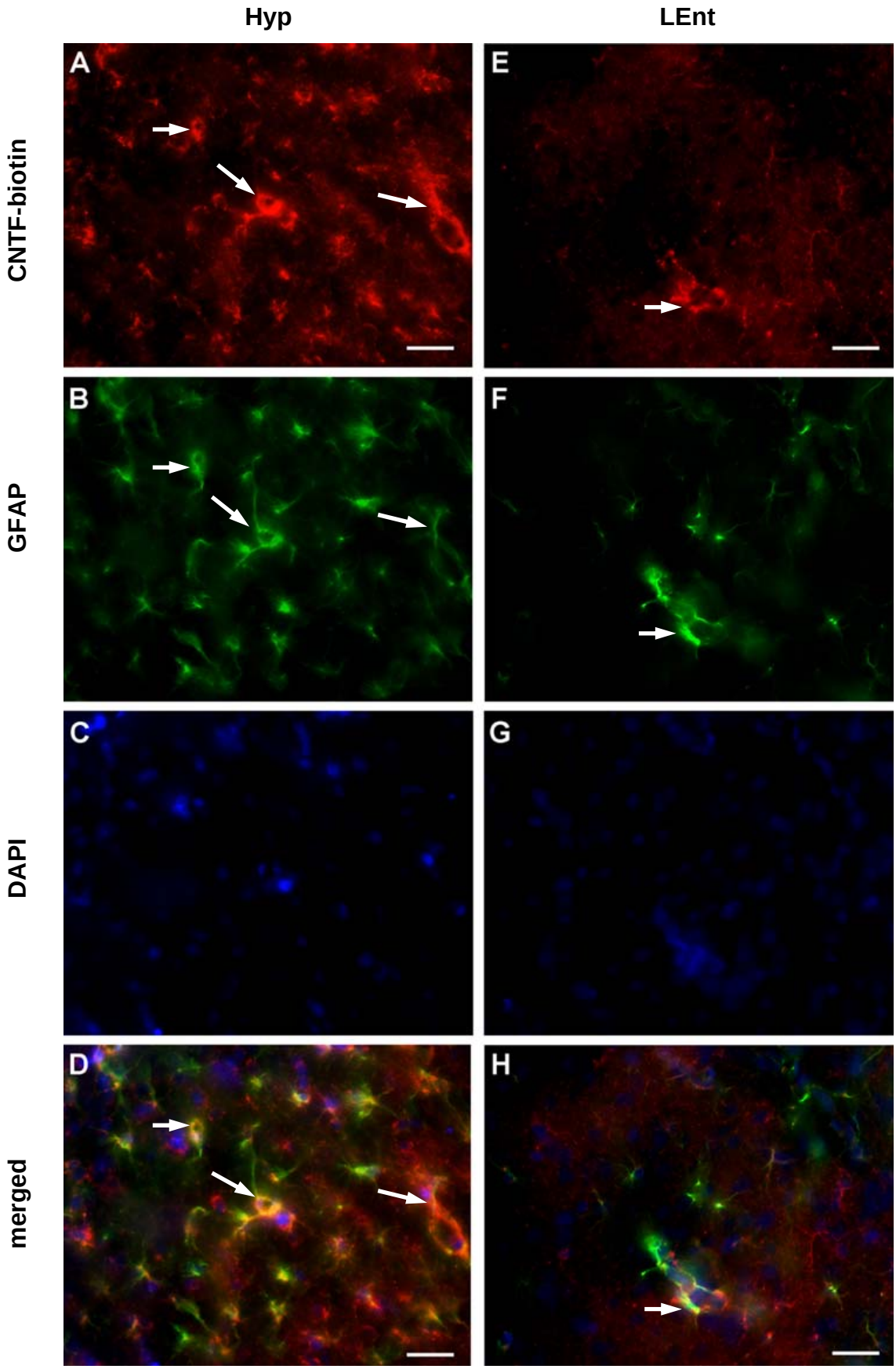
Hyp
LEnt
CNTF-biotin
GFAP
DAPI
merged
A
B
C
D
E
F
G
H

Figure 2.6

CNTF-biotin Cy3 fluorescence was detected in the spinal trigeminal nucleus and the cochlear nucleus of the cerebellum 30mins after intranasal inoculation into $ZnSO_4$-treated rats (A-F).

(A) spinal trigeminal nucleus (sp5); **(B)** Control section of spinal trigeminal nucleus from a BSA-biotin treated animal; **(C-D)** Low and high power images of neuronal cells displaying CNTF-biotin Cy3 fluorescence (arrowheads and arrows) within the spinal trigeminal nucleus. **(E-F)** Neuronal cells (arrowheads and arrows) within the ventral cochlear nucleus, anterior part (VCA). Cellular nuclei (blue) in sections displayed in panels **C-F** were counterstained with DAPI. Scale bars = 25μm. Images A-F correspond to the regions marked on Paxinos' coronal rat brain maps (Paxinos and Watson, 1998).

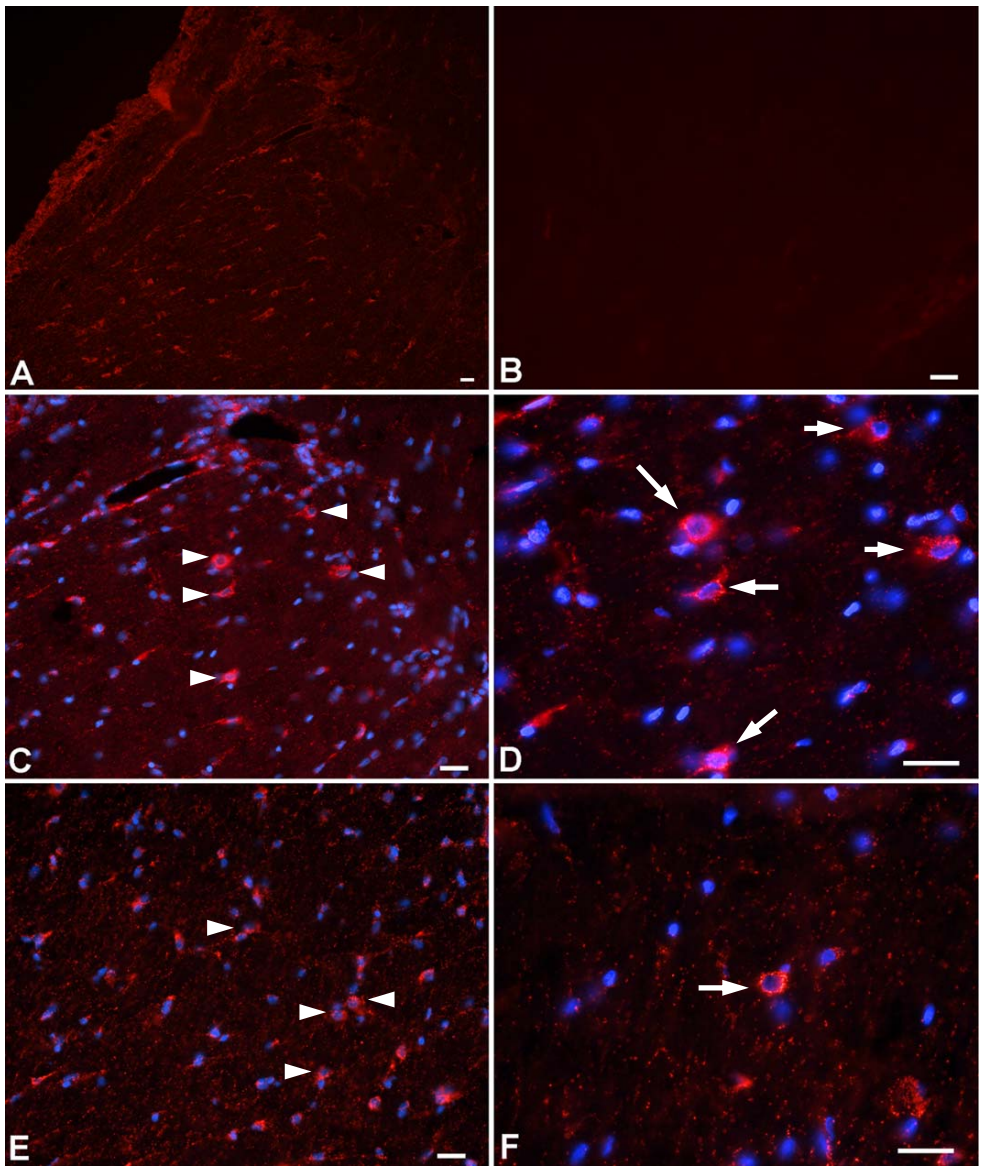

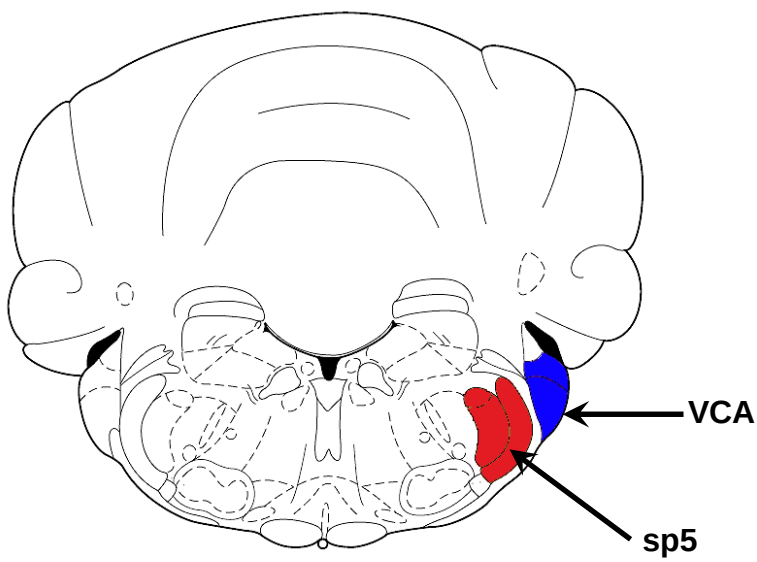

Bregma -10.52 mm, Paxinos and Watson, 1998

trigeminal region **(Fig.2,6 A,C & D)** displayed specific cytoplasmic fluorescence from CNTF-biotin. The anterior ventral cochlear region **(Fig.2.6 E-F)** also contained CNTF-biotin fluorescent neuronal cells. Cellular nuclei were identified by DAPI fluorescence.

Within the hypothalamic brain regions of the $ZnSO_4$-treated animals, specific CNTF-biotin fluorescence was localized in neuronal cells of the medial arcuate nucleus **(Fig.2.7 A-B and E)**. Specific CNTF-biotin fluorescence could also be observed within neurons of the ventromedial hypothalamic nuclei **(Fig.2.7 C-D)**. As seen previously, no specific fluorescence was present in the BSA-biotin control brain hypothalamic region **(Fig. 2.7 F)**.

2.4.4 pSTAT3 immunofluorescence in thalamic and hypothalamic sections 30mins after intranasal delivery of CNTF into SD rats.

To evaluate the molecular mechanisms and signalling pathways activated by intranasal delivery of CNTF and its localization within the hypothalamus, pSTAT3 antibody was used to identify positive pSTAT3 immunoreactive cells. In Sprague-Dawley rats (n=4), recombinant human CNTF induced phosphorylation of STAT3 in neurons of the thalamic and hypothalamic regions 30mins after intranasal delivery of the neurotrophin. Moderate levels of CNTF-induced pSTAT immunoreactivity were concentrated in neurons of the lateral hypothalamus (LH) **(Fig. 2.8 A-B)**. A small group of neuronal cells in the ventral posterolateral thalamic nucleus (VPL) **(Fig. 2.8 C-D)** exhibited positive pSTAT immunoreactivity following CNTF induction. Robust STAT3 activation was also observed in the ventromedial hypothalamic nuclei, dorsomedial part (VMHDM) **(Fig.2.8 G-H)** close to the hypothalamic arcuate nucleus. The paraventricular thalamic nuclei, posterior part (PVP) contained a small group of positive pSTAT3 immunoreactive neuronal cells **(Fig.2.8 E-F)**. In control

Figure 2.7

CNTF-biotin Cy3 fluorescence localized within neurons of the arcuate nucleus (Arc) and ventromedial hypothalamic nucleus (VMH) 30mins after intranasal inoculation into $ZnSO_4$ denervated rats (A-F).

(A & B) Hypothalamic arcuate nucleus medial part (ArcM), **(B)** positive neurons (arrows) in the ArcM, high power image of boxed area in **(A)** ; **(C & D)** CNTF-biotin Cy3 fluorescent neurons (arrowheads & arrows) within the ventromedial hypothalamic nucleus (VMH) ; **(E)** CNTF-biotin localized within arcuate nucleus, medial posterior part ; **(F)** Control section of arcuate nucleus from BSA-biotin intranasal delivered animal. **3V** = 3rd ventricle. Scale bars = 25μm. Images A-F correspond to the arrowed regions (ArcM and VMH) marked on Paxinos' coronal rat brain map (Paxinos and Watson, 1998).

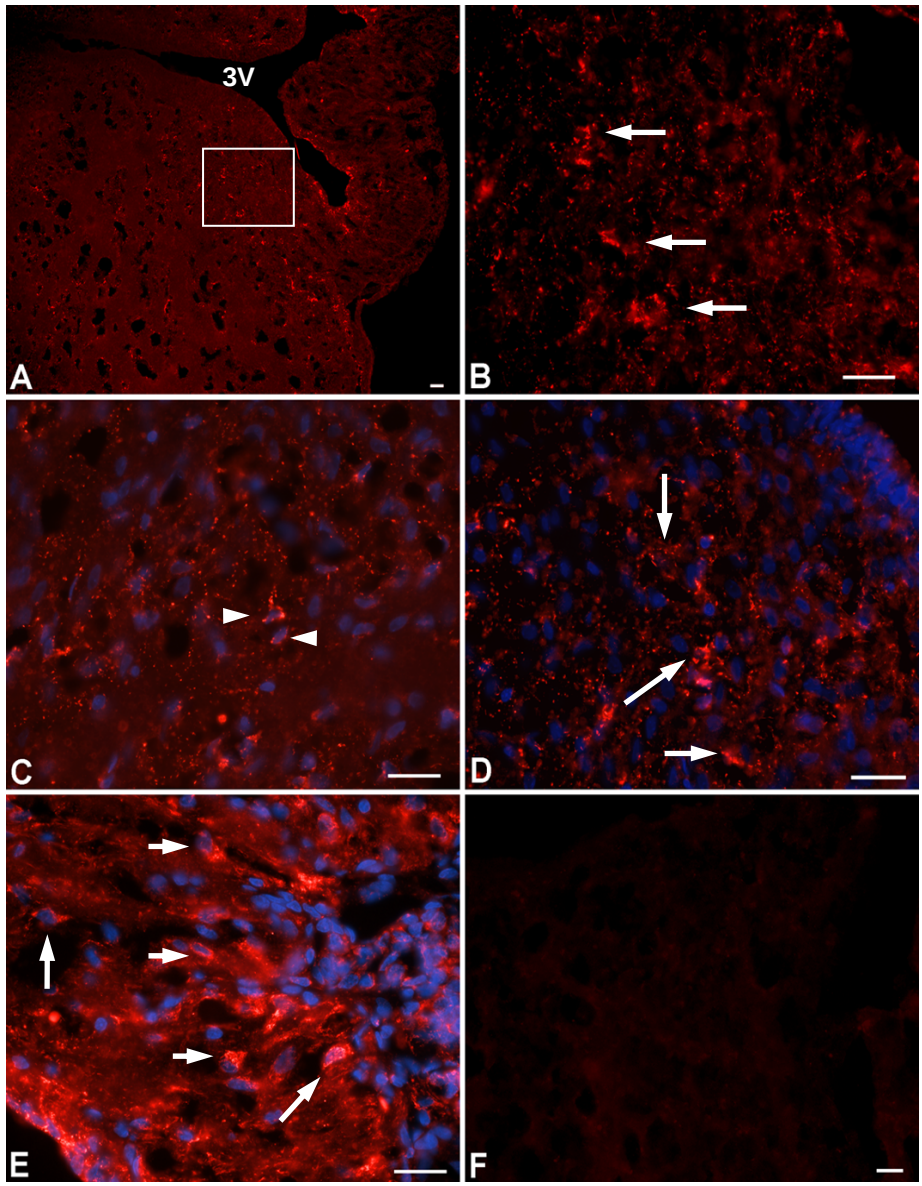

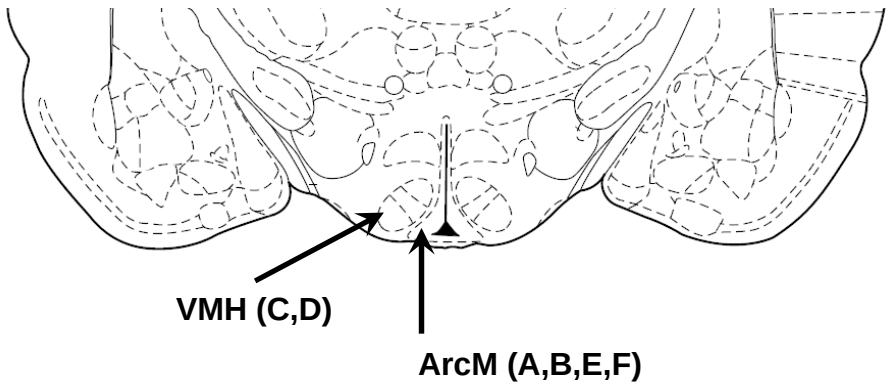

Bregma -2.80 mm, Paxinos and Watson, 1998

Figure 2.8

The localization of intranasal CNTF-induced phospho-STAT3 immunoreactive cells in the hypothalamus and thalamus (A-H).

Boxed regions in image panels **A, C, E & G** are enlarged in panels **B, D, F & H**.

(A & B) pSTAT3 immunoreactive cells in the lateral hypothalamus (LH, arrows); **(C & D)** Positive pSTAT3 cells in the ventral posterolateral thalamic nuclei (VPL, arrows); **(E & F)** pSTAT3 cells in the paraventricular thalamic nuclei, posterior part (PVP, arrows) ; **(G & H)** Positive pSTAT3 immunoreactive cells in the ventromedial hypothalamic nuclei, dorsomedial part (VMHDM, arrows). **(I)** No pSTAT3 immunoreactive cells present in control sections from a 1%BSA-treated animal. **(J)** No positive fluorescence seen in sections incubated in pre-immune serum. Scale bars = 25μm. Images A-J correspond to the regions marked on Paxinos' coronal rat brain map shown on the next overleaf page (Paxinos and Watson, 1998).

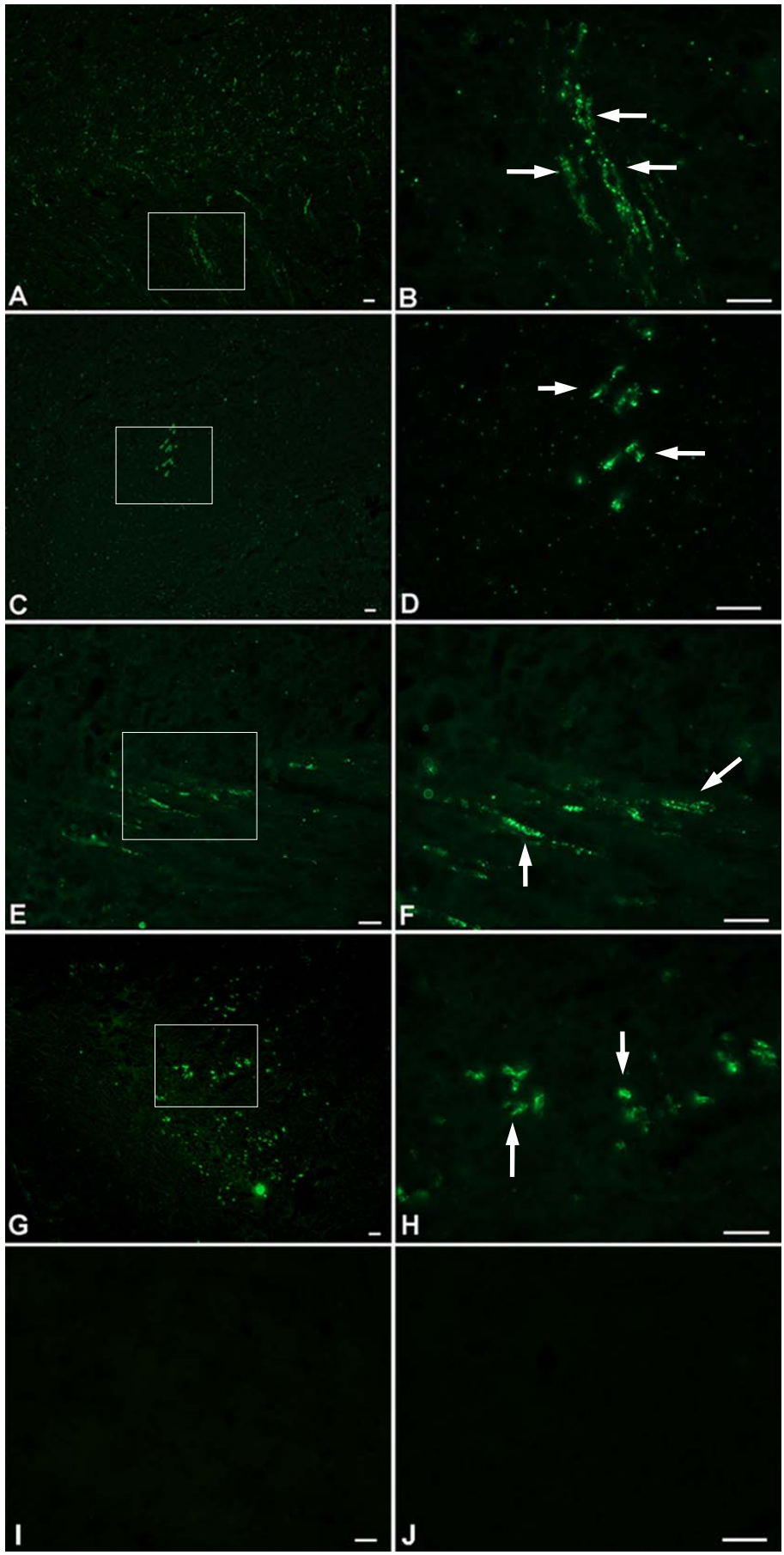
A
B
C
D
E
F
G
H
I
J

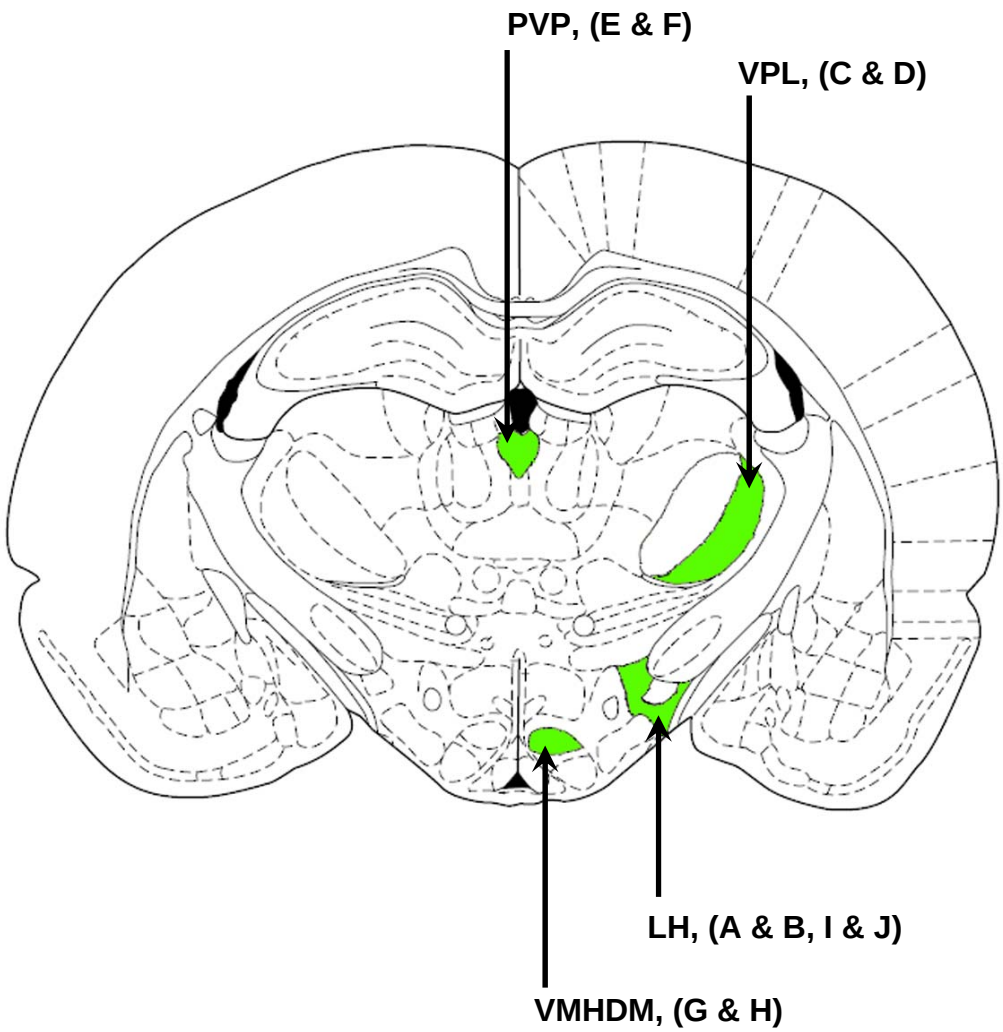

Bregma -3.14 mm, Paxinos and Watson, 1998

animals, intranasal delivered BSA failed to induce any phospho-STAT3 immunoreactivity in thalamic and hypothalamic brain regions **(Fig. 2.8 I)**. No positive fluorescence was seen in sections incubated in pre-immune serum instead of the primary antibody **(Fig. 2.8 J)**.

2.4.5 Temporal and spatial distribution of intranasal applied I^{125}-CNTF in rats.

During the time course from 30min to 24hr following nasal delivery of the I^{125}-CNTF, different brain regions from rostral to caudal displayed varying levels of radioactivity as measured by γ-radiation detection. Intranasal delivered CNTF, represented by I^{125}-CNTF, accumulated in various brain regions and also peripheral tissues. In comparison to the brain average cpm/mg of wet-weight tissue, levels of exogenous intranasal I^{125}-CNTF were significantly higher in the olfactory bulb, trigeminal nerve ($P<0.001$) and forebrain ($P<0.01$) up until 6hrs of the time course **(Fig. 2.9)**. The highest levels of I^{125}-CNTF in olfactory bulb, trigeminal nerve and forebrain compared to the overall brain average were recorded in the earliest time point of 0.5hr. Other brain regions such as the medulla and cervical spinal cord contained similar levels to the brain average.. Compared with the brain average, I^{125}-CNTF levels in other brain regions such as frontal cortex, parietal cortex, pons, hypothalamus/thalamus, cerebellum and hippocampus were the same **(Fig. 2.10)**.

The radioactivity associated with intranasal delivered I^{125}-CNTF was significantly higher in the blood compared to heart, lung, liver, muscle and CSF ($P<0.001$) during the later time-points, 6hr and 24hr **(Fig. 2.11)**. Comparing all peripheral tissue samples heart, lung, liver, muscle and CSF, there was no significance in the radioactivity detected between tissues. Overall, the levels of radioactivity in the CSF were low.

Figure 2.9

A timecourse of CNTF distribution in CNS and brain areas following intranasal delivery of I^{125}CNTF (29ng, $8X10^6$cpm) in 4 groups of rats corresponding to different timepoints, 0.5, 3, 6 and 24 hrs (n=4 per group).

Highest levels of exogenous I^{125}CNTF were detected in olfactory bulb, trigeminal nerve and forebrain. Levels of I^{125}CNTF were significantly higher in olfactory bulb, trigeminal nerve and forebrain compared to brain average. The radioactivity in other brain regions was not statistically different from the brain average, at all time points. Data are expressed as mean ± SEM. *, # : P <0.001 and +: P <0.01 vs brain average as determined by 2-way ANOVA with Bonferroni post-hoc test.

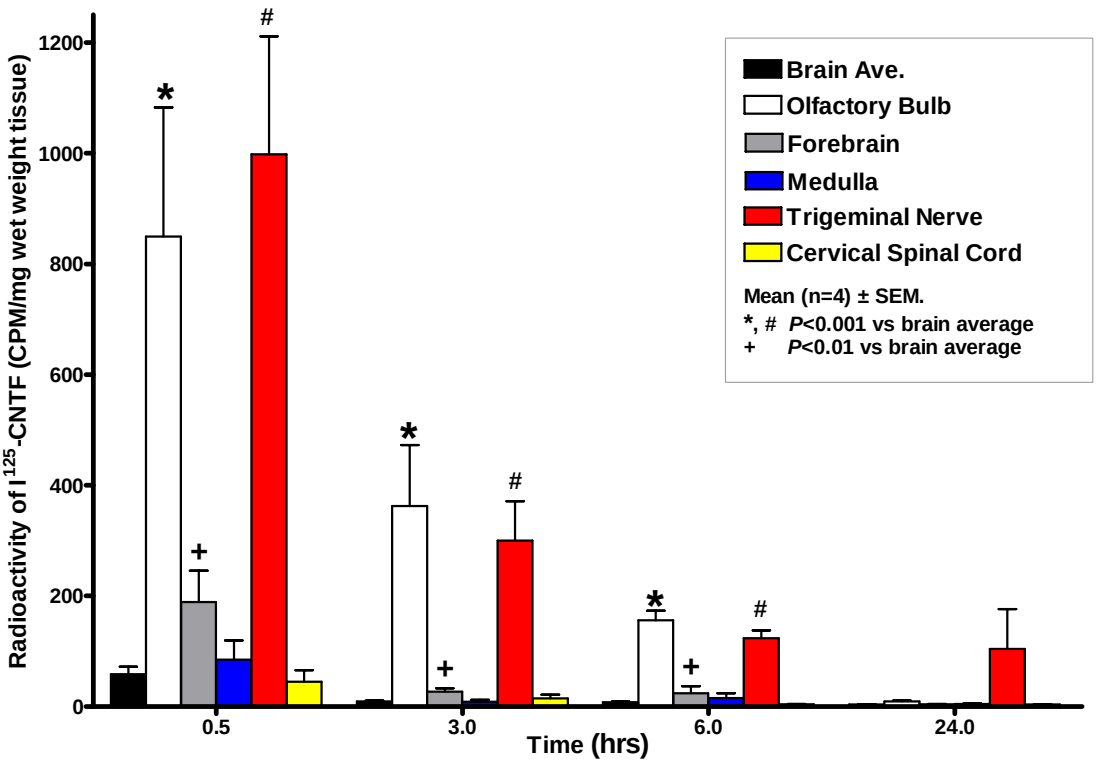
Radioactivity of I125-CNTF (CPM/mg wet weight tissue)
1200
1000
800
600
400
200
0
0.5
3.0
6.0
24.0
Time (hrs)
Brain Ave.
Olfactory Bulb
Forebrain
Medulla
Trigeminal Nerve
Cervical Spinal Cord
Mean (n=4) ± SEM.
*, # P<0.001 vs brain average
+ P<0.01 vs brain average

Figure 2.10

A timecourse (0.5, 3, 6 and 24hr) of CNTF distribution in brain areas following intranasal delivery of I^{125}CNTF (29ng, 8X10^6cpm) in 4 groups of rats (n=4 per group/timepoint).

There were no significant differences between brain areas listed and the brain average within each time group. Highest levels of I^{125}CNTF radioactivity were detected in brain regions of the 0.5hr group. Data represents mean ± SEM.

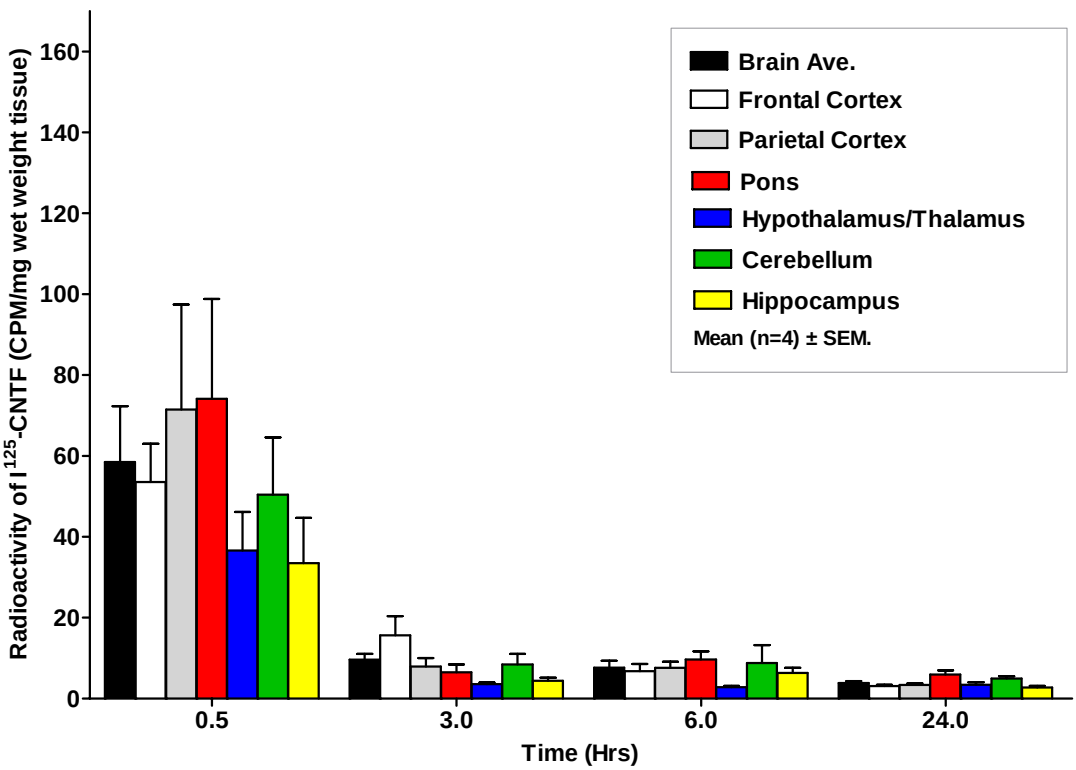
Brain Ave.
Frontal Cortex
Parietal Cortex
Pons
Hypothalamus/Thalamus
Cerebellum
Hippocampus
Mean (n=4) ± SEM.
Radioactivity of I125-CNTF (CPM/mg wet weight tissue)
0
20
40
60
80
100
120
140
160
0.5
3.0
6.0
24.0
Time (Hrs)

Figure 2.11

A timecourse (0.5, 3, 6 and 24hr) of CNTF content in blood and peripheral tissues following intranasal delivery of I^{125}CNTF (29ng, $8X10^6$cpm) in 4 groups of rats (n=4 per group/timepoint).

Levels of I^{125}-CNTF radioactivity in blood increases slightly over the timecourse. Data represent mean ± SEM. *, P <0.001 vs blood as determined by 2-way ANOVA with Bonferroni post-hoc test.

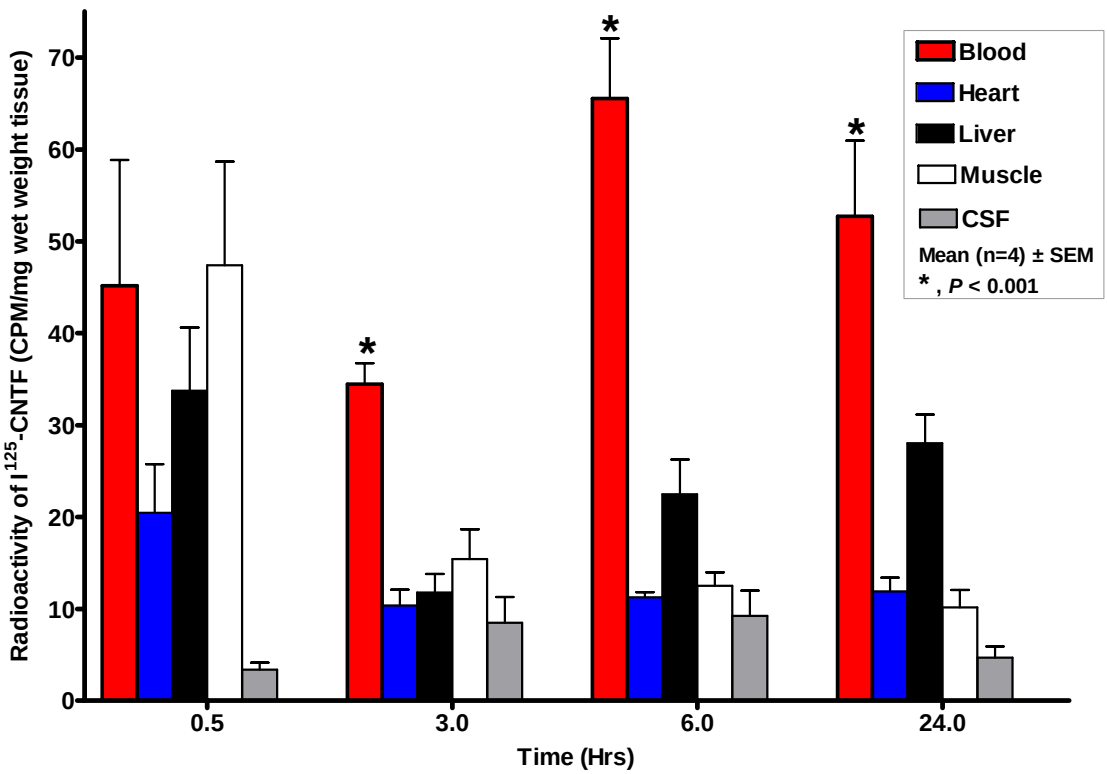
Blood
Heart
Liver
Muscle
CSF
Mean (n=4) ± SEM
*, P < 0.001
Radioactivity of I125-CNTF (CPM/mg wet weight tissue)
0
10
20
30
40
50
60
70
0.5
3.0
6.0
24.0
Time (Hrs)
*
*
*

2.4.6 Spatial distribution of intranasal applied I^{125}-CNTF in rats and effect of unlabelled CNTF.

To determine whether nasal CNTF transport to the olfactory bulb and brain occurs via a receptor mediated mechanism, I^{125} labelled CNTF was intranasally delivered together with 500 fold excess unlabelled CNTF (cold-CNTF) to a group of rats (n=4). Brain and olfactory tissues were collected 30min after delivery and a positive control group of rats (n=4) received an equal concentration of I^{125}-CNTF. In the olfactory bulb, highest levels of radioactivity were detected in the positive control I^{125}-CNTF group and there was a significant reduction in I^{125}-CNTF in the group treated with excess unlabelled CNTF (P<0.01) **(Fig 2.12)**. However, in the trigeminal nerve, there was no significant reduction of I^{125}-CNTF radioactivity as a result of excess unlabelled CNTF. This suggests that delivery of I^{125}-CNTF is competitively hindered by excess unlabelled CNTF in the applied solution. In the other brain regions, excess unlabelled CNTF had no obvious effect on CNTF radioactivity levels, except in the forebrain where there was a possible trend of reduction in I^{125}-CNTF radioactivity as a result of the excess unlabelled CNTF. Overall analysis of the treatment groups by 2-way ANOVA suggests that the effect of the treatment group is significant for all tissues (P< 0.001).

2.4.7 Effect of $ZnSO_4$ denervation of olfactory mucosa prior to I^{125}-CNTF intranasal application.

Zinc sulphate was used to disrupt the olfactory epithelium by ORN denervation in a group of rats (n=4) for 2 days prior to intranasal delivery of I^{125}-CNTF. A positive control group of rats (n=4) received only sterile saline 2 days before I^{125}-CNTF delivery. After analysis of the brain tissue radioactivity, there was a significant reduction in CNTF radioactivity in the $ZnSO_4$ treated group within the

Figure 2.12

Brain and peripheral tissue distribution of intranasal delivered I^{125}-CNTF containing 500 fold excess unlabelled CNTF, measured 30min after delivery.

Tissues from two different groups of rats (n=4) treated with either, I^{125}-CNTF (21.43 ng, $1.2X10^6$ cpm), or I^{125}-CNTF + unlabelled CNTF (10.7ug, n=4). Data are mean ± SEM. *, $P<0.01$, as determined by 2-way ANOVA with Bonferroni post-hoc test. I^{125}CNTF appears to be competitively hindered by excess unlabelled CNTF in the olfactory bulb **(Ob)**. **Bl**, Blood; **CSc**, cervical spinal cord; **Cb**, cerebellum; **Md/Pn**, medulla/pons; **Mb**, midbrain; **Fb**, forebrain; **Hy/Th**, hypothalamus/thalamus; **Hc**, hippocampus; **PCt**, cortex; **FCt**, frontal cortex; **Tg**, trigeminal nerve; **H**, heart; **L**, lung; **Liv** ,liver; **CSF**, cerebral spinal fluid.

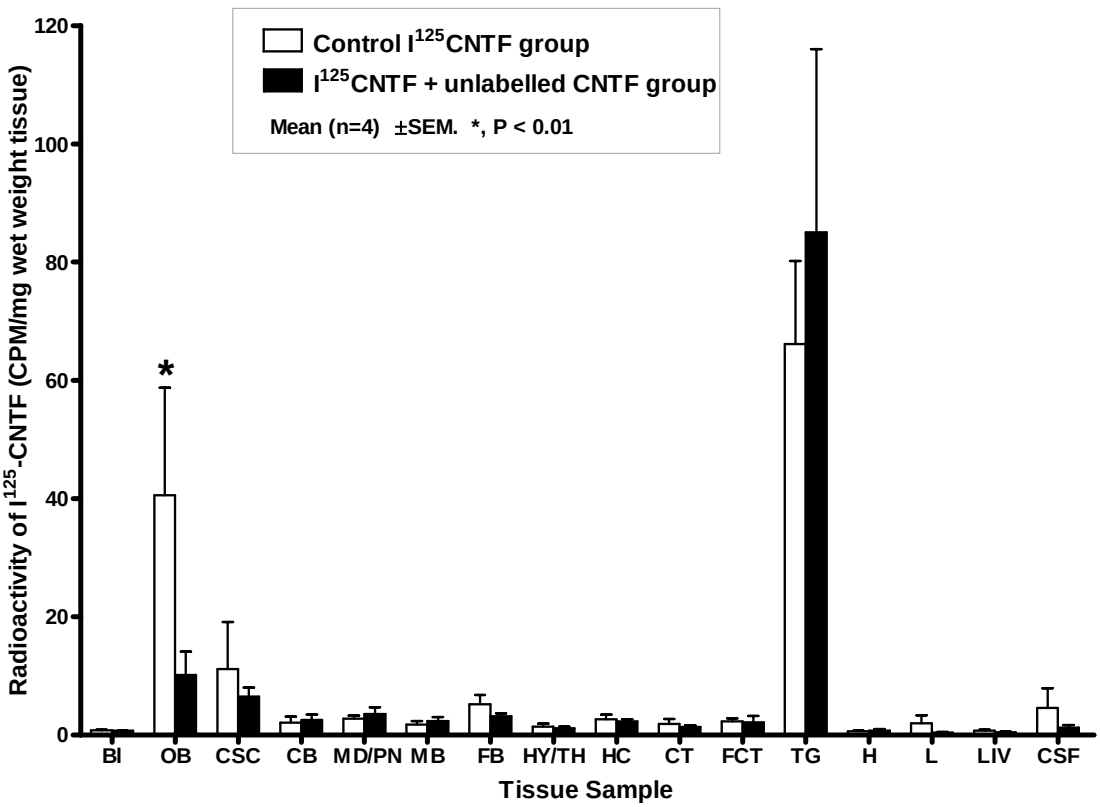
Control I125CNTF group
I125CNTF + unlabelled CNTF group
Mean (n=4) ±SEM. *, P < 0.01
Radioactivity of I125-CNTF (CPM/mg wet weight tissue)
120
100
80
60
40
20
0
*
Bl
OB
CSC
CB
MD/PN
MB
FB
HY/TH
HC
CT
FCT
TG
H
L
LIV
CSF
Tissue Sample

Figure 2.13

Brain and peripheral tissue distribution of intranasal delivered I^{125}-CNTF following denervation of olfactory mucosa by $ZnSO_4$ treatment.

I^{125}-CNTF uptake through the olfactory bulb appears to be significantly reduced by ORN denervation. Transport through the trigeminal nerve appears unaffected. Data are mean ± SEM. *, $P< 0.001$ as determined by 2-way ANOVA with Bonferroni post-hoc test. **Bl**, blood; **Ob**, olfactory bulb; **CSc**, cervical spinal cord; **Cb**, cerebellum; **Md/Pn**, medulla/pons; **Mb**, midbrain; **Fb**, forebrain; **Hy/Th**, hypothalamus/thalamus; **Hc**, hippocampus; **PCt**, cortex; **FCt**, frontal cortex; **Tg**, trigeminal nerve; **H**, heart; **L**, lung; **Liv** ,liver; **CSF**, cerebral spinal fluid.

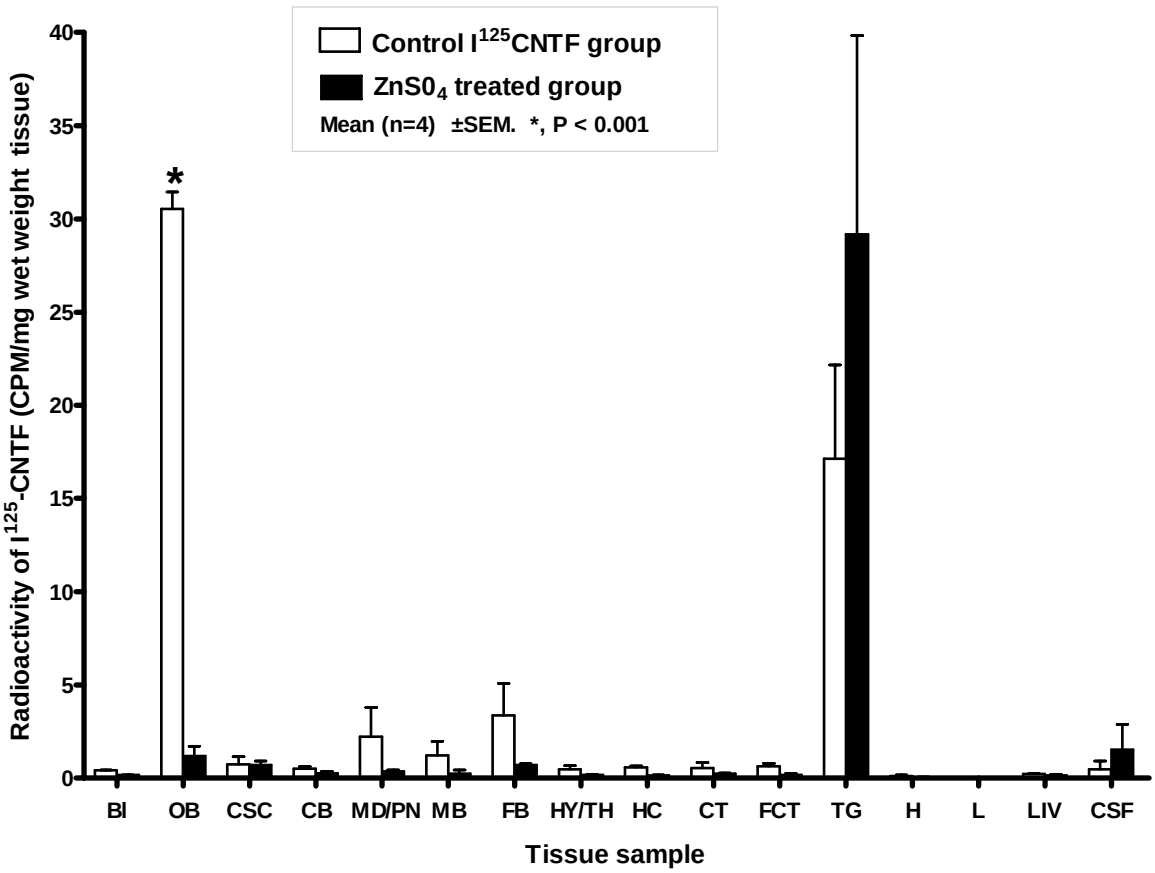
Control I125CNTF group
ZnS04 treated group
Mean (n=4) ±SEM. *, P < 0.001
Radioactivity of I125-CNTF (CPM/mg wet weight tissue)
40
35
30
25
20
15
10
5
0
*
BI
OB
CSC
CB
MD/PN
MB
FB
HY/TH
HC
CT
FCT
TG
H
L
LIV
CSF
Tissue sample

olfactory bulb ($P< 0.001$) **(Fig 2.13)**. Another brain region, such as the forebrain showed a trend of reduction in transported CNTF radioactivity in the $ZnSO_4$-treated group ($P< 0.05$), however, no reduction in transported CNTF occurred in the trigeminal nerve. From an overall analysis of the treatment groups by 2-way ANOVA, the effect of the treatment group (i.e. $ZnSO_4$- treated vs saline treated) is significant for all tissues ($P<0.0001$).

2.4.8 Reduction of body weight induced by intranasal delivered CNTF in obese Zucker rats

During the treatment period, daily intranasal inoculations of 0.06mg/kg/day rhCNTF caused significant weight loss in the (*fa/fa*) OZRs, compared to the vehicle control group **(Fig 2.14)** and **(Fig 2.15)**. In the pre-treatment period, average body weights of both groups of OZRs fluctuated over the nine days, however there was a gradual increase in average body weights **(Fig 2.14)**. Average body weights steadily decreased in the CNTF treated group over the 12 day treatment period, increasing slightly after cessation of treatment. The control group showed a steady increase in average body weight over the treatment period and continual increase after treatment ceased **(Fig 2.14)**. When both groups are compared as a percentage difference of body weight from the first day of treatment, there is a significant decrease in body weight in the CNTF treated group of about 3.5-4% from the Day 0 starting weight **(Fig 2.15)** ($P<0.01$). In comparison, the BSA control group significantly increased in body weight by 0.5-1.5% from Day 0. When the CNTF and BSA intranasal treatment ceased on Day 12, there were increases in percentage body weight change of approximately 0.5 % and 2.0 % for the CNTF and BSA groups respectively. When comparing individual animals, the most significant differences between the two groups were observed on Day 3 ($P<0.05$) and Days 6-15 ($P<0.01$). Overall, the

Figure 2.14

Intranasal treatment of obese (fa/fa) Zucker rats with either rhCNTF (0.06mg/kg/day, n=5) or BSA (1mg/mL, n=5) over a 12 day treatment period.

Body weight was measured daily before, during and after the intranasal treatment period. Average body weight for each group is compared over the pre and post treatment time period. Although average body weights fluctuate over the time period, there is an overall decreasing trend in the CNTF treated group. Data are mean ± SEM. *, $P< 0.01$; #, $P< 0.001$ as determined by 2-way ANOVA with Bonferroni post-hoc test.

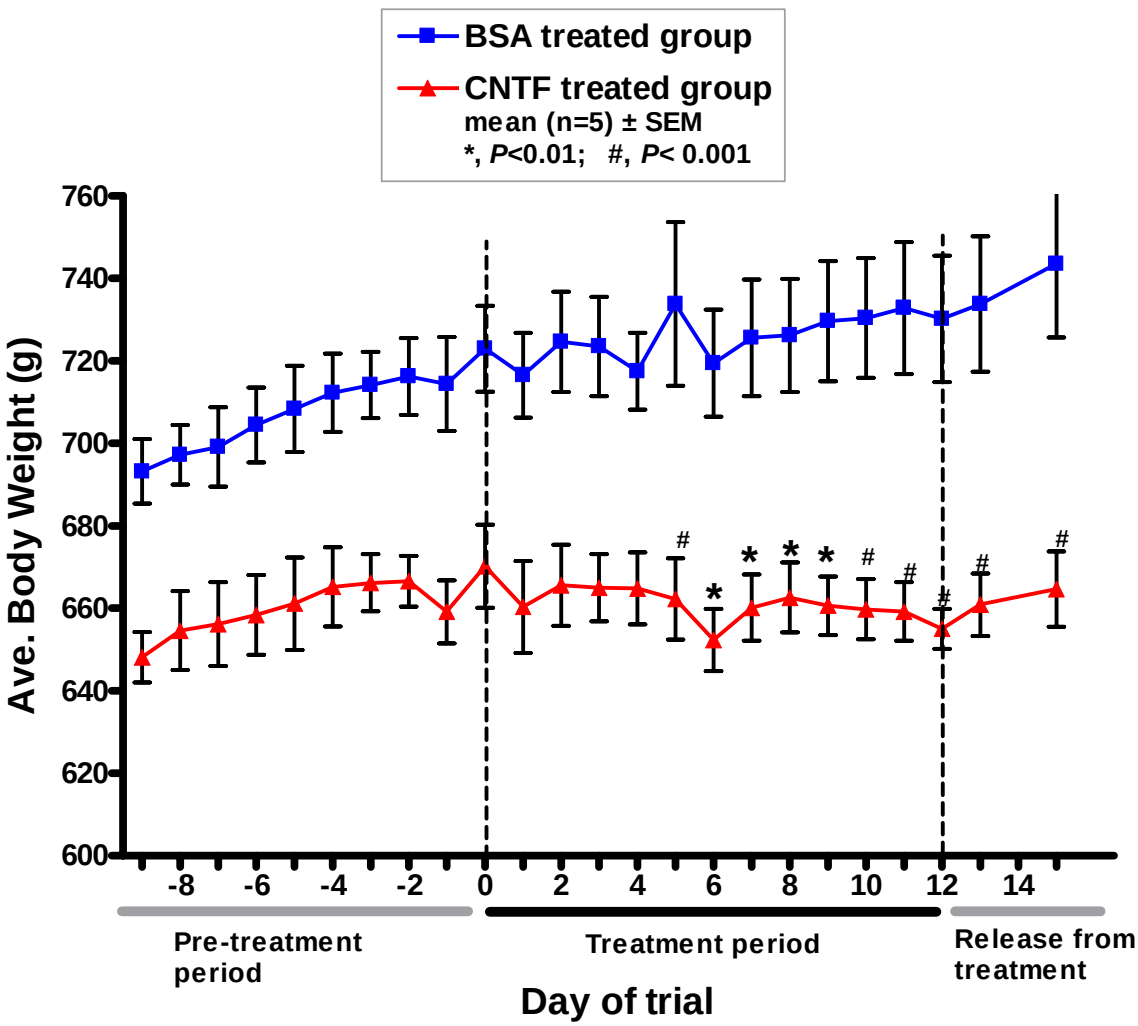
BSA treated group
CNTF treated group
mean (n=5) ± SEM
*, P<0.01; #, P< 0.001
Ave. Body Weight (g)
760
740
720
700
680
660
640
620
600
-8
-6
-4
-2
0
2
4
6
8
10
12
14
Pre-treatment period
Treatment period
Release from treatment
Day of trial

Figure 2.15

Effects of CNTF on body weight in genetically obese (fa/fa) Zucker rats.

Rats received daily intranasal doses of either vehicle BSA (1mg/mL) or human CNTF (0.06mg/kg) for a 12 day period, starting at day 0. Body weight was measured daily and is shown as the percentage difference from the original body weight on day 0. Data are mean ± SEM. *, $P<0.05$; **, $P<0.01$ as determined by 2-way ANOVA with Bonferroni post-hoc test.

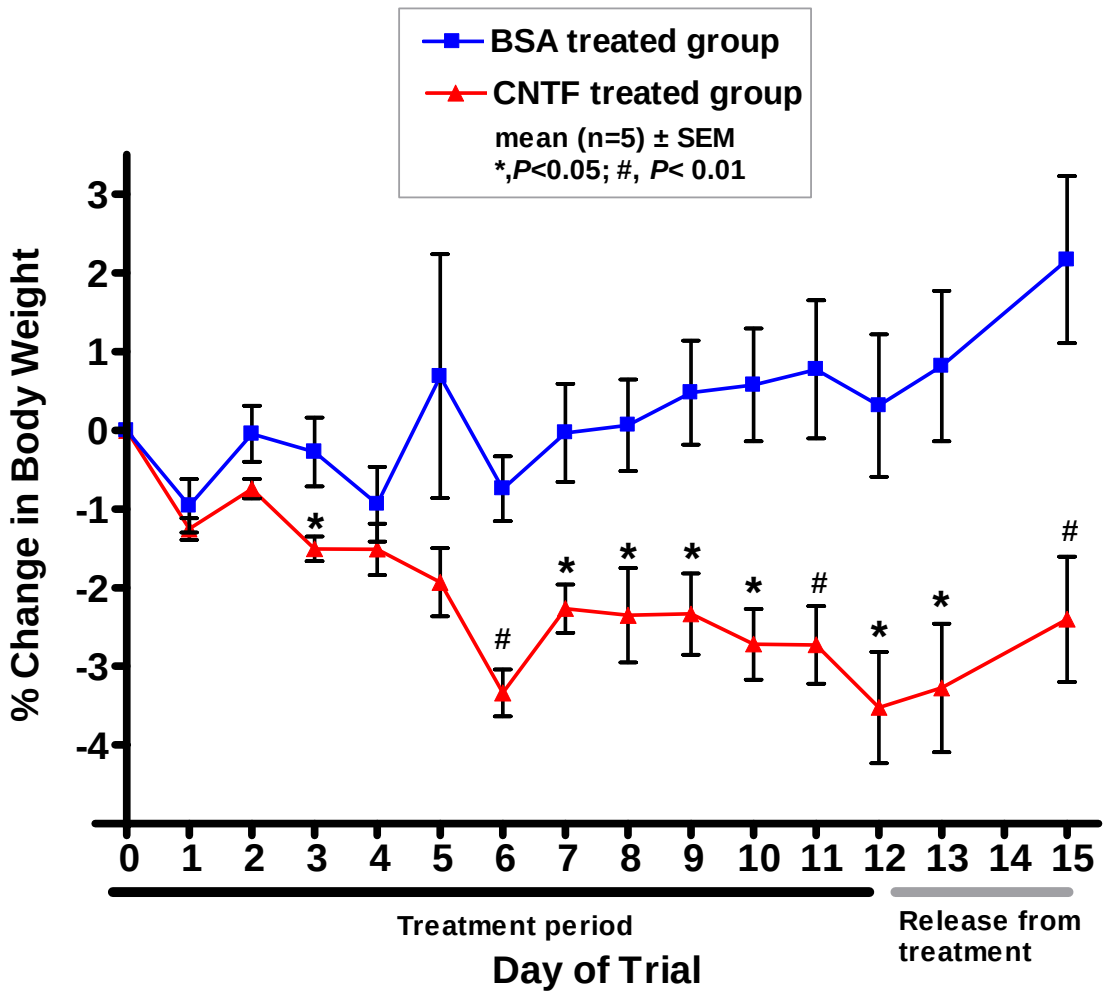
BSA treated group
CNTF treated group
mean (n=5) ± SEM
*,P<0.05; #, P< 0.01
% Change in Body Weight
3
2
1
0
-1
-2
-3
-4
0 1 2 3 4 5 6 7 8 9 10 11 12 13 14 15
Treatment period
Release from treatment
Day of Trial

Figure 2.16

Effects of CNTF on food intake in genetically obese (fa/fa) Zucker rats.

Rats received daily intranasal doses of either vehicle BSA or human CNTF (0.06mg/kg) for a 12 day period, starting at day 0. Percentage change in food intake was measured daily over a 13 day period. Data are mean ± SEM.

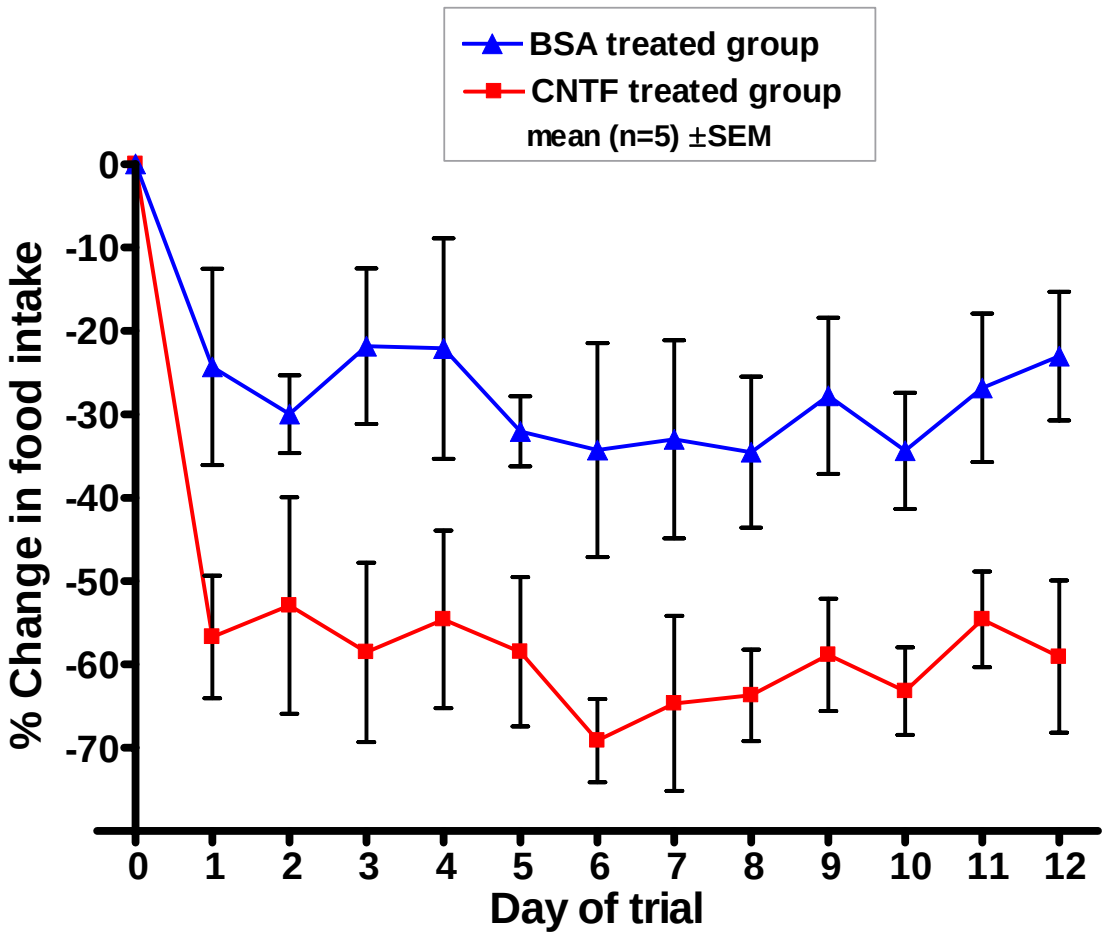
BSA treated group
CNTF treated group
mean (n=5) ±SEM
% Change in food intake
0
-10
-20
-30
-40
-50
-60
-70
0
1
2
3
4
5
6
7
8
9
10
11
12
Day of trial

treatment results in a significant effect between the two groups over the time period ($P<0.01$).

The amount of food intake was measured semi-quantitatively over a 24hr period each day and was expressed as the percentage change in food intake compared to Day 0 of the trial **(Fig 2.16)**. Although there was a large error variation within the groups, the overall trend appeared to be a greater percentage reduction in food intake in the CNTF treated compared to the BSA treated group. By Day 7 of the treatment period, the trend suggested that the CNTF treated group had reduced their overall food intake by approximately 70% compared to their intake on Day 0. The BSA treated group showed a 35% reduction in overall food intake. Therefore the CNTF treated group showed an overall trend of reduced food consumption by 35% compared to the BSA treated group.

2.4.9 Summary

In summary, biotinylated CNTF localized in rat olfactory, cortical and forebrain regions 30mins after intranasal delivery and in other rostral and caudal brain regions 2hrs after delivery. Highest levels of I^{125}-CNTF radioactivity accumulated in olfactory bulb, forebrain and trigeminal nerve after 30mins, and persisted in olfactory bulb and trigeminal nerve up to 6hrs following delivery. Other brain regions contained levels of I^{125}-CNTF radioactivity similar to a brain average. In a separate experiment, excess unlabelled CNTF reduced I^{125}-CNTF radioactivity in the olfactory bulb but not in the trigeminal nerve. $ZnSO_4$ denervated olfactory mucosa did not affect transport of CNTF-biotin to hypothalamic arcuate, ventromedial hypothalamic, ventral cochlear and trigeminal nuclei regions. However $ZnSO_4$ denervation reduced I^{125}-CNTF radioactivity in the olfactory bulb but not in the trigeminal nerve. Activated pSTAT3 was observed in thalamic and hypothalamic

regions after CNTF-biotin delivery. Finally intranasal treatment with CNTF reduced body weight and food intake in an OZR model.

2.5 Discussion

This study has demonstrated that intranasal administration of the neurotrophic factor CNTF results in rapid transport of the protein to multiple brain regions within 30 mins from the start of intranasal delivery. The transported CNTF was biologically active and able to activate STAT3 pathways in hypothalamic neurons. The biologically active CNTF was also able to activate hypothalamic satiety pathways and cause body weight loss in a genetically obese rodent model.

From the radioactive tracing data, it appears that CNTF is transported to the brain via two distinct routes. The two main pathways proposed for direct transport of proteins from the nasal epithelium to the brain are the intracellular and extracellular neuronal routes (Shipley, 1985; Balin et al., 1986; Thorne et al., 1995; Thorne et al., 2004). It is believed that the intracellular transport pathway requires several hours, with protein transport time of 6 hrs in mice (Broadwell and Balin, 1985). Protein transported via the intracellular pathway may be subjected to either receptor-mediated endocytosis into olfactory receptor neurons followed by transcytosis to the olfactory bulb, or non-specific fluid-phase endocytosis into ORN and subsequent intracellular transport to olfactory bulb. However, protein transport via the extracellular pathway occurs rapidly within minutes as peptides travel through open intercellular clefts in the olfactory epithelium and subsequent diffusion into the olfactory bulb or subarachnoid space (Balin et al., 1986; Thorne et al., 2004).

Following intranasal delivery, biotinylated CNTF was localized in several brain regions at 30mins and 2hrs after delivery. As seen in previous studies with different transported proteins, CNTF appeared to be localized in the cellular cytoplasm of neuronal cells within the olfactory bulb, anterior olfactory nucleus, entorhinal cortex, endopiriform cortex, lateral hypothalamus, cerebellum and

trigeminal nucleus **(Fig 2.2, 2.3 & 2.6)**. However further immunofluorescence experiments, involving double-labelling with antibodies to specific neuronal markers, would be required to confirm localization within neuronal populations. The rapid appearance of the biotinylated-CNTF within several rostral brain regions 30 mins after intranasal delivery is consistent with a transport pathway utilizing the peripheral olfactory and trigeminal routes as proposed by Thorne et al.(Thorne et al., 1995; Thorne et al., 2004). CNTF also co-localized with a neurofilament marker N52 within the OB, hypothalamus and lateral entorhinal cortex **(Figs. 2.4)**. In the OB, positive N52 stain and its co-localization with CNTF-biotin positive neurons was only observed in the glomerular and deeper OB layers, not in the outer OB neural layer. This occurred because N52 antibody only recognizes high molecular weight neurofilaments associated with myelinated axons (Lawson and Waddell, 1991; Michael and Priestley, 1999), which are not present in the OB neural layer. The co-localization of CNTF-biotin with GFAP within hypothalamic and cortical regions **(Figs. 2.5)** indicates that the intranasal CNTF is present in astrocytes, which express CNTF receptors (Lee et al., 1997).

The use of $ZnSO_4$ to disrupt the olfactory epithelium did not interfere with the transport of biotinylated-CNTF from the nasal cavity to areas of the cerebellum, trigeminal nucleus and hypothalamus **(Figs. 2.6 & 2.7)**, which would have most likely occurred via the extracellular route. Both sensory trigeminal nuclei and anterior ventral cochlear regions of the cerebellum displayed specific cytoplasmic fluorescence within neuronal cells. Although other studies have demonstrated that i.n. delivered vasoactive intestinal peptide (Gozes et al., 1996; Dufes et al., 2003) results in higher CNS concentrations near the brainstem, the precise mechanisms of this caudally directed CNS transport have not been fully examined. It is possible that i.n. delivered protein may gain access to the olfactory subarachnoid space CSF and

be distributed along the ventral surfaces of the brain, eventually being sequestered near the brainstem and cerebellum (Thorne et al., 2004). Extracellular transport of biotinylated-CNTF from the $ZnSO_4$ disrupted olfactory epithelium to hypothalamic regions seems evident with specific fluorescence observed in cells of the medial arcuate and ventromedial hypothalamic nuclei. The rapid transport of CNTF to hypothalamic satiety centers such as the arcuate and ventromedial hypothalamic nuclei is significant considering many studies using the anti-obesogenic properties of CNTF targeting this region.

Intranasal administration of recombinant human CNTF increased STAT3 phosphorylation in the hypothalamus, close to the arcuate nucleus (Arc). Using immunofluorescence, phosphorylated STAT3 immunoreactive cells were observed in the lateral hypothalamus (LH), ventromedial hypothalamic nuclei (VMH), ventral posterolateral thalamic nuclei (VPL) and the paraventricular thalamic nuclei (PVP) **(Fig. 2.8)**. Localization of CNTF-induced pSTAT3 immunoreactive cells in the LH, VMH and Arc follows previous studies which demonstrate CNTF-induced pSTAT3 activation in hypothalamic satiety centres (Gloaguen et al., 1997; Lambert et al., 2001; Anderson et al., 2003). As these nuclei are involved in the regulation of satiety and energy metabolism, the activation of the STAT pathway by CNTF may result in weight loss in obesity conditions.

Following intranasal delivery of I^{125}-CNTF, quantitation of radioactivity detected revealed that the highest levels of I^{125}CNTF radioactivity, as indicated by CPM/mg I^{125}-CNTF compared to the brain average, accumulated rapidly in the olfactory bulb, forebrain and trigeminal nerve in all rats at the 30 min time-point. Higher levels of I^{125}-CNTF radioactivity persisted within these brain regions throughout the 24hr time course. These results are consistent with previous studies by Thorne et al. who demonstrated an extracellular pathway of rapid transport of

peptides from the olfactory epithelium to the brain via peripheral olfactory and trigeminal routes (Thorne et al., 1995; Frey 2nd et al., 1997; Thorne et al., 2004). Other rostral and caudal brain regions contained the same levels of accumulated I^{125}-CNTF radioactivity as the overall brain average. Peripheral tissues including blood contained varying levels of I^{125}-CNTF radioactivity as a result of I^{125}-CNTF gaining access to the bloodstream via the nasal respiratory mucosa. Only low levels of CNTF radioactivity were detected in the CSF samples which may suggest a possible participation in the overall transport process. Potential transport via the CSF from entry points in the olfactory epithelium is a clear possibility as other proteins and peptide molecules have been shown to gain access to the CSF following i.n. delivery (Born et al., 2002; Banks et al., 2004; Charlton et al., 2008).

When excess unlabelled CNTF was introduced into the I^{125}-CNTF solution which was intranasally administered to a separate group of rats, there was a significant decrease in I^{125}-CNTF radioactivity in the olfactory bulb exclusively. The excess unlabelled CNTF would have competed for receptor binding sites in the olfactory epithelium, reducing the intracellular transport of I^{125}-CNTF from the ORN's to the olfactory bulb. However the transport of I^{125}-CNTF from the olfactory epithelium to the trigeminal nerve was unaffected, suggesting that CNTF transport via the trigeminal nerve is not receptor mediated, but likely via extracellular pathways as suggested by Thorne et al. (Thorne et al., 2004). On the other hand, the reduction in total counts in olfactory bulb by unlabelled CNTF compared with a labeled I^{125}-CNTF group, may suggest that CNTF internalization and transport to the olfactory bulb via ORNs is receptor mediated.

This assumption was further supported by the ORN ablation experiment. Deafferentation of the olfactory neuro-epithelium with intranasal $ZnSO_4$ resulted in an almost total abolition of I^{125}-CNTF accumulation in the olfactory bulb and several

other brain regions including the forebrain, medulla, pons, hippocampus and midbrain, indicating that intact ORNs are essential for the transport of CNTF to the olfactory bulb and related brain structures. However, transport of I^{125}-CNTF via the trigeminal nerve appeared to be unaffected, indicating the accumulation of CNTF in the trigeminal nerve and related structures does not require the intact ORNs. Although previous studies have shown a species variation between rats and mice in the efficacy of this treatment (Slotnick et al., 2000; McBride et al., 2003), the rats in this study received two consecutive treatments of intranasal $ZnSO_4$ irrigation over two days before I^{125}-CNTF delivery. Therefore this result further supports the view that transportation of CNTF via the trigeminal route is predominantly through the extracellular pathway. However, with the degeneration of the olfactory epithelium, including loss of axons, hypertrophy of astroglial cell processes, proliferation of phagocytic cells and other cellular rearrangements, it may also be possible that the extracellular route to the brain could be blocked. Therefore an independent analysis of the olfactory perineural space would be required to assess its cellular structure. Although these results seem to be consistent with studies demonstrating a rapid extracellular peripheral olfactory and trigeminal route, one cannot fully rule out the contribution of the vascular route and extra control experiments involving IV injection of I^{125}-CNTF would be required at the time-points examined.

CNTF is known to be retrogradely transported by primary sensory and motor neurons (Curtis et al., 1993). This study is the first to have demonstrated that CNTF may also be anterogradely transported by ORNs. However, the physiological significance of anterograde transport of CNTF is not yet clear. It is known that ORNs express CNTF (Langenhan et al., 2005) and CNTF receptors (Lee et al., 1997; Young et al., 1997). Therefore CNTF may participate in the proliferation and differentiation of ORN which undergo constant neurogenesis during the postnatal life

(Mackay-Sim and Chuah, 2000). It may also act, like brain derived neurotrophic factor (BDNF) which is anterogradely transported by neurons (Zhou and Rush, 1996), to promote synaptic plasticity in nerve terminals (Lu, 2003).

To examine the biological activity of intranasally administered rhCNTF, we monitored its anti-obesogenic properties in a genetically obese rat model, the (*fa/fa*) OZR. Previous studies have focused on CNTF mediated weight loss in leptin-resistant mouse models of obesity, namely the *db/db* and *ob/ob* mice, and diet-induced obesity (DIO) mouse models (Gloaguen et al., 1997; Lambert et al., 2001; Anderson et al., 2003). The CNTF-mediated weight loss is a practical measurement to look at the function of intranasally delivered CNTF in the brain, in particular in the hypothalamus. Currently there are no studies assessing weight loss in a genetically obese rat model using CNTF. Over the 12 day treatment period the CNTF treated OZR group, receiving intranasal doses of 0.06mg/kg/day rhCNTF, lost a significant amount of body weight when compared to the vehicle BSA treated control group. The 4% overall percentage weight loss from starting weight in the CNTF treated group is comparable to that reported by Lambert *et. al*. who observed a similar weight loss in *ob/ob* mice using 0.1mg/kg/day of the modified $CNTF_{AX15}$ (AXOKINE) (Lambert et al., 2001). $CNTF_{AX15}$ (AXOKINE) is a truncated form of CNTF with the last 15 c-terminal amino acids removed, plus amino acid substitutions Glu63→ Arg and Cys17→ Ala, giving rise to a more potent, stable and soluble molecule (Panayotatos et al., 1993). Gloaguen *et.al.* achieved significant weight loss in *db/db* and *ob/ob* mice using 2-50 μg/mouse daily doses of a modified human CNTF super-agonist variant called DH-CNTF (Di Marco et al., 1996; Gloaguen et al., 1997). As seen in previous studies CNTF mediated weight loss is dose dependent. It is anticipated that a greater weight loss would have been observed in the Zucker rats if higher rhCNTF doses over a longer treatment period was used.

However, higher doses of intranasal administered rhCNTF may have been absorbed into the blood via the respiratory mucosa, eventually crossing into the brain via a saturable mechanism (Pan et al., 1999). Lambert's study found that subcutaneous injected $CNTF_{AX15}$ at 0.03mg/kg/day in mice resulted in little effect on overall weight loss. In our study, the weight loss resulting from the 0.06mg/kg/day intranasal dose of rhCNTF is most likely due to intracellular olfactory or extracellular trigeminal transported rhCNTF rather than blood absorbed rhCNTF, as the level of radioactivity in the blood and peripheral tissues was much lower than specific brain regions such as olfactory bulb and forebrain. However only an experiment using s.c. or i.v. injected 0.06mg/kg/day rhCNTF in a separate group of OZRs would confirm this. The OZRs seemed to tolerate the intranasal delivered rhCNTF treatment well with no adverse side effects. When comparing the overall percentage reduction in food intake between the two groups over the treatment period, the rhCNTF OZR group appeared to have a 55% reduction in food consumption by day 7, compared to day 0 of the treatment period. Although there is no statistical significance between the OZR groups due to a large animal variation, an overall trend in reduced food consumption can be seen in the rhCNTF treated group.

2.6 Conclusions

Overall, these results suggest that intranasal delivered CNTF is rapidly transported from the nasal cavity to several rostral brain regions via both olfactory and trigeminal pathways. It appears that although a large proportion of the exogenous CNTF is transported via an extracellular route through the peripheral trigeminal nerve complex, some of the CNTF may be endocytosed by ORNs and transported to the olfactory bulb and brain via intracellular/axonal transport. The intranasal delivery of CNTF to regions of the brain was accompanied by possible activation of presumptive satiety pathways in the hypothalamus through phosphorylation of STAT3. This activation correlated with an overall body weight loss in an obese rat model, which provides evidence that the intranasal delivered rhCNTF reached hypothalamic target sites functionally intact. Although several studies have shown that $CNTF_{AX15}$ inhibits appetite and reduces body weight via a leptin-like pathway, the subcutaneous or intravenous administration of this drug may illicit unwanted immune response with high levels of anti-$CNTF_{AX15}$ antibodies as seen in recent clinical trials (Ettinger et al., 2003). Therefore intranasal delivery of rhCNTF or AXOKINE may be a more effective, safer and non-invasive method of delivering this drug in weight loss trials, targeting the brain by avoiding the BBB.

CHAPTER 3

VIRAL VECTOR GENE DELIVERY OF ENHANCED-GFP TO THE BRAIN VIA THE OLFACTORY PATHWAY: A FEASIBILITY STUDY

3.1 Summary

Non-invasive delivery of therapeutic gene products into the brain is a critical step towards a feasible gene therapy for neurological diseases. From axonal transport research, it is tempting to speculate that macromolecules such as viral vectors and neurotrophic factors can be delivered into the brain by neurons spanning the blood brain barrier (BBB). Specifically, therapeutic viral vector gene products can be transported into the brain via the olfactory receptor neurons (ORNs). In this section, I investigated the temporal and spatial expression of Enhanced Green Fluorescent Protein (EGFP) transferred by a single dose nasal delivery of either a recombinant adenovirus vector (Ad5CMV-EGFP) or adeno-associated vector (AAV2-EGFP) into Sprague-Dawley rats. Robust EGFP expression was localized in ORNs throughout the olfactory epithelium after 24 hours. EGFP in the ORNs was anterogradely transported along their axons to the olfactory bulb and transferred in glomeruli to second-order neurons, mitral and tufted cells. EGFP was transferred to several brain regions including the lateral entorhinal cortex, amygdala, CA2/CA3 regions of hippocampus, thalamus, striatum, cerebellum and pontine raphae nucleus after 7 days. EGFP expression co-localized with Olfactory Marker Protein (OMP) and was confirmed with EGFP immunofluorescence labeling and Western blotting. Similar distribution patterns of EGFP in the brain were observed after 2 months in animals receiving AAV2-EGFP. However EGFP mRNA was detected by RT-PCR in the olfactory mucosa only. This simple and non-invasive gene delivery method provides ubiquitous macromolecule expression throughout the rodent brain.

3.2 Introduction

Delivery of genes that express neurotrophic factors, polypeptides or other therapeutic enzymes into the brain may be beneficial for a number of neurological diseases, such as Alzheimer's disease, Parkinson's disease and lysosomal storage disorders. In recent years, a number of studies attempt to protect neurons from degeneration by delivering therapeutic genes into the brain using a variety of viral and non-viral vectors (Barkats et al., 1998; Marr et al., 2003; Miana-Mena et al., 2004). However, most of the therapeutic genes are delivered into the brain via an invasive method of intracerebral or intraventricular injections (Bemelmans et al., 2006).

Intranasal administration provides a non-invasive alternative to established administration routes (e.g. intravenous, subcutaneous and intramuscular) for the systemic delivery of therapeutic molecules, such as proteins and viral vectors. As a method of effectively bypassing the BBB, intranasal delivery has only recently been appreciated as a way of direct delivery of protein or viral vector therapeutics to the central nervous system (CNS) (Thorne et al., 1995; Thorne and Frey 2nd, 2001; Jerusalmi et al., 2003).

Olfactory sensory receptor neurons (ORNs) are the easiest accessible bipolar neurons that closely link the outside environment to the brain, and are the shortest linking neurons between the periphery and CNS. Their cell bodies and ciliated dendrites are located in the upper rear part of the nasal cavity and line the nasal septum and turbinates. The function of ORNs is to transmit signals of evaporative odorant from air to the brain (Buck and Axel, 1991). These neurons send their axons through the cribiform plate and enter the olfactory bulb forming synapses with mitral and tufted cells within a glomerular structure in the olfactory bulb. It is known that over 1000 odorant receptor genes are expressed by different types of ORNs (Buck

and Axel, 1991; Chess et al., 1992; Malnic et al., 1999) and an odorant activates thousands of neurons which send converged signals to discrete glomeruli and then to the olfactory cortex (Vassar et al., 1994). The olfactory cilia of ORNs provide a large surface area contacting with the air environment, which is useful for the application of gene vectors or drugs. Due to their unique geometric localization, close linkage with the brain, a large contact surface area of cilia and the diversity of odorant receptors, it may be possible to deliver therapeutic viral vectors or gene products into the brain via axonal transport within ORNs.

Previous studies have demonstrated that ORNs and olfactory sustentacular cells can be efficiently transfected with adenoviral vectors (Holtmaat et al., 1996; Hermens et al., 1997; Holtmaat et al., 1997; Ivic et al., 2000; Soudais et al., 2001; Youngentob et al., 2004).Several studies have used adenoviral mediated expression of lacZ transgenes in ORN cell bodies and their nerve bundles (Draghia et al., 1995; Zhao et al., 1996; Doi et al., 2005).

The aim of the present study is to explore the feasibility for delivery of viral vectors into several different brain regions using olfactory neurons as a transport route bypassing the BBB. We have investigated whether the transgene product can be detected in other brain regions by the non-invasive gene delivery system: an adenovirus or AAV mediated gene transfer by nasal instillation in a rat model. A short time course (24hr-2wks) was used to examine the adenovirus mediated localized expression pattern of a reporter protein Enhanced Green Fluorescence Protein (EGFP) within rat olfactory and brain tissue. A longer time course of 8 weeks was used to examine the expression and distribution pattern of EGFP from nasal delivered AAV2-EGFP.

3.3 Materials and Methods

3.3.1 Animals

Eight-week-old male Sprague-Dawley rats were used for this study under the guidelines of the National Health and Medical Research Council of Australia and with approval from the Animal Ethics Committee of Flinders University, Adelaide, in compliance with approval number 577/04. The principles of laboratory animal care (NIH publication No. 86-23, revised 1985) were followed. All animals were individually caged and housed in a temperature controlled room with a 12 hour / 12 hour light / dark cycle, with unlimited access to normal laboratory chow and water.

3.3.2 Viral Vectors

The Ad5-CMV-eGFP is a replication deficient recombinant adenovirus and was obtained from Vector Development Laboratory (Baylor College of Medicine, Houston, TX) at $5X10^{12}$ particles/ml. The Ad5 vector utilizes the Coxsackie-Adenovirus Receptor (CAR) to enter cells (Bergelson et al., 1997), contains a strong cytomegalovirus (CMV) promoter and an enhanced GFP coding region.

AAV2-EGFP vector was made by our collaborator, Dr. Xiao-Bing Wu (VGTC Biotech Company, Beijing, China) using a proprietary production method which generates very high titre and highly purified AAV particles ($1X10^{12}$ particles/ml),

3.3.3 Intranasal delivery of Ad5CMV-EGFP and AAV2-EGFP into rats

Adult Sprague-Dawley rats (n=4 per time point, 3 groups) were anaesthetized by an intraperitoneal injection of a Ketamine (80mg/kg): Xylazil (15mg/kg) mixture, placed on their backs and Ad5CMV-EGFP ($5 X 10^{10}$ pfu/ml) was administered to the

rat's nasal cavities by micropipette with 5µl droplet solution delivered to each nostril per dose 4 times, for a total of 40µL delivered over a 45 minute period. Rats were allowed to naturally inhale the solution between doses before waking. Control animals received 40uL intranasal inoculations of BSA (Pierce, Rockford, IL). Olfactory and brain tissue samples were collected after a time course of 1 day, 1 week and 2 weeks post-intranasal inoculation **(Fig. 3.1)**.

A separate group of rats (n=4) were anaesthetized as above and received 40µL of AAV2-EGFP administered to the nasal cavities as alternating 5µl droplets between nares. After 6 weeks, brain and olfactory tissue were collected **(Fig. 3.2)**.

Fresh olfactory and brain tissue (i.e non-fixed) was obtained from 2 groups of rats (n=4) which received either AdV-EGFP or AAV2-EGFP. Samples were collected at time points 1 week for AdV and 6 weeks for AAV **(Figs. 3.1 & 3.2)**.

3.3.4 EGFP expression *in vivo*

At serial time points of 1 day, 1 week and 2 weeks (for AdV), and 6 weeks (for AAV), the animals (n=4 per time point) were re-anaesthetized and transcardially perfused with a solution of 4% paraformaldehyde, buffered to pH 7 with 0.1M PB. After perfusion, the brain, olfactory bulb and the nasal cavity containing the septum and olfactory turbinates were dissected out and postfixed in the same fixative for 20 hours. The olfactory tissues and brains were cryoprotected and decalcified in 30% sucrose, 14% EDTA in 0.1M PB at 4^0C for 18 hours before freezing in Tissue Tek OCT tissue protection medium (ProSciTech, Thuringowa Qld) and sectioning on a Leica cryostat (Leica-Microsystems, North Ryde, NSW) to a thickness of 15µm (10 sections per animal). Olfactory tissues were sectioned horizontally and all other brain tissues were sectioned coronally and sagittally. Most tissue sections were collected on gelatin-coated slides, rinsed with PBS and mounted with VECTASHIELD®

Delivery of either:
Ad5CMV-EGFP (5X 10^{10} pfu/ml) (40uL) or
BSA control (40uL)

Group 1

Or

Group 2

Perfusion/fixation
at 1day, 1 & 2wks (n=4)

Fresh brain tissue collection
after 1wk (n=4)

Frozen 15μm sections
(brain, nasal tissues)

Protein extraction
(brain regions , nasal tissues)

Fluorescent
Microscopy
EGFP

Immuno-
Fluorescence
α-EGFP, α-OMP

SDS-PAGE Western blot
using α-EGFP Ab

Fig 3.1 Schematic outline of AdV-EGFP nasal administration experiments

Delivery of either:
AAV2-EGFP (1X 10^9 pfu/ml) (40uL) or
BSA control (40uL)

Group 1

Or

Group 2

Perfusion at 6 wks (n=4)

Fresh brain tissue collection after 6 wks (n=4)

Frozen 15μm sections (brain, nasal tissues)

mRNA extraction (brain regions , nasal tissues)

RT PCR using Fwd and Rev EGFP oligos

Fluorescent Microscopy EGFP

IHC α-EGFP

Immuno-Co-localization EGFP, α-N52

Fig 3.2 Schematic outline of AAV-EGFP nasal administration experiments

(Vector Laboratories, Burlingame, CA) before fluorescent microscopy of expressed EGFP. Some brain sections were mounted with VECTASHIELD® containing DAPI nuclear stain. For immunohistochemistry experiments, 15μm sections were collected free-floating in PBS.

3.3.5 Immunofluorescence

Olfactory tissue sections were washed three times in PBST for 10min each and then incubated in a blocking solution of PBS containing 10% normal horse serum (NHS) for 1 hour at RT. The olfactory sections were incubated overnight at 4^0C in primary antibodies against EGFP (rabbit anti-EGFP; 1:10000) (Millipore, North Ryde, NSW) and OMP (goat anti-Olfactory Marker Protein; 1:10000) (Wako Chemicals, Richmond, VA) (Keller and Margolis 1975). After washing three times in PBST for 10min each, the sections were incubated in secondary antibodies, chicken anti-goat IgG Alexa 647 (1:1000, Invitrogen, Mt. Waverley VIC) and donkey anti-rabbit IgG Cy3 (1:500, Invitrogen, Mt. Waverley VIC) for 1 hour at room temperature. Sections were thoroughly washed in PBS prior to mounting with VECTASHIELD® (Vector Laboratories, Burlingame, CA) and cover-slipping. As negative controls, addition of pre-immune serum instead of a primary antibody on tissue sections in the above procedure was performed, which gave no positive immunofluorescence.

For the N52 double-labelling experiments, coronal brain sections, collected and washed with PBST as described above, were firstly incubated in 10% NHS blocking solution for 1 hr at RT before overnight 4^0C incubation in anti-neurofilament (N52) monoclonal antibody (Sigma-Aldrich, Castle Hill, NSW), diluted 1:500 in the blocking buffer. Sections were then incubated for 1hr in anti-mouse-CY3 conjugated secondary antibody (Sigma-Aldrich, Castle Hill, NSW). Finally sections were washed and mounted as described above.

3.3.6 Immunohistochemistry

Free-floating sections were treated with 0.3% hydrogen peroxide in 50% ethanol for 40 mins and washed thoroughly in PBST, blocked in 10% NHS, and incubated with anti-EGFP monoclonal antibody (Clontech, Mountain View, CA) diluted 1:200 in 3% NHS overnight at RT. For negative control, normal rabbit serum replaced anti-EGFP antibody. After three 10 min washes in PBST, the sections were incubated in biotinylated donkey anti-mouse IgG (Millipore, North Ryde, NSW) in 3% NHS for 2hrs at RT. After PBST washing, sections were continuously incubated in ABC reagents (1:100, VECTASTAIN® ABC kit, Vector Laboratories, Burlingame, CA) for 1.5 hrs. Following extensive PBST washing, sections were developed with the glucose oxidase-DAB nickel method of staining (Shu et al., 1988). Sections were then mounted on slides, dried overnight and coverslipped with Depex mounting medium (Merck, Kilsyth, Vic.) and finally observed under a light microscope.

3.3.7 Protein analysis by western blotting

Brain and olfactory tissue were collected 1 week after intranasal delivery and processed for protein extraction. Tissue specimens were grounded in liquid nitrogen with a mini mortar and pestle, and lysed in homogenisation buffer (pH 7.5) containing 20mM Tris, 1% TritonX-100, 150mM NaCl, 1mM EDTA, 0.5% Na Deoxycholate, 0.1% SDS phosphatase inhibitor cocktail and protease inhibitor cocktail (Roche, Dee Why, NSW). Tissue lysates were sonicated by a microprobe sonicator and clarified by centrifugation in a microfuge (15min, 13000 rpm, 4^0C). Protein concentration of the supernatant was determined using BCA protein assay kit (Pierce, Rockford, IL). Brain tissue extracts (40μg) were denatured (95^0C, 8 mins)

under reducing conditions (100mM DTT) and resolved by electrophoresis on a 10% SDS PAGE using a mini-PROTEAN Electrophoresis cell (BioRad, Gladesville, NSW) along with molecular protein marker (10-250 KDa) (BioRad, Gladesville, NSW). This was followed by protein electro-transfer on to Hybond ECL nitrocellulose membrane (GE Healthcare, Rydalmere, NSW) using a mini-PROTEAN transfer system (BioRad, Gladesville, NSW). After blocking with 5% skim milk in TBS containing 0.1% Tween-20 for 2 hours at RT, membranes were probed with primary antibodies overnight at 4^0C. After removing excess unbound antibodies, membranes were further probed with secondary antibodies labelled with HRP for 1 hour, followed by chemiluminescent ECL detection (GE Healthcare, Rydalmere, NSW). Full details of this procedure can be found in **Appendix 1.1.**

3.3.8 Image acquisition and analysis

Images were acquired using an Olympus BX-50 epifluorescent microscope (Olympus, Vic, Australia) equipped with a CoolSNAP CCD camera (Roper Scientific, Ottobrunn, Germany). Filters 488nm (EGFP), 548nm (Cy3), 650nm (Cy5) and 400 nm (DAPI) were used to visualize fluorescent labeled cells and tissues. Brain tissues were counterstained using the nuclear stain DAPI.

3.3.9 Real-time RT-PCR analysis

Fresh olfactory mucosa, olfactory bulb and brain tissue was harvested from rats, 6wks after nasal delivery with AAV2-EGFP. Tissue samples were ground to a powder form in liquid nitrogen with a mini mortar and pestle, then 0.8 ml of TRIZOL® reagent (Invitrogen, Mt. Waverley VIC) was added to the sample and ground until the sample was uniformly homogeneous in TRIZOL®. Homogenized samples underwent aqueous phase separation, total RNA precipitation and RNA

pellet washing steps according to the TRIZOL® RNA isolation protocol (Invitrogen, Cat # 18064-014) developed from the modified single-step method of RNA isolation (Chomczynski and Sacchi, 1987). RNA pellets were air dried then dissolved in RNAse-free water. The RNA concentration and purity was determined by measuring its absorbance at 260nm and 280nm in a spectrophotometer (Gene Quant2 RNA/DNA calculator, Pharmacia).

First-strand cDNA was synthesized using a Superscript II reverse transcriptase kit (Invitrogen, Mt. Waverley VIC) following the protocol described in the Superscript II manual. All RNA samples were initially treated with RNAse-free DNAse (Promega, Alexandria NSW) following the product manual protocol. For the reverse transcription reaction, **Appendix 1.2 and Appendix Table 1.1** describes the procedure, volumes and concentrations used for the 20μL reactions.

Real-time RT-PCR reactions were performed using the rat olfactory and brain cDNA templates in 0.2 uL PCR tubes with a Rotogene-2000 (Corbett Research, Qiagen, Doncaster, VIC). Hotstart Taq DNA polymerase and dNTPs were included in the QuantiTect SYBR Green PCR kit (Qiagen, Doncaster, VIC). Master mix for forward and reverse EGFP oligonucleotide primers (see **Appendix 1.3**) was prepared according to **Table 3.1**., and 18uL was aliquoted into each tube and mixed with 2uL of different cDNA. Samples were run in duplicates.

Table 3.1 Master mix preparation for real time PCR

Component	Volume/Reaction	Final Concentration
2X QuantiTect SYBR Green PCR mix	110μL	1X
EGFP Fwd primer	22μL of 3M stock	0.3μM
EGFP Rev primer	22μL of 3M stock	0.3μM
RNAse-free water	44 μL	
Template cDNA	22 μL RT product	
Total volume	**220μL**	

The parameters for the PCR were as follows:

95^0C for 10min (1 cycle); 95^0C for 30s, 52^0C for 30s and 72^0C for 1min (35 cycles); 72^0C for 1min (1 cycle).

AAV2-EGFP vector was included as a positive control, run in parallel to the samples, providing the reference gene EGFP for the reactions. Completed PCR products were loaded onto a 2% TAE (Tris, Acetic acid, EDTA) agarose gel for separation by electrophoresis (see (Maniatis et al., 1989)for protocol).

3.4 Results

3.4.1 Adenovirus-mediated EGFP expression in the olfactory epithelium, olfactory bulb and trigeminal nerve *in vivo*.

In this study, rats were infected with 40µl adenoviral solution ($2X10^9$ pfu) intranasally and examined up to 2 weeks post infection. All experimental animals recovered after intranasal viral infection and remained healthy without exhibiting any behavioral abnormalities until being sacrificed. Additionally there was no evidence of tissue damage or cell loss caused by the viral infection.

Figure 3.3.1 A-F shows horizontal cryosections of the olfactory epithelium and olfactory bulb from 1 day to 2 weeks post-intranasal infection, displaying expressed EGFP fluorescence. At 1 day post-intranasal inoculation **(Fig.3.3.1 A & B)**, adenoviral mediated EGFP expression was detected within cells throughout the olfactory epithelial surface. Expression was primarily localized within the olfactory receptor neurons (ORNs, **Fig.3.3.1 B**). Strong fluorescence was observed in the ORN cell bodies and dendritic processes extending towards the apical surface of the olfactory mucosa and ending in dendritic knobs (**Fig. 3.3.1 B**, arrows). The ORNs transduced with Ad5CMV-EGFP had a distinctly bipolar morphology (**Fig. 3.3.1 B**, arrows). In addition to ORN cell bodies lining the olfactory epithelium, EGFP containing axonal bundles were observed in the lamina propria, extending towards the olfactory bulb (**Fig. 3.3.1 A**, arrows).

Within the main olfactory bulb, intense EGFP fluorescence was predominantly detected in the olfactory nerve layer and the glomerular layer at 1 week and 2 weeks following intranasal inoculation (**Fig. 3.3.1 C, D & E**). ORN axon bundles, leaving the olfactory epithelium, projected into the lateral and medial sides of the olfactory bulb and made synaptic connections with mitral and tufted cells

Figure 3.3.1.

Time course of Adenovirus-mediated EGFP expression in the rat olfactory epithelium and main olfactory bulb.

(A) A horizontal section of rat olfactory mucosa, 1day after Ad5CMV-EGFP intranasal inoculation, showing intense EGFP fluorescence within ORNs. Arrows indicate ORN axon bundles passing from the lamina propria to the olfactory bulb. **(B)** In a higher-power view, EGFP expression was predominantly observed in ORNs (arrowhead) and ORN dendrites (arrows) can be seen extending to the mucosal layer (ML). Olfactory epithelium (OE); Lamina propria (LP).

(C) EGFP fluorescence observed in the horizontal lateral side of the olfactory bulb neural layer (NL, arrowhead) and glomeruli (GL, arrows), 1 week after IN inoculation.

(D) Higher-power view of glomerulus showing intense EGFP fluorescence at ORN synapses with mitral and tufted cells, 1 week after IN inoculation.

(E) Olfactory bulb neural (NL, arrowhead) and glomerular layers (GL, arrows) 2 weeks after intranasal inoculation of Ad5CMV-EGFP.

(F) No EGFP expression in olfactory bulb 1 week after intranasal inoculation with BSA. Scale bars = 25μm.

Olfactory mucosa
Olfactory bulb 1wk
Olfactory bulb 2wks
Control OB
A
B
ML
OE
LP
C
GL
NL
GL
D
E
NL
GL
GL
F

Figure 3.3.2.

Localization of EGFP in rat trigeminal lnerve regions 1 week after intranasal inoculation with Ad5CMV-EGFP.

(A, B, C) Horizontal sections of opthalamic (V_1) and maxillary (V_2) segments of rat trigeminal nerve, 1 week after Ad5CMV-EGFP intranasal inoculation, showing intense EGFP fluorescence within neuronal cells (arrows). Panels **A-C** show sections with increasing magnification, scale bar = 25μm.

(D, E, F) Horizontal sections of opthalamic (V_1) and maxillary (V_2) segments of rat trigeminal nerve stained using immunohistochemistry, 1 week after Ad5CMV-EGFP intranasal inoculation, showing EGFP localization by prominent immunostaining within neuronal cells (brown-purple staining). Panels **A-C** show sections with increasing magnification. Scale bar in panel **D** = 100μm. Scale bars in panels **E & F** = 25μm.

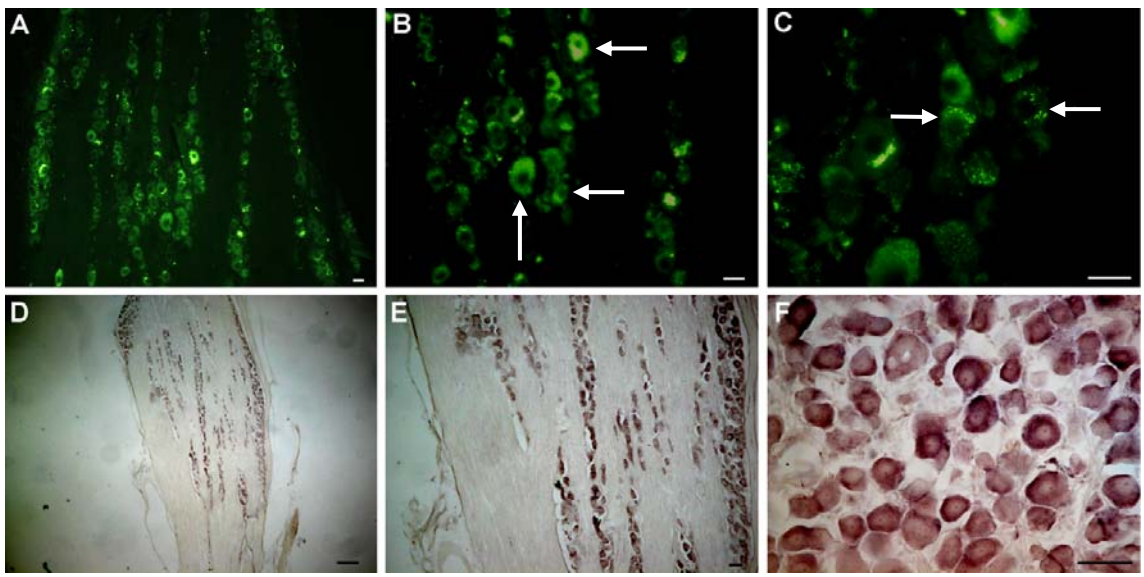
A
B
C
D
E
F

within dense regions of neuropil known as glomeruli (**Fig. 3.3.1 D**). After 2 weeks, EGFP expression was still present in the olfactory nerve and glomerular layers of the lateral and medial side of the olfactory bulb. Control olfactory bulb tissue sections show no EGFP expression 1 week after intranasal inoculation with BSA (**Fig. 3.3.1 F**).

The opthalamic (V_1) and maxillary (V_2) segments of rat trigeminal nerve contained specific regions of EGFP fluorescence localised within cytoplasmic granules of what appeared to be neuronal cells (**Fig. 3.3.2 A-C**). This expressed EGFP fluorescence was confirmed by inmmunohisochemistry conducted on sections of trigeminal nerve from the same animals using anti-EGFP monoclonal antibody. In **Fig. 3.3.2 D-F**, significant brown-purple immunostaining was observed in the same V_1/ V_2 regions of the trigeminal nerve within what appeared to be neuronal cells. However further double-labelling immunofluorescence would be required to confirm the exact cell types.

3.4.2 EGFP detected in other brain regions

One week following Ad5CMV-EGFP intranasal inoculation, EGFP fluorescence was detected in neurons of several brain regions (**Fig. 3.4A-F**). Higher magnifications of coronal rat brain sections revealed strong EGFP fluorescence localized within the cellular cytoplasm of lateral entorhinal cortex neurons and amygdaloid neurons in the central amygdaloid nucleus (**Fig. 3.4A & B**). EGFP fluorescence was also localized within cytoplasmic granules of neurons in the CA2 region of the hippocampus (**Fig. 3.4C**) and also present in the CA3 and dentate gyrus regions. As shown in **Fig. 3.4D**, several striatal neurons containing cytoplasmic EGFP fluorescence were observed. EGFP accumulated within the cytoplasm of

Figure 3.4

Localization of EGFP in rat brain regions 1 week after intranasal inoculation with Ad5CMV-EGFP.

(A-F) High magnification images of coronal and sagittal rat brain sections displaying EGFP fluorescence localized within the cytoplasm of various neuron populations. These include: **(A)** neurons of the lateral entorhinal cortex (arrows), **(B)** neuronal cells (arrowheads) in the central amygdaloid nucleus, **(C)** neuronal cells (arrows) in the CA2 region of hippocampus, **(D)** neurons in the caudate putamen (striatum) (arrowheads), **(E)** cerebellar Purkinje cells (arrows) and neurons in the pontine raphe nucleus (arrowheads). In all neuronal cells observed, EGFP fluorescence appeared to be granular and localized in cellular cytoplasm. Nuclei in panels **A-D** were counterstained with DAPI. Scale bar = 25μm.

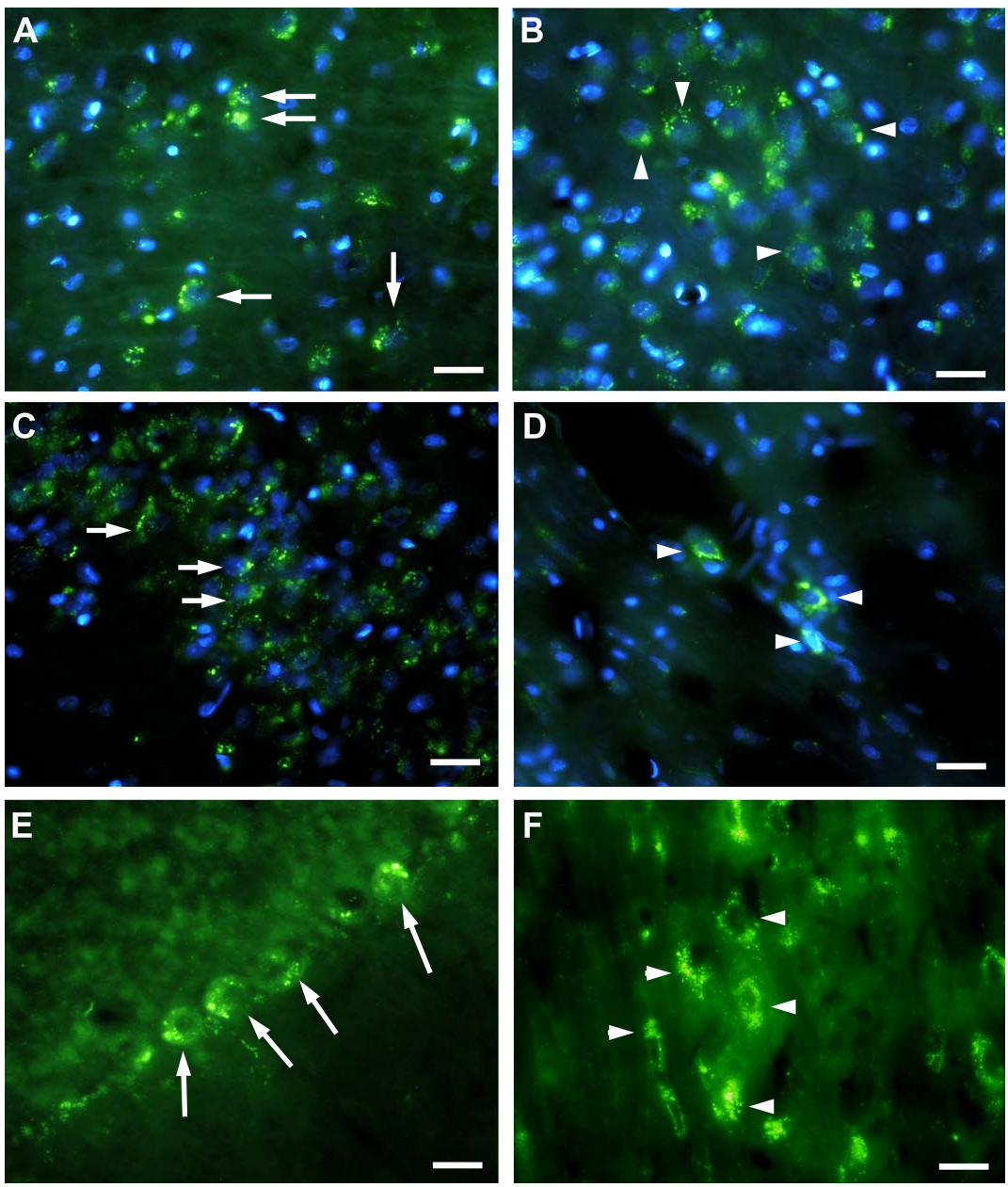
A
B
C
D
E
F

cerebellar Purkinje cells, which displayed strong fluorescence (**Fig. 3.4E**). Sagittal sections of the pons region revealed very intense EGFP fluorescence localized within the cellular cytoplasm of neurons in the pontine raphe nucleus (**Fig. 3.4F**) and the inferior olive nuclei (data not shown). In **Figs. 3.4A-D**, cellular nuclei were counterstained with DAPI for better visualization of nuclei. In all neuronal cells observed, EGFP fluorescence appeared to be granular and localized within the cellular cytoplasm. These results suggest that EGFP expressed in the ORNs by infection of Ad5CMV-EGFP, may be transferred across from the olfactory epithelium to the olfactory bulb and further to other brain regions.

In the same animals which received i.n. delivered Ad5CMV-EGFP and analysed one week later, several regions of respiratory epithelium and olfactory lymphoid tissue was examined for specific EGFP fluorescence. No significant expressed EGFP fluorescence was detected in these tissues. However, greater animal numbers and a more quantitative analysis would be required to confirm this.

3.4.3 Immuno-localization of expressed EGFP

Immunohistochemistry using a polyclonal rabbit anti-EGFP antibody further confirmed the presence of expressed EGFP in the olfactory mucosa and the main olfactory bulb (**Fig. 3.5A & B**). Immuno-localization of EGFP (red) co-localized (yellow) with adenoviral mediated expressed EGFP (green) within ORNs and olfactory sustentacular cells in the olfactory mucosa (**Fig. 3.5A**, arrows). Within the main olfactory bulb, expressed EGFP (green) co-localized (yellow) with anti-EGFP-Cy3 (red) in the olfactory neural layer axonal fibers and in the glomerular layers (**Fig. 3.5B**, arrowheads). Using an anti-Olfactory Marker Protein (OMP) antibody, immunohistochemical staining suggested that Ad5CMV-EGFP transduced cells were ORNs as shown in **Fig. 3.5C & D**. Expressed EGFP (green) in ORN axon fibers co-

Figure 3.5

Immuno-localization of EGFP fluorescence with anti-EGFP antibody and with anti-Olfactory Marker Protein (OMP) antibody in rat olfactory tissue 1-3 days following intranasal Ad5CMV-EGFP inoculation.

(A) In the olfactory epithelium, expressed EGFP (green) co-localized (yellow) with α-EGFP-Cy3 (red) within ORN's and supporting cells (arrows). **(B)** In the main olfactory bulb, expressed EGFP (green) co-localized (yellow) with α-EGFP-Cy3 (red) in the neural and glomerular regions (arrows). **(C-D)** Immuno-localization of α-OMP-Cy3 (red) with expressed EGFP (green) in the ORN fibres (arrows) of the olfactory epithelium and in the neural and glomerular layers of the main olfactory bulb (arrowheads). Scale bar = 25μm.

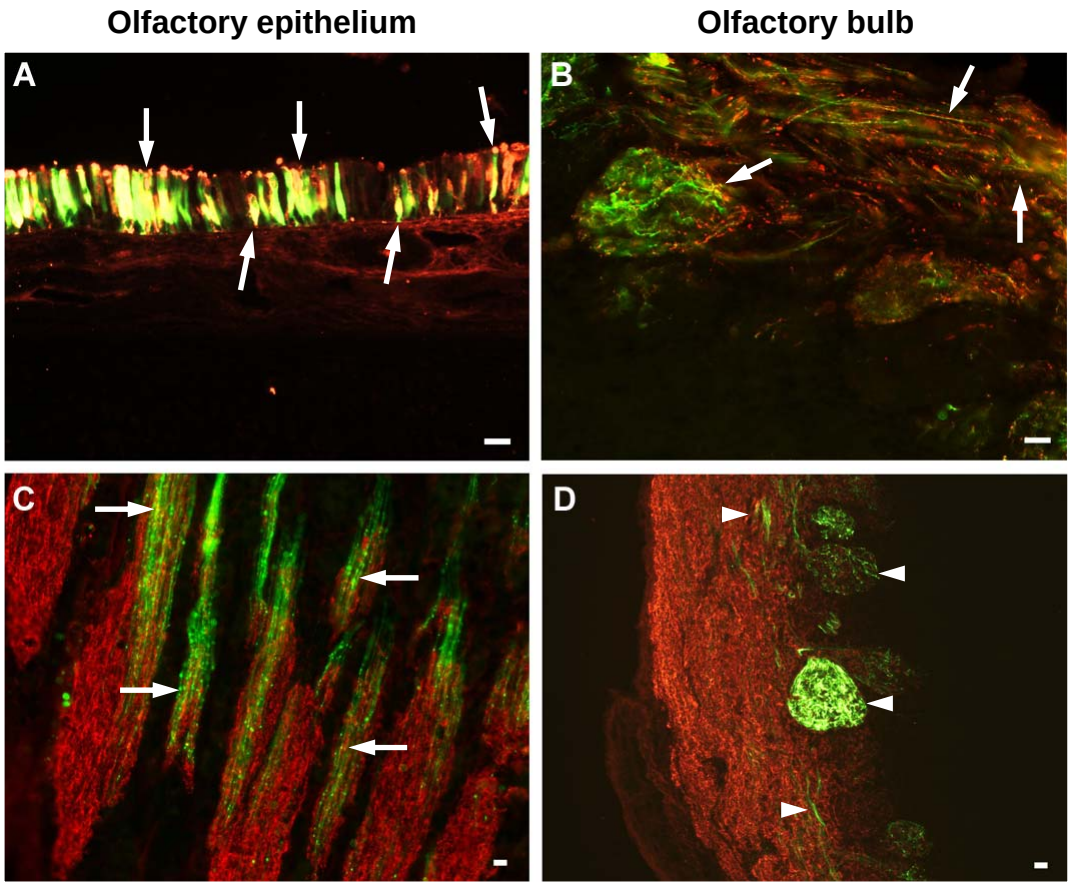
Olfactory epithelium
Olfactory bulb
A
B
C
D

Figure 3.6

Western blot of rat brain tissue extracts, 1 week after intranasal inoculation with Ad5CMV-EGFP.

EGFP was detected in olfactory mucosa **(lane 3)**, olfactory bulb **(lane 4)**, basal forebrain **(lane 5)**, medulla **(lane6)**, cerebellum **(lane 7)**, hippocampus **(lane 8)** and hypothalamus **(lane 9)**. Controls included: recombinant EGFP **(rEGFP, lane 2)** and olfactory tissue from a rat intranasally inoculated with BSA **(lane 10)**. Lane 1 contains a 10-250 KDa protein marker.

β-Tubulin (50kDa) was used as a loading control.

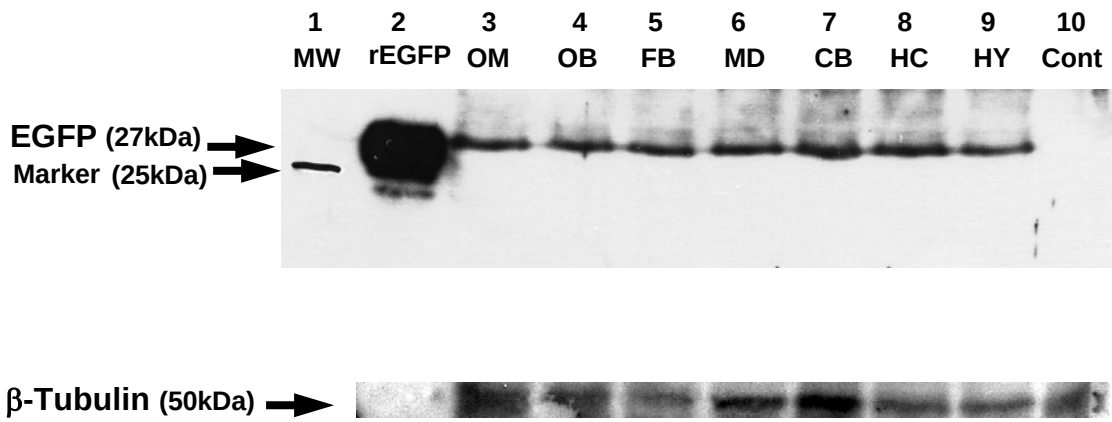
1 MW
2 rEGFP
3 OM
4 OB
5 FB
6 MD
7 CB
8 HC
9 HY
10 Cont
EGFP (27kDa)
Marker (25kDa)
β-Tubulin (50kDa)

localized (yellow) with anti-OMP-Cy3 (red) within the olfactory mucosa (**Fig. 3.5.4A-F**). Co-localization was also observed in the olfactory bulb neural and glomerular layers (**Fig.3.5D**).

3.4.4 Localization of EGFP in brain tissue extracts

Western blot analysis further verified the presence of Ad5CMV-mediated EGFP expression in olfactory mucosa and EGFP distribution within several different brain regions 1 week following intranasal inoculation (**Fig.3.6**). EGFP, with a molecular weight of 27kDa (**Fig.3.6, lane 2**), was detected by immunoblot within rat tissue extracts from the olfactory mucosa, olfactory bulb, basal forebrain, medulla oblongata, cerebellum, hippocampus and hypothalamus (**Fig.3.6, lanes 3-9**). In the control brain tissue sample, obtained from the saline intranasal delivered animal, no EGFP was detected (**Fig.3.6, lane 10**).

3.4.5 AAV delivered EGFP localized in several brain regions after 6wk period

In these experiments, rats were infected with 40µl AAV2-EGFP solution ($1X10^9$ pfu) intranasally and examined 6 weeks post infection. The experimental animals recovered after intranasal viral infection and remained healthy without exhibiting any behavioral abnormalities until being sacrificed. Additionally there was no evidence of tissue damage or cell loss caused by the viral infection.

As shown in **Fig. 3.7 A-I**, specific EGFP fluorescence was detected in several rostral and caudal brain regions including areas of the forebrain (**Fig. 3.7A & B**), cortex (**Fig. 3.7C & D**), hippocampus CA2 region (**Fig. 3.7E &, F**), cerebellar Purkinje cells (**Fig. 3.7G & H**) and neuronal cells in the trigeminal nucleus (**Fig. 3.7I**). In forebrain and cortical areas, positive neuronal cells appeared to contain localized and granular EGFP within their cytoplasm (**Fig. 3.7B & D**, marked by

Figure 3.7

Localization of EGFP in rat rostral and caudal brain regions 6 weeks after intranasal inoculation with AAV-EGFP.

(A-J) High magnification fluorescent images of rat brain sections displaying EGFP fluorescence localized within the cytoplasm of various cell populations.

EGFP appeared to localize in cells (as indicated by arrows in panels **B, D, F, H** & **I**) within the forebrain **(A,B)**, cortex **(C,D)**, hippocampus **(E,F)**, cerebellum **(G,H)** and trigeminal nerve **(I).** In a control animal which received intranasal delivered BSA, no specific EGFP fluorescence was present in cerebellum **(J)** and other brain regions. Boxed areas in **(A, E** & **G)** are enlarged in higher magnification panels **(B, F** & **H)**. Scale bars = 25μm.

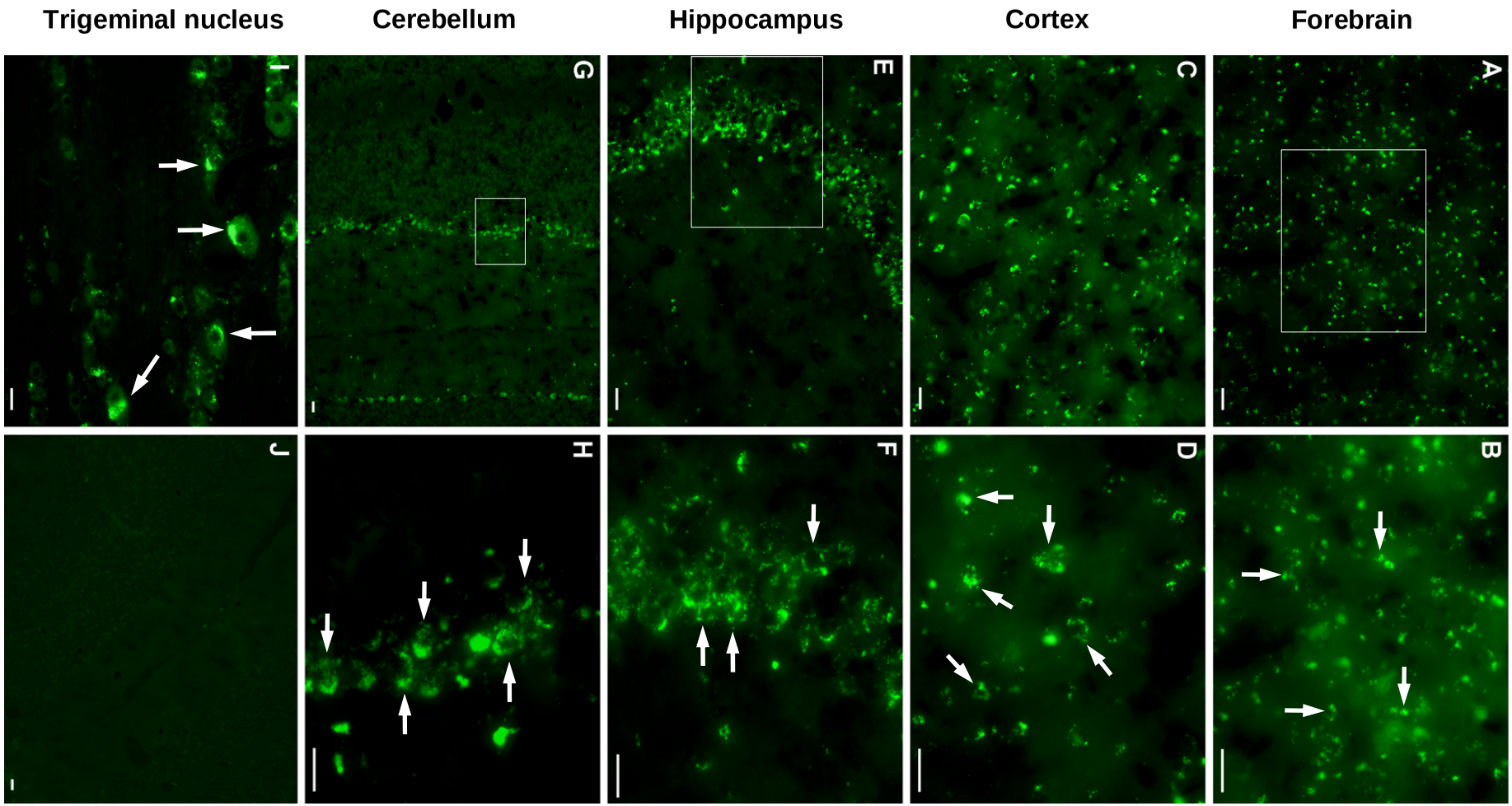
Trigeminal nucleus
Cerebellum
Hippocampus
Cortex
Forebrain
I
G
E
C
A
J
H
F
D
B
Control cerebellum

arrows). The CA2 region of hippocampus and Purkinje cell area of cerebellum (boxed areas in **Figs. 3.7E & G**) contained numerous neuronal cells displaying positive EGFP granular fluorescence (**Fig. 3.7F & H**, marked by arrows). Numerous positively identified neuronal cells were also observed in the trigeminal nucleus (**Fig. 3.7I**, marked by arrows). In the control section of cerebellum (**Fig. 3.7J)** and in other brain regions**,** from an animal which received an equivalent volume of intranasal BSA, no positive EGFP fluorescence was observed.

3.4.6 Immunostaining of EGFP localized in brain regions

Using an α-EGFP polyclonal antibody, EGFP immunoreactivity was observed in several brain regions, including some of the same areas which showed specific EFP fluorescence in the previous experiment. **Fig. 3.8 A-H** shows the positive immuno-staining which indicates EGFP localization within areas of the amygdala (**Fig. 3.8A & B**), thalamus (**Fig. 3.8C & D**), hippocampus CA2 (**Fig. 3.8E & F**) and dentate gyrus (**Fig. 3.8G & H**).

Positive immuno-stained cells were clustered in the central amygdaloid nucleus, (boxed area and arrow in **Figs. 3.8A & B**) and displayed in low and high power images as dark purple-brown staining. Neuronal cells in the thalamus (boxed area and arrowed cells in **Figs. 3.8C & D**) were positive for EGFP immuno-staining and some appear pyramidal in morphology. A similar localization pattern of EGFP in the CA2 region of hippocampus was observed in the immuno-stained sections (**Figs. 3.8E & F**) when compared to the EGFP fluorescence images (**Fig. 3.7E & F**). Also within the hippocampus, the dentate gyrus (**Fig. 3.7G**) contained positive neurons in the polymorph (**Fig. 3.7H**, arrows) and granular layers (**Fig. 3.7H**, arrowheads).

Figure 3.8

Nasal delivery of AAV-EGFP resulted in significant expression of EGFP in the central amygdaloid nucleus, thalamus, hippocampus and dentate gyrus (A-H) of rats as detected by immunohistochemistry using monoclonal antibody to EGFP.

In panels (**A & B**), positive EGFP staining was localized in neuronal cells (boxed area and arrow) of the central amygdaloid nucleus. In the thalamus (boxed area in **C** and enlarged in **D**), several positive neuronal cells (shown by arrows in **D**) appeared to have a pyramidal morphology. Several regions in the hippocampus (**E & F**) displayed positive EGFP staining and in the CA2 region (boxed area in **E**, enlarged in **F**) many positive neurons were localized. Within the dentate gyrus (**G & H**), several positive EGFP stained neurons were observed in the polymorph (arrows) and granular (arrowheads) layers. EGFP was present in dendrites and cell bodies of pyramidal cells and granular neurons. EGFP expression was displayed in some granular particles within cellular cytoplasm.

Sizes of scale bars are marked in figure panels.

Amygdala
Thalamus
Hippocampus
Dentate gyrus
A
B
C
D
E
F
G
H
100 µm
25 µm

3.4.7 EGFP localized within N52 positive neurons in midbrain

Brain sections taken from rats which received intranasal inoculations of AAV2-EGFP, were examined using neurofilament marker (N52) and fluorescent images are shown in **Fig. 3.9 A-I**. Expressed EGFP fluorescence (green) was observed within neuronal cells of several different brain regions including areas of the midbrain (**Fig. 3.9 B, E & H**). Neuronal cells displaying positive N52 immunofluorescence (red) (shown by arrows in **Fig. 3.9 A, D & G**) were found to co-localize with EGFP positive cells when the images were merged (yellow cells shown by arrows in **Fig. 3.9 C, F &, I**).

3.4.8 EGFP mRNA expression in olfactory epithelium only, 6 wks after i.n. delivery

The real-time PCR of internal control, AAV2-EGFP vector, was performed in parallel with cDNA samples from brain and olfactory tissue, originating from animals which received i.n. delivery of either AAV2-EGFP or BSA control 6wks ago. The PCR products included olfactory mucosa, olfactory bulb and hippocampus from AAV2-EGFP delivered animals, and olfactory mucosa from BSA control delivered animals. All PCR products were examined on a 2% agarose gel (**Fig. 3.10**) and a single 211 bp EGFP product band was obtained for the AAV2-EGFP control and AAV delivered olfactory mucosa. With single bands only in these two products, there were no non-specific or primer dimers present. In the other reactions, no specific EGFP product was observed indicating that EGFP mRNA was expressed only in the cells of the olfactory mucosa and not in other brain regions.

Figure 3.9

AAV expressed EGFP co-localizes with neurofilament N52 in midbrain after 6wks

(Panels A, D & G) N52 positive neuronal cells (red, shown by arrows) within the rat midbrain co-localized with midbrain cells containing AAV expressed EGFP (green) **(Panels B, E & H)**. Merged images **(Panels C, F & I)** showing co-localization (yellow, arrowed cells) between N52 and expressed EGFP in the midbrain.

Scale bars= 25μm

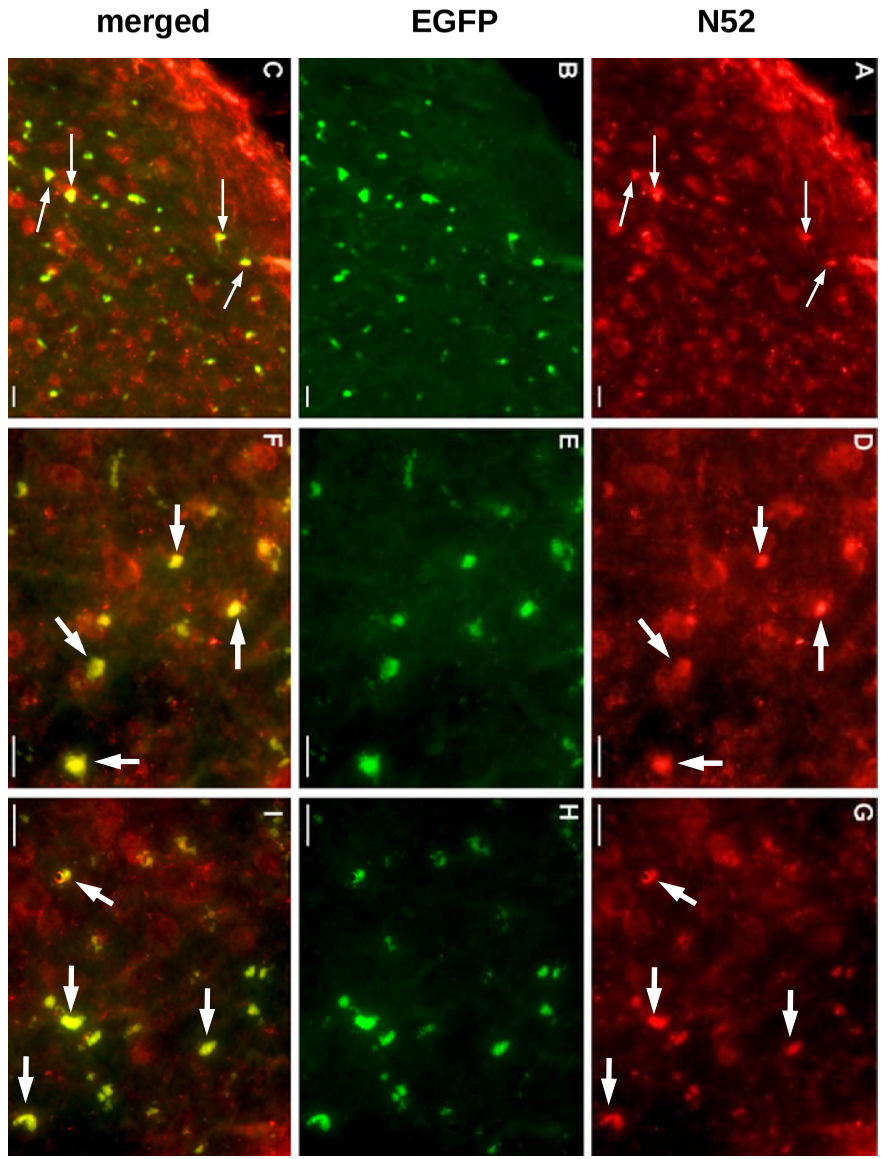
merged
EGFP
N52
C
B
A
F
E
D
I
H
G

Figure 3.10

Amplification of EGFP mRNA transcript in olfactory mucosa 6 wks after intranasal inoculation.

Preliminary RT-PCR results show that EGFP mRNA was detected in AAV2-EGFP positive control **(lane 1)** and AAV2-EGFP delivered nasal mucosa **(lane 5)** as shown by a 211bp single band PCR product which was resolved on a 2% agarose gel. No PCR product was detected in olfactory bulb **(lane 2)** and hippocampus **(lane 3)** from AAV delivered animals. In the control animals which received intranasal BSA, no PCR product was detected in olfactory mucosa **(lane 4)**. A no template PCR control was also included **(lane 6).**

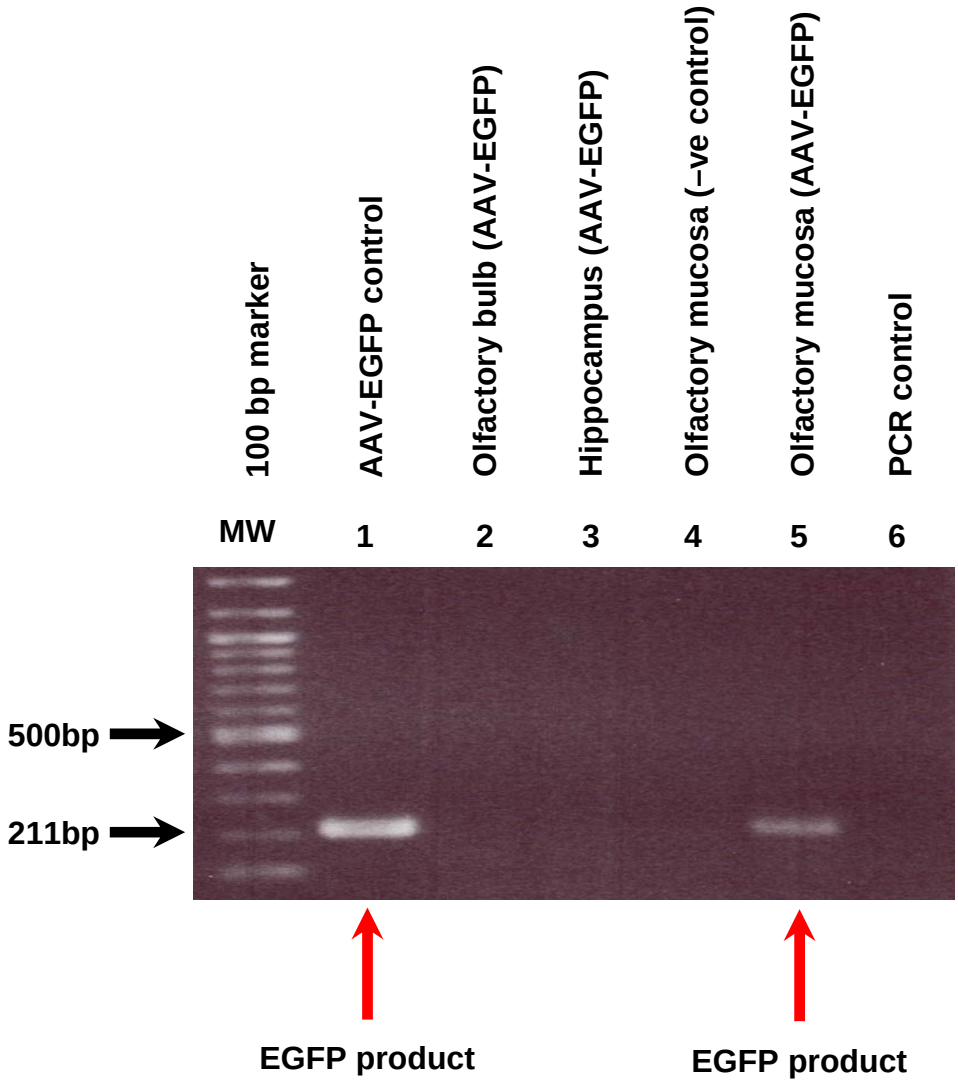
100 bp marker
AAV-EGFP control
Olfactory bulb (AAV-EGFP)
Hippocampus (AAV-EGFP)
Olfactory mucosa (–ve control)
Olfactory mucosa (AAV-EGFP)
PCR control
MW
1
2
3
4
5
6
500bp
211bp
EGFP product
EGFP product

3.5 Discussion

In this study, we have established that adenoviral and AAV vectors, when applied to the olfactory epithelium of a rodent model by intranasal instillation, robustly infected the ORNs. Furthermore, we found that the EGFP transgene product, which accumulated in the cell bodies of the adenoviral infected ORNs, was axonally transported in an anterograde direction to the nerve terminals in the olfactory bulb glomeruli and further transported to other regions of the brain, as detected by EGFP fluorescence, immunohistochemistry and by Western blot. Adenovirus mediated EGFP expression was observed in the olfactory epithelium 1 day post-inoculation and transported EGFP identified in the olfactory bulb glomeruli, trigeminal nerve and several brain regions within 7 days. Even after 2 weeks, strong EGFP expression was detected in the olfactory bulb neural and glomerular layers. EGFP localization was confirmed in the trigeminal nerve using immunohistochemistry with an anti EGFP monoclonal antibody. However, to fully confirm an anterograde axonal transport pathway of the viral transgene product from ORNs to olfactory cortex at a mechanistic level, further experimental studies need to be performed. Future intranasal tracing experiments would include initial destruction of the ORNs by either zinc sulfate inhalation (Cancalon, 1982; Slotnick et al., 2000) or surgical ablation of the olfactory bulb prior to nasal delivery of the viral vectors.

From AAV2 mediated EGFP expression in the olfactory epithelium, a similar pattern of EGFP localization in different brain regions (**Fig. 3.7**) was observed 6 weeks post-inoculation. EGFP localization was confirmed by immunoreactivity to anti-EGFP antibody within neurons of the central amygdala, thalamus, hippocampus, dentate gyrus (**Fig. 3.8**), and the cortex, cerebellum and brainstem (data not shown). Morphologically the EGFP positive neurons appeared pyramidal in some of these regions (**Fig. 3.8D**). The EGFP positive neurons also co-localized with neurofilament

marker N52 in the midbrain (**Fig. 3.9**). From a preliminary real-time RT-PCR experiment, it was found that EGFP mRNA was expressed in cells of the olfactory mucosa only and not in olfactory bulb and brain regions 6 weeks after nasal inoculation (**Fig. 3.10**). This result suggests that the AAV vector itself is not transported from the olfactory mucosa to the brain by either intracellular or extracellular routes, but the EGFP transgene product is transported by one or both of these routes. However, this preliminary real-time RT-PCR is not conclusive and further reactions need to be done using oligonucleotide primers to viral vector DNA, examining different olfactory and brain regions at several different time points post-inoculation.

Several previous studies have reported the use of a recombinant, replication-deficient, adenoviral vector construct for examining the rodent olfactory system (Draghia et al., 1995; Holtmaat et al., 1996; Zhao et al., 1996; Arimoto et al., 2002; Kinoshita et al., 2002; Doi et al., 2005). Studies conducted by Draghia et al., Zhao et al. and Doi et al. all involved intranasal inoculation of rodents with adenoviral vectors containing the lacZ gene which encodes the E.coli enzyme β-galactosidase (Draghia et al., 1995; Zhao et al., 1996; Doi et al., 2005). These studies all reported expression of transgene in olfactory mucosa ORNs and olfactory axons were traced to their targets in the glomerular layer of the olfactory bulb. We have confirmed that the transgene is expressed by ORNs in the olfactory epithelium and olfactory bulb. EGFP co-localized with anti-EGFP antibody within the ORNs in the olfactory neural and glomerular layers in the olfactory bulb. Olfactory Marker Protein (OMP), which is highly restricted to mature ORNs (Buiakova et al., 1994), co-localized with expressed EGFP within ORN axon bundles in the olfactory epithelium and the olfactory bulb neural layer.

Previously, only Draghia et al. reported expressed β-galactosidase in the rat anterior olfactory nucleus, locus coeruleus and area postrema 12 days post-infection. In contrast, we found the presence of expressed EGFP within neurons of several brain regions. These regions included the amygdala, hippocampus CA2/CA3 regions, and the lateral entorhinal cortex. Expressed EGFP was also detected in the caudate putamen (striatum), pontine raphe nucleus and cerebellar Purkinje cells. Analysis of brain tissue regions by Western blot, using an anti-EGFP antibody, confirmed the localization of expressed EGFP within the olfactory regions, basal forebrain, thalamus, medulla and hypothalamic regions. How the gene product accumulates in the brain regions in addition to the olfactory bulb are not fully known. It is possible that the transgene product is either transsynaptically transported and endocytosed by neurons projecting to the olfactory bulb (intracellular pathway), or gains access to the peripheral olfactory and trigeminal perineural spaces (extracellular pathway) to be transported to more caudal brain regions such as the cerebellum. Another possibility is that the viral vector itself crosses the olfactory bulb glomerular synapses to be transported to further CNS regions. However the real-time RT-PCR result from the AAV2-EGFP experiments seems to question this possibility. Although this may be clarified by immunohistochemical assay to viral proteins, the granular EGFP fluorescence localized in the cytoplasm of neuronal cells (**Fig. 3.4**) suggests transport of the viral vector gene product to distinct neuronal populations. The specificity of the fluorescence was further confirmed with correct size of EGFP by Western blot.

Other studies have found that intranasal administration of WGA protein leads to visualization of the primary and secondary olfactory pathways, from the olfactory mucosa to olfactory bulb and then to the cortex (Shipley, 1985; Itaya, 1987). Kinoshita et al. demonstrated transsynaptic labelling of mouse olfactory neural pathways by using a WGA-expressing adenoviral vector containing a strong CAG

promoter (Kinoshita et al., 2002). They reported anterograde transfer of WGA protein from the olfactory epithelium to the olfactory bulb and further to olfactory cortical areas including, the anterior olfactory nucleus, olfactory tubercle, piriform cortex and lateral entorhinal cortex. In addition, retrograde transsynaptic labelling was observed from the olfactory bulb to nuclei such as the horizontal limb of diagonal band, median raphe nucleus and locus coeruleus. These studies suggest that protein expressed by adenoviral vector infected ORNs is anterogradely transported along their axons to the olfactory bulb and may be transsynaptically transferred in glomeruli to dendrites of second-order neurons, mitral and tufted cells. Our results are consistent with those which suggest that anterograde transsynaptic transport enables ORN expressed proteins to enter the CNS via innervation of primary and secondary olfactory tract targets. However to fully confirm transneuronal transport via the olfactory nerve, further spacial and temporal i.n. tracing experiments need to be conducted to closely examine regions of the primary olfactory cortex listed in chapter 1.4.6 and figures 1.7 and 1.8.

In the rat olfactory epithelium, we found that the adenoviral vector predominantly infected ORNs, however, was also observed to a lesser degree in sustentacular cells. This may be due to the variation of cellular distribution of Coxsackie Adenovirus Receptor (CAR) which adenovirus use for internalization (Bergelson et al., 1997). ORNs express abundant CAR mRNA and are therefore highly susceptible to adenoviral infection (Venkatraman et al., 2005). The reason of why an obvious variation exists among different studies is not fully understood and the method of delivery may cause the variation. In these previous studies, the methods of virus application into the olfactory epithelium vary. Kinoshita et al. injected the viral solution (50-70µl) by droplets at the entrance of the nasal cavity and allowing the mice to inhale it spontaneously over 60 min, thus achieving

relatively uniform adenoviral infection of ORNs throughout the epithelium (Kinoshita et al., 2002). Zhao et al. injected the 10µl adenoviral solution through a small hole in the bone/cartilage at the top of the rat nasal cavity (Zhao et al., 1996), but did not achieve uniform infection throughout the olfactory epithelium. In our study, rat olfactory epithelium ORNs were infected by injecting individual 5µl droplets of adenoviral solution into each nasal cavity and allowing the rats to naturally inhale it during a 45 min period for a total volume of 40uL. Using this procedure, we were able to infect a large proportion of ORNs within the olfactory epithelium (**Fig. 3.3A**); however we did not achieve total EGFP labeling of all glomeruli in the olfactory bulb (**Fig. 3.3C & E**). This was probably a result of the lower total volume (40µl) of adenoviral vector delivered, compared to other studies which used 50-70µl. Our study also utilized a CMV promoter where some other studies used a strong CAG promoter for robust gene expression.

3.6 Conclusions

This study together with previous studies provides evidence suggesting the feasibility of using either adenoviral or AAV vectors to deliver therapeutic genes and gene products into the brain via a non-invasive nasal delivery protocol. Although the precise mechanisms of ORN transneuronal transport to brain regions is still to be elucidated, nasal delivery of therapeutic viral vectors remains a promising non-invasive method of transgene delivery to the CNS.

CHAPTER 4

GENERAL DISCUSSION AND CONCLUSIONS

4.1 General Summary

Over the last two decades, intranasal delivery has been recognised as a novel approach to directly targeting the CNS, cerebrovascular and perivascular spaces, and lymphatics for therapeutic studies. As first developed by Frey's group in 1991, this non-invasive method of delivering therapeutic agents to the CNS could allow drugs that do not cross the BBB gain access to the CNS (Frey, 1991; Thorne et al., 1995; Frey, 2002). Furthermore drugs which are able to cross the BBB can be directly targeted to regions of the CNS, avoiding the unwanted side effects encountered through systemic delivery. This is important in human therapeutic studies where a reduction in systemic exposure is desirable. Intranasal protein therapeutics have been shown to be effective in humans, reaching the brain without altering blood levels. An example of this is a charged molecule such as insulin which enters the brain from the nasal cavity without altering blood levels of glucose or endogenous insulin (Born et al., 2002).

The concept of direct nose to brain transport of a neurotrophic factor and viral vectors by both intracellular and extracellular olfactory and trigeminal pathways has been further explored by the work presented in this PhD thesis. As a strategy of effectively bypassing the BBB, and delivering either protein or viral vector therapeutic macromolecules directly to rostral and caudal brain regions, the intranasal delivery method has been successfully demonstrated by this study and others.

The results presented in this PhD project demonstrate that a neurotrophic factor, CNTF, can bypass the BBB and be transported to several regions within the brain around 30 mins after the commencement of IN delivery (reported in Chapter 2). The rapid transportation of endogenous CNTF from the nasal cavity is consistent with extracellular diffusion of CNTF through components of the peripheral olfactory

and trigeminal complex. Although the competitive binding and lesioning experiments suggested that CNTF transport via the trigeminal nerve is not receptor mediated and likely through the extracellular pathway, the reduced CNTF radioactivity in OB may suggest a receptor-mediated intracellular transport mechanism involving the ORNs. CNTF was delivered to brain regions functionally intact as supported by the demonstration of pSTAT3 signal pathway activation in multiple brain regions 30 mins after IN delivery. In a preliminary weight loss trial, it has been shown for the first time that IN delivered rhCNTF causes significant body weight loss in an obese rat model.

Following several previous studies which examine IN delivery of viral vectors, the second part of this thesis examined the feasibility of targeting different brain regions using IN administered adenovirus and AAV vectors containing an EGFP reporter (reported in Chapter 3). From the results presented in this chapter, it was found that the EGFP transgene product, which was expressed in the cell bodies of the adenoviral infected ORNs, was axonally transported in an anterograde direction to the nerve terminals in the olfactory bulb glomeruli, and further transported to other regions of the brain, as detected by EGFP fluorescence and Western blot 1 week after initial IN inoculation. Similarly, from AAV2 mediated EGFP expression in the olfactory mucosa, as confirmed by RT-PCR, a similar pattern of EGFP localization in different brain regions was observed 6 weeks post-inoculation. In consideration of the time frames involved in which EGFP fluorescence was observed in various rostral and caudal brain regions (i.e 1 week for AdV-EGFP and 6 weeks for AAV2-EGFP), it is possible that the expressed EGFP is axonally transported to the brain within ORNs via the intracellular pathway. However the extracellular pathway cannot be fully ruled out as a possible route of

entry into the brain from nasal mucosa for either the viral vector or transgene product.

4.2 Understanding the pathways of nose to brain transport

4.2.1 Animal models

Sprague-Dawley rats (in Chapters 2 and 3) and Obese Zucker rats (in Chapter 2) were used as the experimental animal models for the work presented in this thesis. Rats have been widely used in animal experiments and are established as excellent animal models to study the pathways involved in transport of macromolecules to the CNS from the nasal cavity. Although most studies investigating the nose-to-brain pathways have been performed in rodents, some studies in primates have also been reported (see Chapter 1, Table 1.1). As mentioned in section 1.4.5 (Chapter 1), animal models such as rodents are classified as macrosmatic while humans are considered to be microsmatic. While the olfactory mucosa in rats is spread throughout the posterior part of their nasal cavity covering 50% of the area, in humans, it appears to be more anteriorly distributed than previously assumed and constitutes approximately 3% of the area (Leopold et al., 2000)(Morrison and Costanzo, 1992). Others have reported the presence of ORNs in the anterior and medium part of the middle turbinate, the superior turbinate, and the dorsoposterior regions of the septum (Feron et al., 1998) In addition, CSF volume is replaced every 1hr in rats and every 5hrs in humans. Furthermore, as shown by Zhang et.al., CSF in the rat drains rapidly along selective and directional pathways from the ventral surface of the brain forward to the region of the cribiform plate and finally draining into nasal lymphatics (Zhang et al., 1992). Therefore careful consideration must be

exercised when extrapolating results seen in rat nose-to-brain studies to human trials due to these anatomical differences.

4.2.2 Intranasal delivery of a neurotrophic factor

The neurotrophic factor CNTF, which has considerable therapeutic potential for the treatment of several neurological diseases, is an excellent candidate for examining the pathways from olfactory mucosa to the CNS. The results presented in Chapter 2 demonstrate: (1) rapid IN delivery of CNTF to the brain along both olfactory and trigeminal extracellular pathways, (2) distribution of CNTF throughout the brain including key regions such as the hypothalamus, (3) effects of $ZnSO_4$ on CNTF transport along the olfactory neural pathway, (4) pSTAT3 signalling in the brain resulting from biologically active IN delivered CNTF, and (5) reduced body weight as a result of IN CNTF treatment.

As reported by Frey and Thorne *et. al.*, the neurotrophic factors NGF, IGF-1 and IFN- β, all undergo rapid extracellular transport to rostral and caudal regions of the brain along peripheral olfactory and trigeminal pathways (Frey 2nd et al., 1997; Thorne et al., 2004; Thorne et al., 2008). In these studies, the highest levels of radioiodinated protein were recorded in olfactory bulb and trigeminal nerve, along with regions in close proximity to these areas within 30 mins following IN delivery. Similarly, as reported in Chapter 2, CNS levels of I^{125}-CNTF peaked at an earlier time-point than did levels in the blood, which is consistent with a rapid extracellular entry into the CNS and a slower absorption into bloodstream from nasal epithelia. The I^{125}-CNTF radioactivity levels in the olfactory bulb, forebrain and trigeminal nerve did not follow the same pattern of I^{125}-CNTF radioactivity in the blood, which may add further support of a delivery mechanism to the brain which did not involve

systemic distribution from the bloodstream. At the earlier time-points of 30min and 3hrs, most of the transport along the olfactory pathway is not likely to involve axonal transport through ORNs, but rather be extracellular which occurs within 30mins as opposed to axonal transport which requires at least 6hrs to several days (Broadwell and Balin, 1985; Shipley, 1985; Baker and Spencer, 1986). To further clarify whether I^{125}-CNTF detected in CNS and peripheral tissues originated from the bloodstream following IN delivery, a separate group of rats would receive IV injection of I^{125}-CNTF to determine the area under the blood-concentration time curve (AUC) over a 30min time period when compared to a group which received IN I^{125}-CNTF. The amount of I^{125}-CNTF absorbed into the blood would be reflected by the AUC (Thorne et al., 2004). Therefore rats receiving IV I^{125}-CNTF could provide a measure of expected I^{125}-CNTF penetration from bloodstream into peripheral and central tissues following IN delivery.

Rapid extracellular entry of CNTF to rostral and caudal brain regions was further confirmed by the appearance of biotinylated-CNTF in neuronal cells of specific regions including: the anterior olfactory nucleus, entorhinal cortex, endopiriform cortex, lateral hypothalamus, cerebellum and trigeminal nucleus. The CNTF localised in these neuronal cells appeared to be cytoplasmic. However, to further reveal which cellular components contain biotinylated–CNTF, double-labelling using antibodies to vesicular and endosomal markers, such as Rab4 (an early endosomal marker), would be required.

The competitive binding experiment using unlabelled CNTF and the $ZnSO_4$ lesioning experiments, presented in Chapter 2, both showed a significant reduction in I^{125}-CNTF in the olfactory bulb but not in the trigeminal nerve, when compared to control groups. These results certainly provide additional support to the view that transportation of CNTF from the nasal cavity to the CNS via the trigeminal route is

not receptor mediated and predominantly through the extracellular pathway as seen in other studies using different proteins (Frey 2nd et al., 1997; Ross et al., 2004; Thorne et al., 2004; Yang et al., 2008). However, this result may also suggest that CNTF is internalised by ORNs through a receptor-mediated mechanism and axonally transported to the olfactory bulb. Although this route of CNS entry is certainly possible for the later time-points (i.e after 6hrs post IN delivery), it is still not entirely clear if CNTF is transported via this pathway during the 30 min period. However it is possible that the CNTF transport could occur via a fast axonal mechanism within the ORNs, travelling the short distance between olfactory epithelium and OB within the 30 min period, although further anterograde tracing experiments would be needed to clarify this. Alternatively the unlabelled CNTF may also be simply reducing the binding of labelled CNTF to receptors present in the olfactory bulb, as it has been reported by Lee *et. al.* (1997) that CNTF receptor-α mRNA is present in adult rat olfactory bulb (Lee et al., 1997).

It is known that CNTF activates the JAK and pSTAT3 signalling pathways of neurons in hypothalamic nuclei (Ip and Yancopoulos, 1996; Lambert et al., 2001; Anderson et al., 2003). Therefore the activation of the pSTAT3 signalling pathway, as seen by immunoreactive cells in the hypothalamus and thalamus, following IN delivery suggests that CNTF is delivered to the CNS intact and biologically active. As demonstrated in a study examining IN delivered vasoactive intestinal peptide (Dufes et al., 2003), a similar method could be used to determine whether IN delivered CNTF is intact compared to IV delivered CNTF. Samples of brain tissue and blood would be analysed by HPLC following IN and IV administration of I^{125}-CNTF.

Further evidence supporting the idea that IN delivered CNTF reaching the brain is functionally and biologically active is the successful body weight loss which

was observed in a genetically obese rat model as a result of IN CNTF treatment. Over the 12 day trial period, the CNTF (0.06mg/kg/day) treated OZR group experienced a 4% overall weight loss, comparable to that reported by Lambert *et. al*. who observed a similar weight loss in *ob/ob* mice using 0.1mg/kg/day of the modified $CNTF_{AX15}$ (AXOKINE) (Lambert et al., 2001). It is therefore anticipated that if the weight loss trial and CNTF treatments had been extended to one month, with IN administration of several different CNTF concentrations and more animals, greater weight loss may have been observed in the OZRs. The semi- quantitative measurement of food consumption by the CNTF treated OZRs, showed an overall reduced food consumption of 35% compared to the BSA treated group. However there was a large error variation observed which may have been eliminated by the use of properly controlled metabolic cages which were not available at the time of the trial. During the IN delivery trial period, at days 0 and 6, blood samples were collected from both OZR groups. Terminal blood was also collected and serum levels of glucose, insulin, cholesterol and triglycerides were measured in these samples. However, due to a large variation and error between the samples, differences between the treated and untreated groups could not be seen.

Although the results presented in Chapter 2 suggest rapid uptake of CNTF to the brain along both olfactory and trigeminal extracellular pathways, acting on satiety centres in the hypothalamus, one cannot rule out possible contributions for uptake via multiple mechanisms. For example, concerning the weight loss trial, the food intake may drop because the food is less palatable to the animals. This situation may occur if some of the IN delivered CNTF leaked out the back of the nasal cavity into the esophagus affecting gut sensory nerves or motor nerves causing the animal to feel nauseous. This is certainly possible as the 30-40uL i.n. delivered volume

would take up a 30-40mm^3 area of the nasal cavity and a proportion of this volume would end up being swept to the back of the nasal cavity and down the esophagus.

Another very important question which was not fully examined and resolved within the scope of this thesis was the potential CSF spread from the entry points of the olfactory nerve and trigeminal nerve. As suggested in Chapter 2, it is possible that the i.n. administered protein could rapidly gain access to the olfactory subarachnoid space CSF, where it could be distributed along the brain's ventral surface and be sequestered near the cerebellum and brainstem.

4.2.3 Intranasal delivery of viral vectors

With the increasing popularity of viral vectors as a vehicle for delivering therapeutic genes to specific targets in the CNS (Hermens and Verhaagen, 1998), several studies have examined the pathways of nose-to-brain transfer using different viral vectors (Draghia et al., 1995; Holtmaat et al., 1996; Kinoshita et al., 2002; Jerusalmi et al., 2003; Doi et al., 2005; Ozduman et al., 2008). The results presented in Chapter 3 follow these studies in examining the transport and brain distribution of adenoviral and AAV expressed transgene product. It was demonstrated that: (1) IN administered AdV-EGFP successfully infected ORNs and expressed EGFP which appeared to be axonally transported to the glomerular layer of the OB; (2) one week after IN delivery, EGFP was localised in several rostral and caudal brain regions; (3) AAV2-EGFP IN delivery resulted in similar EGFP brain localisation 6 weeks after initial inoculation; (4) EGFP mRNA was detected in the olfactory mucosa only.

It is known from several previous studies that adenoviral vectors efficiently transfect both ORNs and sustentacular cells in the olfactory epithelium (Holtmaat et al., 1996; Hermens et al., 1997; Holtmaat et al., 1997; Ivic et al., 2000; Soudais et al., 2001; Youngentob et al., 2004). Other studies have examined olfactory pathways

into the CNS using adenoviral vectors expressing the lacZ gene or WGA (Draghia et al., 1995; Zhao et al., 1996; Kinoshita et al., 2002; Doi et al., 2005). From the fluorescent imaging results presented in Chapter 2, ORNs and sustentacular cells in the olfactory epithelium were expressing EGFP 1 day after AdV-EGFP IN inoculation, however no EGFP expression was observed in the OB. After 1-2 weeks EGFP fluorescence was seen in the OB neural and glomerular layers, as well as several different rostral and caudal brain regions. The questions which arise from this study is; 1) whether adenoviral particles are internalized by ORNs and axonally transported to the OB, where they are released and transported into other brain regions; or 2) whether the transgene product EGFP is only synthesized in ORNs, but transported into the brain transsynaptically? To answer these questions, a real-time RT-PCR would need to be performed on different olfactory and brain regions using viral vector DNA sequence in the primers. These questions may be further clarified using biotinylated adenovirus in an IN delivery timecourse and immunohistochemistry to determine the geographical virus localisation. Additionally, immunostaining for markers of typical intracellular organelles such as large dense core vesicles, endosomes, and golgi, with imaging taken at high resolution with confocal microscopy, would determine which compartment the EGFP resides if it is transported transsynaptically. To further help resolve the mechanisms of viral vector transport through olfactory pathways, it would be useful to conduct a timecourse of i.n. delivery with varying doses of viral vector.

A recent study by Damjanovic *et. el.* (2008) found that IN inoculation of adenoviral vectors (Ad-GFP and Ad-Luc) lead to little or no viral dissemination to the brain (Damjanovic et al., 2008). However, all of their fluorescence imaging data was obtained from whole organ fluorescence imaging of the brain on a stereomicroscope, unlike the high power images of cellular EGFP fluorescence and

EGFP immunohistochemistry in specific rostral and caudal brain regions presented in Chapter 3 of this thesis. The Damjanovic study also generated quantitative data using adenoviral mediated luciferase expression in various central and peripheral organs. Although their luciferase activity was quite high in the OB, the whole brain gave very low activity levels which may have been different if individual brain regions were assayed. The fact that the study used n=3 mice per timepoint for the luciferase assay, an initial lower adenoviral dose of $5X10^7$ pfu/mouse and no indication of the mouse orientation during nasal delivery, may contribute to low luciferase activity in the brain. However the PCR analysis for adenoviral sequence in CNS and peripheral tissues found no adenoviral DNA in the brain which would be consistent with the idea that adenoviral vector remains in the ORNs following IN delivery.

Using IN administration of an AAV2-EGFP vector, as reported in Chapter 3, a similar localisation pattern of EGFP fluorescence as that of the AdV-EGFP study, was observed 6 weeks after inoculation. This neuronal cell localised fluorescence was confirmed by cytoplasmic EGFP localisation determined by immunohistochemistry and double-labelling with an anti-neurofilament antibody. Although the PCR data showed that EGPF mRNA was not detected in OB and brain 6 weeks after AAV IN delivery, it is conceivable that viral particles were degraded by DNAase and undetectable. It is also possible that AAV particles should be transported via a fast axonal transport mechanism and likely to be detectable in earlier time points. Thus, it would be useful to perform the same experiment by taking samples at 6 hrs, 16 hrs and 3 days after IN AAV delivery. mRNA from olfactory mucosa, olfactory bulb and several different brain regions would be extracted, and the synthesised cDNA analysed by PCR. Detection of AAV DNA in other brain regions will suggest that AAV2-EGFP is transported to the brain.

Successful detection of AAV DNA in olfactory mucosa but failure of detection in other brain regions will suggest that AAV particles are only present in the olfactory mucosa but not transported to the brain.

4.3 Thesis Conclusion

This PhD project has demonstrated that a significantly important neurotrophic factor, such as CNTF, can be rapidly targeted to multiple rostral and caudal CNS regions via an extracellular peripheral olfactory and trigeminal pathway, which bypasses the BBB through a non-invasive IN administration technique. In a rat model, it was revealed that the majority of IN delivered CNTF was transported via a previously discovered extracellular pathway to brain regions, such as the forebrain and ventromedial hypothalamus, in a biologically active form as determined by downstream signalling pathway activation. However, a proportion of the IN delivered CNTF may be transported to rostral brain areas via the intracellular pathway through ORNs, reaching secondary neurons in the OB glomerular layer. For the first time, IN delivered CNTF caused body weight loss in a genetically obese rat model which correlated to the biologically active CNTF localised in the hypothalamus. Finally it was demonstrated that both adenoviral and AAV vectors delivered a transgene product to various brain regions, via a possible intracellular pathway, through ORN axonal transport. The EGFP transgene product was observed in neuronal cell up to 6 weeks after initial IN inoculation.

4.4 Future Directions

Olfactory pathways into the brain have been successfully visualized by several groups using different types of IN delivered viral vector (Draghia et al., 1995; Holtmaat et al., 1996; Hermens et al., 1997; Soudais et al., 2001; Kinoshita et al.,

2002; Jerusalmi et al., 2003). However, most studies have used adenoviral vectors for visualisation of olfactory pathways. A further refinement to the use of AdV-EGFP and AAV2-EGFP vectors in visualising the olfactory intracellular pathway would be to introduce a WGA transgene to the existing viral vector constructs. As WGA is known to be efficiently internalised by neurons and transported retrogradely and anterogradely along axons (Dumas et al., 1979; Fabian and Coulter, 1985), it enables visualisation of primary and secondary olfactory pathways (Shipley, 1985; Baker and Spencer, 1986; Itaya, 1987). Additionally, a retrograde direction-specific transneuronal tracer, such as tetanus toxin C fragment (TTC), could be used as a transgene (Coen et al., 1997). This would enable a simultaneous expression of three molecules (EGFP ,WGA and TTC) which could provide detailed information on the neuronal connectivity patterns of the infected neurons (Kinoshita et al., 2002).

Although the IN CNTF treatment weight loss trial exhibited promising results in the OZR model, how well could this preliminary study be expanded towards an eventual human trial? Firstly, the CNTF weight loss trial was conducted in a genetically obese rat model and did not include a diet induced obesity model, which has been used in previous studies (Gloaguen et al., 1997; Lambert et al., 2001). Furthermore, only male OZRs were used in the trial because female rats were excluded due to their estrogen fluctuations which would result in large animal variations. Essentially, this preliminary CNTF weight loss trial would need to be expanded over a much longer period, including an IN treatment phase of up to one month and a post IN delivery phase to measure possible rebound weight gain when treatment is ceased. As the original $CNTF_{AX15}$ (AXOKINE) human antiobesity study (Ettinger et al., 2003) was discontinued due to insufficient efficacy and the presence of unwanted serum anti-CNTF antibodies, a new study utilising the non-invasive nasal delivery system may achieve better long term results.

As seen in several recent studies, IN protein therapeutics have been demonstrated to be effective in humans reaching the brain without altering systemic blood levels and in some cases, such as IN insulin, improving memory, altering food consumption, body weight and body fat for example. Nasal administration of the neuropeptides, melanocortin (4-10), vasopressin and insulin to the CSF in humans has been documented to bypass the bloodstream, reaching the CSF within 30 mins (Born et al., 2002). It has also been found that IN insulin improves memory and mood in healthy adults (Benedict et al., 2004; Benedict et al., 2007; Benedict et al., 2008), in obese men (Hallschmid et al., 2008), and also improved memory in patients with Alzheimer's disease without altering blood levels of insulin or glucose (Reger et al., 2006). A trial involving 21 days of IN delivered insulin resulted in significantly improved verbal memory, attention span and functioning in Alzheimer's patients (Reger et al., 2008; Reger et al., 2008). More recently it has been discovered that nasal delivered insulin attenuates the response to psychosocial stress in males (Bohringer et al., 2008). Oxytocin delivered by the nasal route has been found to increase trust following direct nose to brain delivery (Kosfeld et al., 2005).

Overall, the potential advantages of the IN delivery route to CNS include the ability to achieve some degree of CNS targeting without significant increase in systemic bloodstream drug concentrations, its non-invasiveness and relatively simple administration procedure. Possible disadvantages may include the need for higher doses due to relatively low CNS bioavailabilities, enzymatic degradation and mucociliary clearance by nasal proteases and peptidases (Thorne and Frey 2nd, 2001). However, growing evidence highlights that several neuropeptide drugs can selectively influence the CNS following IN delivery in humans while remaining ineffective following IV administration (Pietrowsky et al., 1996). Therefore the

intranasal delivery strategy will continue to be an effective, non-invasive method of delivering neurotrophic factors and viral vectors, attracting continues investigation.

APPENDICES

Appendix 1. Experimental Protocols Used in Chapter 3

Appendix 1.1 Western Blotting Analysis

Western Buffer Preparation – Solutions

Most solutions were adapted from:

- Sambrook, J., Fritsch, E.F., and Maniatis, T. (1989) Molecular Cloning: A laboratory manual Second edition. Cold Spring Harbour Laboratory Press, USA. Page 18.51-18.65. (Maniatis et al., 1989)
- Protocol manual for EGFP polyclonal antibodies from Cell Signalling Technology, Australia.

2× SDS gel-loading buffer (Cell Signalling Technology protocol, Australia)

125 mM Tris-Cl (pH 6.8 at 25^{o}C)

100 mM dithiothreitol (DTT)

2% SDS (electrophoresis grade)

0.1% bromophenol blue

10% glycerol

2× SDS gel-loading buffer lacking dithiothreitol can be stored at room temperature. DTT should be added just before the loading buffer is used, from a 1 M stock*.

* Prepare 1M DTT stock in Sodium Acetate (0.01M) at pH=5.2. store at –20^{o}C.

Tris-glycine electrophoresis buffer (Maniatis et al., 1989)

25 mM Tris

250 mM glycine (electrophoresis grade) (pH 8.3)

0.1% SDS

A 5× stock can be made by dissolving 15.1 g of Tris base and 94 g of glycine in 900 ml of MilliQ H_2O. Then 50 ml of a 10% (w/v) SDS stock solution is added, and the volume is adjusted to 1L with H_2O.

Transfer buffer (1×) (Maniatis et al., 1989)

39mM glycine
48mM Tris base
0.037% SDS
20% methanol
Make a 10× glycine and Tris base stock requiring:

390mM glycine → 29.28g
480mM Tris base → 58.08g in 1L, pH 8.3

Prepare 1L of transfer buffer (pH 8.3) by adding 100ml of 10 × glycine and Tris base (pH=8.3) to 200ml of methanol and 3.7ml of 10%SDS, then make solution up to 1L with MilliQ H_2O.

Preparation of 30% acrylamide (Sambrook et al., 1989)

Dissolve 29 g of acrylamide and 1 g of Bis-acrylamide in 100 ml of H_2O.
Heat to dissolve and stir with a magnetic stirrer.

10× TBS (Tris-buffered saline) (Cell Signalling Technology,)

To prepare 1 litre of 10× TBS: add 24.2 g Tris base, 80 g NaCl into MilliQ H_2O, adjust pH to 7.6 with HCl (always use at 1×).

1× TBS, 0.1% Tween-20 (TBST)

Add 100ml of 10× TBS, and dissolve 1ml of Tween-20 in 800ml MilliQ H2O, then make solution to 1L.

Blocking Buffer (5% skim milk block)

1× TBST with 5% w/v skim milk powder; for 50 ml, add 2.5g of milk powder into 50ml of 1× TBST.

Primary antibody dilutions

- For polyclonal rabbit anti-EGFP (1:2000) (Chemicon Millipore, North Ryde, NSW), 1%BSA in 1× PBS is used.

- For mouse anti-β-Tubulin E7 (1:1000) (Sigma-Aldrich, Castle Hill, NSW), 1%BSA in 1× PBS is used

HRP conjugated Secondary antibody dilutions

- For EGFP detection, anti-rabbit IgG-HRP pre-absorbed in 2% rat serum (1:10,000) from Sigma (Castle Hill, NSW) was used.
- For β-tubulin detection, the rabbit anti mouse IgG-HRP (1:20,000) was used.

Ponceau Red A Protein dye

Add 0.2% w/v Ponceau S to 3% TCA (trichloroacetic acid) in MilliQ H_2O, then mix and filter dye through 1M Whatmann paper. Store at RT in the dark.

SDS Polyacrylamide Gel Electrophoresis

1. Set up polyacrylamide gel mini-PROTEAN electrophoresis equipment from BioRad, (Gladesville, NSW) according to manufacture instructions.
2. Preparation of 10 % SDS PAGE (5 ml)

H_2O	1.9 ml
30% acrylamide mix	1.7 ml
1.5M Tris (pH 8.8)	1.3 ml
10% SDS	0.05 ml
10% ammonium persulfate	0.05 ml

   Mix all, then add 2µl TEMED , mix immediately
3. Load gel using syringe immediately and add a layer of water to prevent gel from drying. Allow 20-30min for gel to set.
4. Preparation of 5% stacking gel (1ml)

H_2O	0.68 ml
30% acrylamide mix	0.17 ml
1M Tris (pH = 6.8)	0.13 ml
10% SDS	0.01 ml
10% ammonium persulfate	0.01 ml

   Mix all, then add TEMED 1µl, mix immediately. Insert comb into position and load stacking gel using 1 ml tips.

5. Preparing the loading sample:

   Add 30 μg of growth plate protein in 1× loading buffer plus 50mM DTT.
6. Boil samples for 6 mins, and then place them immediately on ice.
7. Load samples:
   1) Remove the comb from stacking gel and briefly run under water to remove gel residue.
   2) Place the gel into gel tank and add 1× Tris-glycine electrophoresis buffer. Especially in the well.
   3) Using a 20 μl pipette and fine pipette tip slowly load samples.
   4) Lastly, load 5μl of protein marker (Bio RAD, Australia).
   5) Place electrode lid on the tank and run gel at 50V and then increase to 200V when the loading dye has reached the resolving gel. Stop electrophoresis when dye front is 1cm away the bottom of resolving gel.

Electrotransfer of proteins on to Nitrocellulose membrane using mini-PROTEAN transfer system.

1. In a shallow container place 6 sponges and nitrocellulose membrane (cut to the right size) and add 1× transfer buffer
2. Firstly, wet the apparatus and then place 3 sponges plus the SDS gel on top, and then place the nitrocellulose membrane on top of the gel (make sure there are no air bubbles). Lastly, place the last 3 sponges and then the electrode lid.
3. Run transfer at 60mA for 1 hr and 15 mins.
4. After stopping the transfer, label makers clearly with colour pencils and place the membrane into water.
5. Pour the water out and add Ponceau red to check the quality of transfer (1 min).
6. Remove Ponceau red using water, for 5 mins.

Western blotting detection of EGFP and β-tubulin

1. Wash in 1× TBST for 5 mins (3×)
2. Block membrane in 5% milk in 1× TBST blocking buffer
3. Wash with TBST for 5 mins 3×
4. Incubate membrane in 1ml primary antibody (anti-EGFP or β-tubulin at the appropriate dilution describe in Western blotting solution section).

5. Add the primary antibody on a large plastic dish (petri-dish), and then slowly place the membrane with the protein side facing directly down onto the antibody solution (make sure no air bubble is formed). To prevent the membrane form drying out during the overnight incubation at 4^{o}C, parafilm is used to cover the membrane, and the plastic dish is further sealed with a lid or plastic wrap.
6. Wash 3× for 5 mins each with TBST.
7. Incubate membrane with HRP-conjugated secondary antibodies in 1 ml Blocking Buffer for 1 hr at RT.
8. Wash with 1× TBST for 5 mins (3×).
9. Prepare enhanced chemiluminescence solution A and B

   Solution A: 5ml Tris, pH 8 (0.1M),
   22µl Coumaric acid in DMSO (90mM) stock (stored at -20^{o}C),
   50µl Luminol in DMSO (250mM) stock (stored at –20^{o}C).

   Solution B: 5ml Tris, pH 8 (0.1M)
   3ml 30% H_2O_2.

Finally, incubate membrane in Solution A and B for 1 min in dark room, and expose to X-ray film (10min). Develop and fix x-ray film using Kodak developer and fixer (Kodak, Australia).

Appendix 1.2 Reverse transcription of total RNA to cDNA using SuperScript™ II

(Adapted from Invitrogen, Cat # 18064-014 instructions)

Solution Required:

- SuperScript II RNase H$^-$ reverse transcriptase (Invitrogen, Australia)
- 5× First strand buffer (Invitrogen, Mt. Waverley VIC)
- 0.1M DTT (Invitrogen, Mt. Waverley VIC)
- Oligo dT Primer (GeneWorks, Adelaide, SA)*
- dNTPs mix (Geneworks, Adelaide, SA)
- RNase OUT (Invitrogen, Mt. Waverley VIC)

* Reconstitute 100 µg of Oligo dTs in 1 ml of water to obtain concentration of 100ng/µl. Prepare batches of 10 µl and 100 µl aliquot

Methods:

To prepare total RNA for cDNA transcription, 2 μl of 200ng Oligo dTs and 1μl of dNTPs mix was added to separate 2μg olfactory or brain RNA samples, and then RNase-free water was added to make each sample up to 12 μl. The sample mixtures were heated to 65 ^{o}C for 5min and quick chilled on ice. Tubes were centrifuge briefly to collect the contents (remember to set heat block to 70 ^{o}C). 4μl of 5X first-strand buffer, 2 μl of 0.1M DTT and 1 μl of RNase OUT were added to the sample mixtures, mixed gently and incubated at 25 ^{o}C for 10min. Mixtures were incubate at 42 ^{o}C for 2 min, then 1 μl of SuperScript were added and mixed by pipetting gently up and down, and mixtures were further incubated at 42 ^{o}C for 50 min. Finally reactions were inactivated by heating the mixtures at 70 ^{o}C for 15 min. The 20 μl cDNA samples, which will be used as templates for amplication in real time RT-PCR, were stored cDNA at -20 ^{o}C.

Appendix Table 1.1

Component	Volume/Reaction	Final Concentration
template RNA		2μg (per 20μL reaction)
dNTP mix (10mM)	1μL	0.5mM
Oligo dT Primer (10μM)	2μL	1μM
5X First-strand buffer	4 μL	1X
0.1M DTT	2 μL	0.01M
RNAse inhibitor (10U/μL)	1 μL	10M (per 20μL reaction)
Superscript II	1μL	200 U (per 20μL reaction)
RNAse-free water	up to 20μL Total Vol.	

Appendix 1.3 Real-time RT-PCR

All Forward (Fwd) and Reverse (Rev) oligonucleotide primers were synthesized by Geneworks (Adelaide, SA).

EGFP-Fwd:	5'-GCAGTGCTTTTCCAGATACCCAC-3'	Tm=57.6^{0}C
EGFP-Rev:	5'-GCCGAGAATGTTTCCATCCTCC-3'	Tm=58.4^{0}C

211 bp major product.

Appendix 2. Personal Publications (2000-2007)

1) Karageorgos L, Brooks DA, **Pollard A**, Melville EL, Hein LK, Clements PR, Ketteridge D, Swiedler SJ, Beck M, Giugliani R, Harmatz P, Wraith JE, Guffon N, Leão Teles E, Sá Miranda MC, Hopwood JJ. (2007) Mutational analysis of 105 mucopolysaccharidosis type VI patients. **Hum Mutat.** Sep;28(9):897-903.

2) Karageorgos L, Brooks DA, Harmatz P, Ketteridge D, **Pollard A**, Melville EL, Parkinson-Lawrence E, Clements PR and Hopwood JJ.(2007) Mutational analysis of mucopolysaccharidosis type VI patients undergoing a phase II trial of enzyme replacement therapy. **Mol Genet Metab**. Feb;90(2):164-70. Epub 2006 Dec 11.

3) Karageorgos L, Harmatz P, Simon J, **Pollard A**, Clements PR, Brooks DA and Hopwood JJ. (2004) Mutational analysis of mucopolysaccharidosis type VI patients undergoing a trial of enzyme replacement therapy.
Hum Mutat. Mar;23(3):229-33.

4) Jolly RD, Johnstone AC, Hubbard DE, Yogalingam G and **Pollard A.** (2002) Screening for the Mucopolysaccharidosis-IlIA gene in Huntaway dogs. **N Z Vet J**. Jun;50(3):122.

5) Yogalingam G, **Pollard T**, Gliddon B, Jolly RD and Hopwood JJ. (2002) Identification of a mutation causing mucopolysaccharidosis type IIIA in New Zealand Huntaway dogs. **Genomics**. Feb;79(2):150-3.

6) Paton BC, Solly PB, Nelson PV, **Pollard AN**, Sharp PC and Fietz MJ. (2002) Molecular analysis of genomic DNA allows rapid, and accurate, prenatal diagnosis of peroxisomal D-bifunctional protein deficiency. **Prenat Diagn.** Jan;22(1):38-41.

7) Paton BC and **Pollard AN.** (2000) Molecular changes in the D-bifunctional protein cDNA sequence in Australasian patients belonging to the bifunctional protein complementation group. **Cell Biochem Biophys**.;32 Spring:247-51.

BIBLIOGRAPHY

Adams DR (1992). "Fine structure of the vomeronasal and septal olfactory epithelia and of glandular structures." Microsc Res Tech **23**(1): 86-97.

Adler R, Landa KB, Manthorpe M and Varon S (1979). "Cholinergic neuronotrophic factors: intraocular distribution of trophic activity for ciliary neurons." Science **204**(4400): 1434-1436.

Aebischer P, Schluep M, Deglon N, Joseph J-M, Hirt L, Heyd B, Goddard M, Hammang JP, Zurn AD, Kato AC, Regli F and Baetge EE (1996). "Intrathecal delivery of CNTF using encapsulated genetically modifiedxenogeneic cells in amyotrophic lateral sclerosis patients." Nat Med **2**(6): 696-699.

Akli S, Caillaud C, Vigne E, Stratford-Perricaudet LD, Poenaru L, Perricaudet M, Kahn A and Peschanski MR (1993). "Transfer of a foreign gene into the brain using adenovirus vectors." Nat Genet **3**(3): 224-228.

Als, Cntf, Treatment, Study and Group (1996). "A double-blind placebo-controlled clinical trial of subcutaneous recombinant human ciliary neurotrophic factor (rHCNTF) in amyotrophic lateral sclerosis." Neurology **46**(5): 1244-.

Alvarez-Buylla A and Garcia-Verdugo JM (2002). "Neurogenesis in adult subventricular zone." J Neurosci **22**(3): 629-34.

Anand Kumar T, David G, Kumar K, Umberkoman B and Krishnamomorthy M (1974). A new approach to fertility regulation by interfering with neuroendocrine pathways. Proceedings of the International Symposium on Neuroendocrine Regulation of Fertility, Simla, India, Karger, Basel, Switzerland.

Anand Kumar TC, David GF, Sankaranarayanan A, Puri V and Sundram KR (1982). "Pharmacokinetics of progesterone after its administration to ovariectomized rhesus monkeys by injection, infusion, or nasal spraying." Proc Natl Acad Sci U S A **79**(13): 4185-9.

Anderson KD, Lambert PD, Corcoran TL, Murray JD, Thabet KE, Yancopoulos GD and Wiegand SJ (2003). "Activation of the Hypothalamic Arcuate Nucleus Predicts the Anorectic Actions of Ciliary Neurotrophic Factor and Leptin in Intact and Gold Thioglucose-Lesioned Mice." Journal of Neuroendocrinology **15**(7): 649-660.

Anton F and Peppel P (1991). "Central projections of trigeminal primary afferents innervating the nasal mucosa: A horseradish peroxidase study in the rat." Neuroscience **41**(2-3): 617-628.

Arimoto Y, Nagata H, Isegawa N, Kumahara K, Isoyama K, Konno A and Shirasawa H (2002). "In vivo Expression of Adenovirus-mediated lacZ Gene in Murine Nasal Mucosa." Acta Oto-Laryngologica **122**(6): 627-633.

Baker H and Genter MB (2003). The Olfactory System and the Nasal Mucosa as Portals of Entry of Viruses, Drugs, and Other Exogenous Agents into the Brain. Handbook of Olfaction and Gustation, Second Edition. Doty RL, Informa Healthcare**:** 549 - 574.

Baker H and Spencer RF (1986). "Transneuronal transport of peroxidase-conjugated wheat germ agglutinin (WGA-HRP) from the olfactory epithelium to the brain of the adult rat." Exp Brain Res **63**(3): 461-73.

Balin BJ, Broadwell RD, Salcman M and el-Kalliny M (1986). "Avenues for entry of peripherally administered protein to the central nervous system in mouse, rat, and squirrel monkey." J Comp Neurol **251**(2): 260-80.

Bancroft JD and Stevens A (1982). Theory and practice of histological techniques Edinburgh ; New York Churchill Livingstone.

Banks WA, During MJ and Niehoff ML (2004). "Brain Uptake of the Glucagon-Like Peptide-1 Antagonist Exendin(9-39) after Intranasal Administration." J Pharmacol Exp Ther **309**(2): 469-475.

Barkats M, Bilang-Bleuel A, Buc-Caron MH, Castel-Barthe MN, Corti O, Finiels F, Horellou P, Revah F, Sabate O and Mallet J (1998). "Adenovirus in the brain: recent advances of gene therapy for neurodegenerative diseases." Prog Neurobiol **55**(4): 333-341.

Barnett EM and Perlman S (1993). "The Olfactory Nerve and Not the Trigeminal Nerve Is the Major Site of CNS Entry for Mouse Hepatitis Virus, Strain JHM." Virology **194**(1): 185-191.

Bauer S, Rasika S, Han J, Mauduit C, Raccurt M, Morel G, Jourdan F, Benahmed M, Moyse E and Patterson PH (2003). "Leukemia Inhibitory Factor Is a Key Signal for Injury-Induced Neurogenesis in the Adult Mouse Olfactory Epithelium." J. Neurosci **23**(5): 1792-1803.

Bemelmans A-P, Husson I, Jaquet M, Mallet J, Kosofsky BE and Gressens P (2006). "Lentiviral-mediated gene transfer of brain-derived neurotrophic factor is neuroprotective in a mouse model of neonatal excitotoxic challenge." Journal of Neuroscience Research **83**(1): 50-60.

Benedict C, Hallschmid M, Hatke A, Schultes B, Fehm HL, Born J and Kern W (2004). "Intranasal insulin improves memory in humans." Psychoneuroendocrinology **29**: 1326 - 1334.

Benedict C, Hallschmid M, Schmitz K, Schultes B, Ratter F, Fehm HL, Born J and Kern W (2007). "Intranasal insulin improves memory in humans: superiority of insulin aspart." Neuropsychopharmacology **32**: 239 - 243.

Benedict C, Kern W, Schultes B, Born J and Hallschmid M (2008). "Differential Sensitivity of Men and Women to Anorexigenic and Memory-Improving Effects of Intranasal Insulin." J Clin Endocrinol Metab **93**(4): 1339-1344.

Bergelson JM, Cunningham JA, Droguett G, Kurt-Jones EA, Krithivas A, Hong JS, Horwitz MS, Crowell RL and Finberg RW (1997). "Isolation of a common receptor for Coxsackie B viruses and adenoviruses 2 and 5." Science **275**(5304): 1320-3.

Bodian D and Howe HA (1941). "Experimental studies on intraneural spread of poliomyelitis virus." Bulletin of the Johns Hopkins Hospital **68**: 248-267.

Bohringer A, Schwabe L, Richter S and Schachinger H (2008). "Intranasal insulin attenuates the hypothalamic-pituitary-adrenal axis response to psychosocial stress." Psychoneuroendocrinology **33**(10): 1394-400.

Born J, Lange T, Kern W, McGregor GP, Bickel U and Fehm HL (2002). "Sniffing neuropeptides: a transnasal approach to the human brain." Nature Neurosci **5**(6): 514.

Bradbury MW, Cserr HF and Westrop RJ (1981). "Drainage of cerebral interstitial fluid into deep cervical lymph of the rabbit." Am J Physiol **240**(4): F329-36.

Bradbury MW and Westrop RJ (1983). "Factors influencing exit of substances from cerebrospinal fluid into deep cervical lymph of the rabbit." J Physiol **339**: 519-34.

Brightman MW (1977). "Morphology of blood-brain interfaces." Exp Eye Res **25**(Supplement 1): 1-25.

Brinker T, Ludemann W, Berens von Rautenfeld D and Samii M (1997). "Dynamic properties of lymphatic pathways for the absorption of cerebrospinal fluid." Acta Neuropathol **94**(5): 493-8.

Brittebo EB and Eriksson C (1995). "Taurine in the olfactory system: effects of the olfactory toxicant dichlobenil." Neurotoxicology **16**(2): 271-80.

Broadwell RD (1989). "Transcytosis of macromolecules through the blood-brain barrier: a cell biological perspective and critical appraisal." Acta Neuropathol **79**(2): 117-28.

Broadwell RD and Balin BJ (1985). "Endocytic and exocytic pathways of the neuronal secretory process and trans-synaptic transfer of wheat germ agglutinin-horseradish peroxidase in vivo." J Comp Neurol **242**(4): 632-50.

Brownless J and Williams CH (1993). "Peptidases, peptides, and the mammalian blood-brain barrier." J Neurochem **60**(3): 793-803.

Buck L and Axel R (1991). "A novel multigene family may encode odorant receptors: a molecular basis for odor recognition." Cell **65**(1): 175-87.

Buck LB (1996). "Information coding in the vertebrate olfactory system." Annu Rev Neurosci **19**: 517-44.

Buckland ME and Cunningham AM (1999). "Alterations in expression of the neurotrophic factors glial cell line-derived neurotrophic factor, ciliary neurotrophic factor and brain-derived neurotrophic factor, in the target-deprived olfactory neuroepithelium." Neuroscience **90**(1): 333-347.

Buiakova OI, Krishna NSR, Getchell TV and Margolis FL (1994). "Human and Rodent OMP Genes: Conservation of Structural and Regulatory Motifs and Cellular Localization." Genomics **20**(3): 452-462.

Burd GD, Davis BJ, Macrides F, Grillo M and Margolis FL (1982). "Carnosine in primary afferents of the olfactory system: an autoradiographic and biochemical study." J Neurosci **2**(2): 244-55.

Cancalon P (1982). "Degeneration and regeneration of olfactory cells induced by ZnSO4 and other chemicals." Tissue and Cell **14**(4): 717-33.

Capsoni S, Giannotta S and Cattaneo A (2002). "Nerve growth factor and galantamine ameliorate early signs of neurodegeneration in anti-nerve growth factor mice." Proc Natl Acad Sci U S A **99**(19): 12432-12437.

Carson KA (1984). "Quantitative localization of neurons projecting to the mouse main olfactory bulb." Brain Res Bull **12**(6): 629-34.

Carter LA and Roskams AJ (2002). "Neurotrophins and their receptors in the primary olfactory neuraxis." Microsc Res Tech **58**(3): 189-196.

Cedarbaum J, Chapman C and Charatan M, et al. (1996). "A double-blind placebo-controlled clinical trial of subcutaneous recombinant human ciliary neurotrophic factor (rHCNTF) in amyotrophic lateral sclerosis. ALS CNTF Treatment Study Group." Neurology **46**(5): 1244-9.

Cedarbaum J, Chapman C and Charatan Mea (1995). "A phase I study of recombinant human ciliary neurotrophic factor (rHCNTF) in patients with amyotrophic lateral sclerosis. The ALS CNTF Treatment Study (ACTS) Phase I-II Study Group." Clin Neuropharmacol **18**(6): 515-32.

Charlier N, Leyssen P, Paeshuyse J, Drosten C, Schmitz H, Van Lommel A, De Clercq E and Neyts J (2002). "Infection of SCID mice with Montana Myotis leukoencephalitis virus as a model for flavivirus encephalitis." J Gen Virol **83**(Pt 8): 1887-96.

Charlton S, Whetstone J, Fayinka S, Read K, Illum L and Davis S (2008). "Evaluation of Direct Transport Pathways of Glycine Receptor Antagonists and an Angiotensin Antagonist from the Nasal Cavity to the Central Nervous System in the Rat Model." Pharm Res. **25**(7): 1531-1543.

Chen XQ, Fawcett JR, Rahman YE, Ala TA and Frey 2nd WH (1998). "Delivery of Nerve Growth Factor to the Brain via the Olfactory Pathway." J Alzheimers Dis **1**(1): 35-44.

Chess A, Buck L, Dowling MM, Axel R and Ngai J (1992). "Molecular biology of smell: expression of the multigene family encoding putative odorant receptors." Cold Spring Harb Symp Quant Biol **57**: 505-16.

Chomczynski P and Sacchi N (1987). "Single-step method of RNA isolation by acid guanidinium thiocyanate-phenol-chloroform extraction." Anal Biochem **162**(1): 156-9.

Chou K-J and Donovan MD (1998). "Lidocaine distribution into the CNS following nasal and arterial delivery: a comparison of local sampling and microdialysis techniques." Int J Pharm **171**(1): 53-61.

Chow HS, Chen Z and Matsuura GT (1999). "Direct transport of cocaine from the nasal cavity to the brain following intranasal cocaine administration in rats." J Pharm Sci **88**(8): 754-8.

Cleland TA and Linster C (2003). Central Olfactory Structures. Handbook of Olfaction and Gustation, Second Edition. Doty RL. New York, Informa Healthcare**:** 165 - 180.

Coen L, Osta R, Maury M and Brulet P (1997). "Construction of hybrid proteins that migrate retrogradely and transynaptically into the central nervous system." Proc Natl Acad Sci U S A **94**(17): 9400-9405.

Cometto-Muz JE and Doty RL (2003). Trigeminal Chemosensation. Handbook of Olfaction and Gustation, Second Edition. Doty RL, Informa Healthcare**:** 981 - 1000.

Curtis R, Adryan KM, Zhu Y, Harkness PJ, Lindsay RM and DiStefano PS (1993). "Retrograde axonal transport of ciliary neurotrophic factor is increased by peripheral nerve injury." Nature **365**(6443): 253-255.

Dahlin M (2000). Nasal administration of compounds active in the central nervous system: Exploring the olfactory system. Medicinska vetenskapsområdet, Faculty of Pharmacy, Department of Pharmacy. Uppsala Uppsala University. **Doctoral thesis**.

Dahlin M, Bergman U, Jansson B, Björk E and Brittebo E (2000). "Transfer of Dopamine in the Olfactory Pathway Following Nasal Administration in Mice." Pharm Res. **17**(6): 737-742.

Damjanovic D, Zhang X, Mu J, Fe Medina M and Xing Z (2008). "Organ distribution of transgene expression following intranasal mucosal delivery of recombinant replication-defective adenovirus gene transfer vector." Genet Vaccines Ther **6**(5): 5.

Davis S, Aldrich TH, Ip NY, Stahl N, Scherer S, Farruggella T, DiStefano PS, Curtis R, Panayotatos N, Gascan H and et a (1993). "Released form of CNTF receptor alpha component as a soluble mediator of CNTF responses." Science **259**(5102): 1736-1739.

Davson H (1967). Physiology of Cerebralspinal Fluid. London, J & A Churchill Ltd.

De Lorenzo A (1970). The olfactory neuron and the blood-brain barrier. Taste and Smell in vertebrates. Wolstenholme G and Knigh tJ. London, Churchill, J. and A. Churchill Ltd.**:** 151–176.

De Lorenzo AJ (1957). "Electron microscopic observations of the olfactory mucosa and olfactory nerve." J. Cell Biol. **3**(6): 839-850.

de Olmos J, Hardy H and Heimer L (1978). "The afferent connections of the main and the accessory olfactory bulb formations in the rat: an experimental HRP-study." J Comp Neurol **181**(2): 213-44.

De Rosa R, Garcia AA, Braschi C, Capsoni S, Maffei L, Berardi N and Cattaneo A (2005). "Intranasal administration of nerve growth factor (NGF) rescues recognition memory deficits in AD11 anti-NGF transgenic mice." Proc Natl Acad Sci U S A **102**(10): 3811-3816.

Deguchi Y, Naito T, Yuge T, Furukawa A, Yamada S, Pardridge WM and Kimura R (2000). "Blood-Brain Barrier Transport of 125I-Labeled Basic Fibroblast Growth Factor." Pharm Res. **17**(1): 63-69.

Di Marco A, Gloaguen I, Graziani R, Paonessa G, Saggio I, Hudson KR and Laufer R (1996). "Identification of ciliary neurotrophic factor (CNTF) residues essential for leukemia inhibitory factor receptor binding and generation of CNTF receptor antagonists." Proc Natl Acad Sci U S A **93**(17): 9247-9252.

Doi K, Nibu K, Ishida H, Okado H and Terashima T (2005). "Adenovirus-mediated gene transfer in olfactory epithelium and olfactory bulb: a long-term study." Annals of Otology, Rhinology & Laryngology **114**(8): 629-633.

Doucette R (1993). "Glial cells in the nerve fiber layer of the main olfactory bulb of embryonic and adult mammals." Microsc Res Tech **24**(2): 113-30.

Draghia R, Caillaud C, Manicom R, Pavirani A, Kahn A and Poenaru L (1995). "Gene delivery into the central nervous system by nasal instillation in rats." Gene Therapy **2**(6): 418-23.

Dufes C, Olivier J-C, Gaillard F, Gaillard A, Couet W and Muller J-M (2003). "Brain delivery of vasoactive intestinal peptide (VIP) following nasal administration to rats." Int J Pharm **255**(1-2): 87-97.

Dumas M, Schwab ME and Thoenen H (1979). "Retrograde axonal transport of specific macromolecules as a tool for characterizing nerve terminal membranes." J Neurobiol **10**(2): 179-97.

Esiri MM and Tomlinson AH (1984). "Herpes simplex encephalitis: Immunohistological demonstration of spread of virus via olfactory and trigeminal pathways after infection of facial skin in mice." Journal of the Neurological Sciences **64**(2): 213-217.

Ettinger MP, Littlejohn TW, Schwartz SL, Weiss SR, McIlwain HH, Heymsfield SB, Bray GA, Roberts WG, Heyman ER, Stambler N, Heshka S, Vicary C and Guler HP (2003). "Recombinant variant of ciliary neurotrophic factor for weight loss in obese adults: a randomized, dose-ranging study." Jama **289**(14): 1826-32.

Evans C (2003). Vomeronasal chemoreception in vertebrates : a study of the second nose. London; River Edge, N.J., Imperial College Press ; Distributed by World Scientific Pub.

Evans J and Hastings L (1992). "Accumulation of Cd(II) in the CNS depending on the route of administration: intraperitoneal, intratracheal, or intranasal." Fundam Appl Toxicol **19**(2): 275-8.

Fabian RH and Coulter JD (1985). "Transneuronal transport of lectins." Brain Res **344**(1): 41-8.

Fairbrother R and Hurst E (1930). "The pathogenesis of, and propagation of the virus in, experimental poliomyelitis." J. Path. Bact. **33**: 17-45.

Febbraio MA (2007). "gp130 receptor ligands as potential therapeutic targets for obesity." J Clin Invest **117**(4): 841-9.

Ferguson IA, Schweitzer JB, Bartlett PF and Johnson Jr. EM (1991). "Receptor-mediated retrograde transport in CNS neurons after intraventricular administration of NGF and growth factors." J Comp Neurol **313**(4): 680-692.

Feron F, Perry C, Cochrane J, Licina P, Nowitzke A, Urquhart S, Geraghty T and Mackay-Sim A (2005). "Autologous olfactory ensheathing cell transplantation in human spinal cord injury." Brain **128**(12): 2951-2960.

Feron F, Perry C, McGrath JJ and Mackay-Sim A (1998). "New Techniques for Biopsy and Culture of Human Olfactory Epithelial Neurons." Arch Otolaryngol Head Neck Surg **124 (8)**: 861-866.

Finiels F, Gimenez y Ribotta M, Barkats M, Samolyk ML, Robert JJ, Privat A, Revah F and Mallet J (1995). "Specific and efficient gene transfer strategy offers new potentialities for the treatment of motor neurone diseases." Neuroreport **6**(18): 2473-8.

Fliedner S, Schulz C and Lehnert H (2006). "Brain Uptake of Intranasally Applied Radioiodinated Leptin in Wistar Rats." Endocrinology **147**(5): 2088-2094.

Frenkel D and Solomon B (2002). "Filamentous phage as vector-mediated antibody delivery to the brain." Proc Natl Acad Sci U S A **99**(8): 5675-5679.

Frey 2nd WH, Liu J, Chen X, Thorne RG, Fawcett JR, Ala TA and Rahman YE (1997). "Delivery of 125I-NGF to the brain via the olfactory route." Drug Deliv **4**(2): 87-92.

Frey WH (1991). Neurologic Agents for Nasal Administration to the Brain. Organization WIP. Geneva, Switzerland:, Frey, W. H. **WO/1991/007947**.

Frey WH (2002). "Bypassing the blood-brain barrier to delivery therapeutic agents to the brain and spinal cord." Drug Delivery Technol **5**: 46 - 49.

Getchell ML and Getchell TV (1992). "Fine structural aspects of secretion and extrinsic innervation in the olfactory mucosa." Microsc Res Tech **23**(2): 111-27.

Geurkink N (1983). "Nasal anatomy, physiology, and function." J Allergy Clin Immunol **72**(2): 123-8.

Gizurarson S, Thorvaldsson T, Sigurdsson P and Gunnarsson E (1997). "Selective delivery of insulin into the brain: Intraolfactory absorption." Int J Pharm **146**(1): 135-141.

Gloaguen I, Costa P, Demartis A, Lazzaro D, Di Marco A, Graziani R, Paonessa G, Chen F, Rosenblum CI, Van der Ploeg LH, Cortese R, Ciliberto G and Laufer R (1997). "Ciliary neurotrophic factor corrects obesity and diabetes associated with leptin deficiency and resistance." Proc Natl Acad Sci U S A **94**(12): 6456-61.

Goldstein BJ and Schwob JE (1996). "Analysis of the Globose Basal Cell Compartment in Rat Olfactory Epithelium Using GBC-1, a New Monoclonal Antibody against Globose Basal Cells." J. Neurosci **16**(12): 4005-4016.

Gozes I, Bardea A, Reshef A, Zamostiano R, Zhukovsky S, Rubinraut S, Fridkin M and Brenneman DE (1996). "Neuroprotective strategy for Alzheimer disease: intranasal administration of a fatty neuropeptide." Proc Natl Acad Sci U S A **93**(1): 427-432.

Graziadei PP (1970). "The mucous membranes of the nose." Ann Otol Rhinol Laryngol **79**(3): 433-42.

Graziadei PPC (1971). The olfactory mucosa of vertebrates. Olfaction. Beidler LM and Amoore JE. Berlin, New York, Springer-Verlag. **4:** 518.

Graziadei PPC and Monti-Graziadei GA (1979). "Neurogenesis and neuron regeneration in the olfactory system of mammals. I. Morphological aspects of differentiation and structural organization of the olfactory sensory neurons." Journal of Neurocytology **8**(1): 1-18.

Haberly LB and Price JL (1978). "Association and commissural fiber systems of the olfactory cortex of the rat II. Systems originating in the olfactory peduncle." J Comp Neurol **181**(4): 781-807.

Haberly LB and Price JL (1978). "Association and commissural fiber systems of the olfactory cortex of the rat. I. Systems originating in the piriform cortex and adjacent areas." J Comp Neurol **178**(4): 711-740.

Hallschmid M, Benedict C, Schultes B, Born J and Kern W (2008). "Obese men respond to cognitive but not to catabolic brain insulin signaling." Int J Obes (Lond) **32**(2): 275-82.

Hanson L and Frey W (2007). "Strategies for Intranasal Delivery of Therapeutics for the Prevention and Treatment of NeuroAIDS." Journal of Neuroimmune Pharmacology **2**(1): 81-86.

Henriksson J, Tallkvist J and Tjalve H (1997). "Uptake of nickel into the brain via olfactory neurons in rats." Toxicol Lett **91**(2): 153-62.

Henry RJ, Ruano N, Casto D and Wolf RH (1998). "A pharmacokinetic study of midazolam in dogs: nasal drop vs. atomizer administration." Pediatr Dent **20**(5): 321-6.

Hermens WTJMC, Giger RJ, Holtmaat AJGD, Dijkhuizen PA, Houweling DA and Verhaagen J (1997). "Transient gene transfer to neurons and glia: Analysis of adenoviral vector performance in the CNS and PNS." Journal of Neuroscience Methods **71**(1): 85-98.

Hermens WTJMC and Verhaagen J (1998). "Viral vectors, tools for gene transfer in the nervous system." Prog Neurobiol **55**(4): 399-432.

Hinds JW, Hinds PL and McNelly NA (1984). "An autoradiographic study of the mouse olfactory epithelium: evidence for long-lived receptors." Anat Rec **210**(2): 375-83.

Holl A (1965). "Vital staining by trypan blue; its selectivity for olfactory receptor cells of the brown bullhead, Ictalurus natalis." Stain Technol **40**(5): 269-73.

Holtmaat AJGD, Hermens WTJMC, Beate Oestreicher A, Hendrik Gispen W, Kaplitt MG and Verhaagen J (1996). "Efficient adenoviral vector-directed

expression of a foreign gene to neurons and sustentacular cells in the mouse olfactory neuroepithelium." Molecular Brain Research **41**(1-2): 148-156.

Holtmaat AJGD, Hermens WTJMC, Sonnemans MAF, Giger RJ, Van Leeuwen FW, Kaplitt MG, Oestreicher AB, Gispen WH and Verhaagen J (1997). "Adenoviral Vector-Mediated Expression of B-50/GAP-43 Induces Alterations in the Membrane Organization of Olfactory Axon Terminals In Vivo." J. Neurosci **17**(17): 6575-6586.

Howe HA and Bodian D (1941). "Second Attacks of Poliomyelitis: An Experimental Study." J. Exp. Med. **74**(2): 145-166.

Hussain AA (1998). "Intranasal drug delivery." Advanced Drug Delivery Reviews **29**(1-2): 39-49.

Ichimura T, Fraser PA and Cserr HF (1991). "Distribution of extracellular tracers in perivascular spaces of the rat brain." Brain Res **545**(1-2): 103-13.

IFNB MSG (1995). "Interferon beta-1b in the treatment of multiple sclerosis: final outcome of the randomized controlled trial. The IFNB Multiple Sclerosis Study Group and The University of British Columbia MS/MRI Analysis Group." Neurology **45**(7): 1277-1285.

Illum L (1996). "Nasal delivery. The use of animal models to predict performance in man." J Drug Target **3**(6): 427-42.

Illum L (2000). "Transport of drugs from the nasal cavity to the central nervous system." Eur J Pharm Sci **11**(1): 1-18.

Illum L (2002). "Nasal drug delivery: new developments and strategies." Drug Discovery Today **7**(23): 1184-1189.

Illum L (2003). "Nasal drug delivery--possibilities, problems and solutions." Journal of Controlled Release **87**(1-3): 187-198.

Illum L (2004). "Is nose-to-brain transport of drugs in man a reality?" J Pharm Pharmacol **56**(1): 3-17.

Ip NY and Yancopoulos GD (1996). "The Neurotrophins and CNTF: Two Families of Collaborative Neurotrophic Factors." Annual Review of Neuroscience **19**(1): 491-515.

Isaacs A and Lindenmann J (1987). "Virus interference. I. The interferon. By A. Isaacs and J. Lindenmann, 1957." J Interferon Res **7**(5): 429-38.

Itaya SK (1987). "Anterograde transsynaptic transport of WGA-HRP in rat olfactory pathways." Brain Res **409**(2): 205-214.

Ivic L, Pyrski MM, Margolis JW, Richards LJ, Firestein S and Margolis FL (2000). "Adenoviral vector-mediated rescue of the OMP-null phenotype in vivo." Nat Neurosci **3**(11): 1113-1120.

Iwai N, Zhou Z, Roop DR and Behringer RR (2008). "Horizontal Basal Cells Are Multipotent Progenitors in Normal and Injured Adult Olfactory Epithelium." Stem Cells **26**(5): 1298-1306.

Jackson RT, Tigges J and Arnold W (1979). "Subarachnoid space of the CNS, nasal mucosa, and lymphatic system." Arch Otolaryngol **105**(4): 180-184.

Jerusalmi A, Morris-Downes MM, Sheahan BJ and Atkins GJ (2003). "Effect of intranasal administration of Semliki Forest virus recombinant particles expressing reporter and cytokine genes on the progression of experimental autoimmune encephalomyelitis." Mol Ther **8**(6): 886-94.

Jin K, Xie L, Childs J, Sun Y, Mao XO, Logvinova A and Greenberg DA (2003). "Cerebral neurogenesis is induced by intranasal administration of growth factors." Annals of Neurology **53**(3): 405-409.

Jin Y, Dons L, Kristensson K and Rottenberg ME (2001). "Neural Route of Cerebral Listeria monocytogenes Murine Infection: Role of Immune Response Mechanisms in Controling Bacterial Neuroinvasion." Infect. Immun. **69**(2): 1093-1100.

Kasowski HJ, Kim H and Greer CA (1999). "Compartmental organization of the olfactory bulb glomerulus." J Comp Neurol **407**(2): 261-74.

Kastin AJ and Pan W (2006). "Intranasal Leptin: Blood-Brain Barrier Bypass (BBBB) for Obesity?" Endocrinology **147**(5): 2086-2087.

Keller A and Margolis FL (1975). "Immunological studies of the rat olfactory marker protein." J Neurochem **24**(6): 1101-6.

Kennedy PG and Chaudhuri A (2002). "Herpes simplex encephalitis." J Neurol Neurosurg Psychiatry **73**(3): 237-8.

Kinoshita N, Mizuno T and Yoshihara Y (2002). "Adenovirus-mediated WGA Gene Delivery for Transsynaptic Labeling of Mouse Olfactory Pathways." Chem. Senses **27**(3): 215-223.

Kishimoto T, Akira S, Narazaki M and Taga T (1995). "Interleukin-6 family of cytokines and gp130." Blood **86**(4): 1243-1254.

Kosfeld M, Heinrichs M, Zak PJ, Fischbacher U and Fehr E (2005). "Oxytocin increases trust in humans." Nature **435**(7042): 673-6.

Kratskin I and Belluzzi O (2003). Anatomy and Neurochemistry of the Olfactory Bulb. Handbook of Olfaction and Gustation, Second Edition. Doty RL. New York, Informa Healthcare**:** 139 - 164.

Kristensson K and Olsson Y (1971). "Uptake of exogenous proteins in mouse olfactory cells." Acta Neuropathologica **19**(2): 145-154.

Kroin JS (1992). "Intrathecal drug administration. Present use and future trends." Clin Pharmacokinet **22**(5): 319-26.

Lafay F, Coulon P, Astic L, Saucier D, Riche D, Holley A and Flamand A (1991). "Spread of the CVS strain of rabies virus and of the avirulent mutant AvO1 along the olfactory pathways of the mouse after intranasal inoculation." Virology **183**(1): 320-330.

Laing JM, Gober MD, Golembewski EK, Thompson SM, Gyure KA, Yarowsky PJ and Aurelian L (2006). "Intranasal Administration of the Growth-Compromised HSV-2 Vector [Delta]RR Prevents Kainate-Induced Seizures and Neuronal Loss in Rats and Mice." Mol Ther **13**(5): 870-881.

Lambert PD, Anderson KD, Sleeman MW, Wong V, Tan J, Hijarunguru A, Corcoran TL, Murray JD, Thabet KE, Yancopoulos GD and Wiegand SJ (2001). "Ciliary neurotrophic factor activates leptin-like pathways and reduces body fat, without cachexia or rebound weight gain, even in leptin-resistant obesity." Proc Natl Acad Sci U S A **98**(8): 4652-7.

Landsteiner K and Levaditi C (1910). "Etude experimentale de la Poliomyelite aigue (Maladiede Heine Medin)." Ann Inst Pasteur **24**: 833-878.

Langenhan T, Sendtner M, Holtmann B, Carroll P and Asan E (2005). "Ciliary neurotrophic factor-immunoreactivity in olfactory sensory neurons." Neuroscience **134**(4): 1179-1194.

Lansbury PT, Jr. (2004). "Back to the future: the 'old-fashioned' way to new medications for neurodegeneration." Nat Med **10 Suppl**(7): S51-7.

Lawson SN and Waddell PJ (1991). "Soma neurofilament immunoreactivity is related to cell size and fibre conduction velocity in rat primary sensory neurons." J Physiol **435**(1): 41-63.

Lee M-Y, Deller T, Kirsch M, Frotscher M and Hofmann H-D (1997). "Differential Regulation of Ciliary Neurotrophic Factor (CNTF) and CNTF Receptor alpha Expression in Astrocytes and Neurons of the Fascia Dentata after Entorhinal Cortex Lesion." J. Neurosci **17**(3): 1137-1146.

Lee MY, Hofmann HD and Kirsch M (1997). "Expression of ciliary neurotrophic factor receptor-[alpha] messenger RNA in neonatal and adult rat brain: an in situ hybridization study." Neuroscience **77**(1): 233-246.

Leopold DA, Thomas H, James ES, Seok Chen H, Michael K and Gerd K (2000). "Anterior Distribution of Human Olfactory Epithelium." The Laryngoscope **110**(3): 417-421.

Leung CT, Coulombe PA and Reed RR (2007). "Contribution of olfactory neural stem cells to tissue maintenance and regeneration." Nat Neurosci **10**(6): 720-726.

Lidow MS and Menco BP (1984). "Observations on axonemes and membranes of olfactory and respiratory cilia in frogs and rats using tannic acid-supplemented fixation and photographic rotation." J Ultrastruct Res **86**(1): 18-30.

Lin LF, Armes LG, Sommer A, Smith DJ and Collins F (1990). "Isolation and characterization of ciliary neurotrophic factor from rabbit sciatic nerves." J. Biol. Chem. **265**(15): 8942-8947.

Liu X-F, Fawcett JR, Hanson LR and Frey WH (2004). "The window of opportunity for treatment of focal cerebral ischemic damage with noninvasive intranasal insulin-like growth factor-I in rats." J Stroke Cerebrovasc Dis **13**(1): 16-23.

Liu X-F, Fawcett JR, Thorne RG and Frey Ii WH (2001). "Non-invasive intranasal insulin-like growth factor-I reduces infarct volume and improves neurologic function in rats following middle cerebral artery occlusion." Neurosci Lett. **308**(2): 91-94.

Lu B (2003). "BDNF and activity-dependent synaptic modulation." Learn Mem **10**(2): 86-98.

Ma Y-P, Ma M-M, Ge S, Guo R-B, Zhang H-J, Frey Ii WH, Xu G-L and Liu X-F (2007). "Intranasally delivered TGF-[beta]1 enters brain and regulates gene expressions of its receptors in rats." Brain Res Bull **74**(4): 271-277.

Mackay-Sim A and Chuah MI (2000). "Neurotrophic factors in the primary olfactory pathway." Prog Neurobiol **62**(5): 527-559.

Mackay-Sim A. and Kittel PW (1991). "On the Life Span of Olfactory Receptor Neurons." Eur J Neurosci **3**(3): 209-215.

Macrides F, Davis BJ, Youngs WM, Nadi NS and Margolis FL (1981). "Cholinergic and catecholaminergic afferents to the olfactory bulb in the hamster: a neuroanatomical, biochemical, and histochemical investigation." J Comp Neurol **203**(3): 495-514.

Mahoney MJ and Saltzman WM (1996). "Controlled release of proteins to tissue transplants for the treatment of neurodegenerative disorders." Journal of Pharmaceutical Sciences **85**(12): 1276-1281.

Malnic B, Hirono J, Sato T and Buck LB (1999). "Combinatorial receptor codes for odors." Cell **96**(5): 713-23.

Maniatis T, Fritsch EF and Sambrook J (1989). Molecular cloning : a laboratory manual / J. Sambrook, E.F. Fritsch, T. Maniatis, New York : Cold Spring Harbor Laboratory Press.

Manthorpe M., Louis J. C., Hagg T. and S. V (1993). Ciliary neuronotrophic factor. Neurotrophic Factors. Loughlin S. E. and H. FJ. San Diego, Academic Press**:** 443-473.

Marr RA, Rockenstein E, Mukherjee A, Kindy MS, Hersh LB, Gage FH, Verma IM and Masliah E (2003). "Neprilysin gene transfer reduces human amyloid pathology in transgenic mice." J Neurosci **23**(6): 1992-6.

Masiakowski P, Liu HX, Radziejewski C, Lottspeich F, Oberthuer W, Wong V, Lindsay RM, Furth ME and Panayotatos N (1991). "Recombinant human and rat ciliary neurotrophic factors." J Neurochem **57**(3): 1003-12.

Mathison S, Nagilla R and Kompella UB (1998). "Nasal route for direct delivery of solutes to the central nervous system: fact or fiction?" J Drug Target **5**(6): 415-41.

McBride K, Slotnick B and Margolis FL (2003). "Does intranasal application of zinc sulfate produce anosmia in the mouse? An olfactometric and anatomical study." Chem Senses **28**(8): 659-70.

McLean JH and Shipley MT (1987). "Serotonergic afferents to the rat olfactory bulb: I. Origins and laminar specificity of serotonergic inputs in the adult rat." J. Neurosci **7**(10): 3016-3028.

McLean JH, Shipley MT, Nickell WT, Aston-Jones G and Reyher CK (1989). "Chemoanatomical organization of the noradrenergic input from locus coeruleus to the olfactory bulb of the adult rat." J Comp Neurol **285**(3): 339-49.

Meisami E and Safari L (1981). "A quantitative study of the effects of early unilateral olfactory deprivation on the number and distribution of mitral and tufted cells and of glomeruli in the rat olfactory bulb." Brain Res **221**(1): 81-107.

Meisami E and Sendera TJ (1993). "Morphometry of rat olfactory bulbs stained for cytochrome oxidase reveals that the entire population of glomeruli forms early in the neonatal period." Developmental Brain Research **71**(2): 253-257.

Menco BP (1984). "Ciliated and microvillous structures of rat olfactory and nasal respiratory epithelia. A study using ultra-rapid cryo-fixation followed by freeze-substitution or freeze-etching." Cell Tissue Res **235**(2): 225-41.

Menco BP, Birrell GB, Fuller CM, Ezeh PI, Keeton DA and Benos DJ (1998). "Ultrastructural localization of amiloride-sensitive sodium channels and Na+,K(+)-ATPase in the rat's olfactory epithelial surface." Chem Senses **23**(2): 137-49.

Menco BP and Jackson JE (1997). "A banded topography in the developing rat's olfactory epithelial surface." J Comp Neurol **388**(2): 293-306.

Menco BPM and Morrison EE (2003). Morphology of the Mammalian Olfactory Epithelium: Form, Fine Structure, Function, and Pathology. Handbook of Olfaction and Gustation, Second Edition. Doty RL, Informa Healthcare**:** 17 - 50.

Merkus FWHM and van den Berg MP (2007). "Can Nasal Drug Delivery Bypass the Blood-Brain Barrier?: Questioning the Direct Transport Theory. [Article]." Drugs in R & D **8**(3): 133-144.

Miana-Mena FJ, Muñoz MJ, Roux S, Ciriza J, Zaragoza P, Brûlet P and Osta R (2004). "A Non-Viral Vector for Targeting Gene Therapy to Motoneurons in the CNS." Neurodegenerative Diseases **1**(2-3): 101-108.

Michael GJ and Priestley JV (1999). "Differential Expression of the mRNA for the Vanilloid Receptor Subtype 1 in Cells of the Adult Rat Dorsal Root and Nodose Ganglia and Its Downregulation by Axotomy." J. Neurosci **19**(5): 1844-1854.

Monath TP, Cropp CB and Harrison AK (1983). "Mode of entry of a neurotropic arbovirus into the central nervous system. Reinvestigation of an old controversy." Lab Invest **48**(4): 399-410.

Moran DT, Rowley JC, 3rd and Jafek BW (1982). "Electron microscopy of human olfactory epithelium reveals a new cell type: the microvillar cell." Brain Res **253**(1-2): 39-46.

Mori K, Kishi K and Ojima H (1983). "Distribution of dendrites of mitral, displaced mitral, tufted, and granule cells in the rabbit olfactory bulb." J Comp Neurol **219**(3): 339-55.

Morrison EE and Costanzo RM (1992). "Morphology of olfactory epithelium in humans and other vertebrates." Microsc Res Tech **23**(1): 49-61.

Morse JK, Wiegand SJ, Anderson K, You Y, Cai N, Carnahan J, Miller J, DiStefano PS, Altar CA and Lindsay RM (1993). "Brain-derived neurotrophic factor (BDNF) prevents the degeneration of medial septal cholinergic neurons following fimbria transection." J. Neurosci **13**(10): 4146-4156.

Mufson EJ, Kroin JS, Liu YT, Sobreviela T, Penn RD, Miller JA and Kordower JH (1996). "Intrastriatal and intraventricular infusion of brain-derived neurotrophic factor in the cynomologous monkey: distribution, retrograde

transport and co-localization with substantia nigra dopamine-containing neurons." Neuroscience **71**(1): 179-91.

Mufson EJ, Kroin JS, Sendera TJ and Sobreviela T (1999). "Distribution and retrograde transport of trophic factors in the central nervous system: functional implications for the treatment of neurodegenerative diseases." Prog Neurobiol **57**(4): 451-84.

Naldini L, Blomer U, Gage FH, Trono D and Verma IM (1996). "Efficient transfer, integration, and sustained long-term expression of the transgene in adult rat brains injected with a lentiviral vector." Proc Natl Acad Sci U S A **93**(21): 11382-8.

Newman MP, Feron F and Mackay-Sim A (2000). "Growth factor regulation of neurogenesis in adult olfactory epithelium." Neuroscience **99**(2): 343-50.

Oliver KR and Fazakerley JK (1997). "Transneuronal spread of Semliki Forest virus in the developing mouse olfactory system is determined by neuronal maturity." Neuroscience **82**(3): 867-877.

Orona E, Scott JW and Rainer EC (1983). "Different granule cell populations innervate superficial and deep regions of the external plexiform layer in rat olfactory bulb." J Comp Neurol **217**(2): 227-37.

Ozduman K, Wollmann G, Piepmeier JM and van den Pol AN (2008). "Systemic Vesicular Stomatitis Virus Selectively Destroys Multifocal Glioma and Metastatic Carcinoma in Brain." J. Neurosci **28**(8): 1882-1893.

Pan W, Kastin AJ, Maness LM and Brennan JM (1999). "Saturable entry of ciliary neurotrophic factor into brain." Neurosci Lett. **263**(1): 69-71.

Panayotatos N, Radziejewska E, Acheson A, Pearsall D, Thadani A and Wong V (1993). "Exchange of a single amino acid interconverts the specific activity and gel mobility of human and rat ciliary neurotrophic factors." J. Biol. Chem. **268**(25): 19000-19003.

Pardridge WM (1991). Peptide drug delivery to the brain. New York, Raven Press.

Pardridge WM (1998). "CNS Drug Design Based on Principles of Blood-Brain Barrier Transport." Journal of Neurochemistry **70**(5): 1781-1792.

Pardridge WM (2002). "Drug and Gene Delivery to the Brain: The Vascular Route." Neuron **36**(4): 555-558.

Pardridge WM (2002). "Drug and gene targeting to the brain with molecular Trojan horses." Nat Rev Drug Discov **1**(2): 131-9.

Pardridge WM (2005). "The blood-brain barrier: bottleneck in brain drug development." NeuroRx **2**(1): 3-14.

Penn RD, Kroin JS, York MM and Cedarbaum JM (1997). "Intrathecal ciliary neurotrophic factor delivery for treatment of amyotrophic lateral sclerosis (phase I trial)." Neurosurgery **40**(1): 94-9; discussion 99-100.

Perl DP and Good PF (1987). "Uptake of aluminium into central nervous system along nasal-olfactory pathways." Lancet **1**(8540): 1028.

Perlman S, Jacobsen G and Afifi A (1989). "Spread of a neurotropic murine coronavirus into the CNS via the trigeminal and olfactory nerves." Virology **170**(2): 556-560.

Perlman S, Jacobsen G, Olson AL and Afifi A (1990). "Identification of the spinal cord as a major site of persistence during during chronic infection with a murine coronavirus." Virology **175**(2): 418-426.

Pietrowsky R, Struben C, Molle M, Fehm HL and Born J (1996). "Brain potential changes after intranasal vs. intravenous administration of vasopressin: evidence for a direct nose-brain pathway for peptide effects in humans." Biological Psychiatry **39**(5): 332-340.

Plendl J and Sinowatz F (1998). "Glycobiology of the olfactory system." Acta Anat (Basel) **161**(1-4): 234-53.

Prentis RA, Lis Y and Walker SR (1988). "Pharmaceutical innovation by the seven UK-owned pharmaceutical companies (1964-1985)." Br J Clin Pharmacol **25**(3): 387-96.

Price JL (1968). "The termination of centrifugal fibres in the olfactory bulb." Brain Res **7**(3): 483-486.

Price JL and Powell TP (1970). "The morphology of the granule cells of the olfactory bulb." J Cell Sci **7**(1): 91-123.

Rake G (1937). "THE RAPID INVASION OF THE BODY THROUGH THE OLFACTORY MUCOSA." J. Exp. Med. **65**(2): 303-315.

Reger MA, Watson GS, Frey Ii WH, Baker LD, Cholerton B, Keeling ML, Belongia DA, Fishel MA, Plymate SR, Schellenberg GD, Cherrier MM and Craft S (2006). "Effects of intranasal insulin on cognition in memory-impaired older adults: Modulation by APOE genotype." Neurobiol Aging **27**(3): 451-458.

Reger MA, Watson GS, Green PS, Baker LD, Cholerton B, Fishel MA, Plymate SR, Cherrier MM, Schellenberg GD, Frey WH and Craft S (2008). "Intranasal insulin administration dose-dependently modulates verbal memory and plasma amyloid-beta in memory-impaired older adults." J Alzheimers Dis **13**: 323 - 331.

Reger MA, Watson GS, Green PS, Wilkinson CW, Baker LD, Cholerton B, Fishel MA, Plymate SR, Breitner JC, DeGroodt W, Mehta P and Craft S (2008). "Intranasal insulin improves cognition and modulates beta-amyloid in early AD." Neurology **70**: 440 - 448.

Ross TM, Martinez PM, Renner JC, Thorne RG, Hanson LR and Frey WH (2004). "Intranasal administration of interferon beta bypasses the blood-brain barrier to target the central nervous system and cervical lymph nodes: a non-invasive treatment strategy for multiple sclerosis." Journal of Neuroimmunology **151**(1-2): 66-77.

Sakane T, Akizuki M, Taki Y, Yamashita S, Sezaki H and Nadai T (1995). "Direct drug transport from the rat nasal cavity to the cerebrospinal fluid: the relation to the molecular weight of drugs." J Pharm Pharmacol **47**(5): 379-81.

Sakane T, Akizuki M, Yamashita S, Sezaki H and Nadai T (1994). "Direct drug transport from the rat nasal cavity to the cerebrospinal fluid: the relation to the dissociation of the drug." J Pharm Pharmacol **46**(5): 378-9.

Sakane T, Akizuki M, Yoshida M, Yamashita S, Nadai T, Hashida M and Sezaki H (1991). "Transport of cephalexin to the cerebrospinal fluid directly from the nasal cavity." J Pharm Pharmacol **43**(6): 449-51.

Schaefer ML, Böttger B, Silver WL and Finger TE (2002). "Trigeminal collaterals in the nasal epithelium and olfactory bulb: A potential route for direct modulation of olfactory information by trigeminal stimuli." J Comp Neurol **444**(3): 221-226.

Schulz C, Paulus K and Lehnert H (2004). "Central Nervous and Metabolic Effects of Intranasally Applied Leptin." Endocrinology **145**(6): 2696-2701.

Schwab ME and Thoenen H (1977). "Retrograde axonal and transsynaptic transport of macromolecules: physiological and pathophysiological importance." Agents Actions **7**(3): 361-8.

Schwob JE (2002). "Neural regeneration and the peripheral olfactory system." The Anatomical Record **269**(1): 33-49.

Seki T, Sato N, Hasegawa T, Kawaguchi T and Juni K (1994). "Nasal absorption of zidovudine and its transport to cerebrospinal fluid in rats." Biol Pharm Bull **17**(8): 1135-7.

Shantha TR and Bourne GH (1968). The perineural epithelium-a new concept. The Structure and Function of the Nervous System. Bourne GH. New York, Academic Press. **1:** 168-189.

Shepherd GM, R CW and Greer CA (1998). The Olfactory Bulb. The Synaptic Organization of the Brain. Shepherd GM. New York, Oxford University Press**:** 236.

Shimizu H, Oh-I S, Okada S and Mori M (2005). "Inhibition of appetite by nasal leptin administration in rats." Int J Obes Relat Metab Disord **29**(7): 858-863.

Shipley MT (1985). "Transport of molecules from nose to brain: Transneuronal anterograde and retrograde labeling in the rat olfactory system by wheat germ agglutinin-horseradish peroxidase applied to the nasal epithelium." Brain Res Bull **15**(2): 129-142.

Shipley MT and Ennis M (1996). "Functional organization of olfactory system." J Neurobiol **30**(1): 123-176.

Shipley MT, Ennis M and Puche AC (2004). Olfactory System. The Rat Nervous System (Third Edition). George P. Burlington, Academic Press**:** 923-964.

Shipley MT, Halloran FJ and de la Torre J (1985). "Surprisingly rich projection from locus coeruleus to the olfactory bulb in the rat." Brain Res **329**(1-2): 294-9.

Shu SY, Ju G and Fan LZ (1988). "The glucose oxidase-DAB-nickel method in peroxidase histochemistry of the nervous system." Neurosci Lett **85**(2): 169-71.

Sicard G, Feron F, Andrieu JL, Holley A and Mackay-Sim A (1998). "Generation of neurons from a nonneuronal precursor in adult olfactory epithelium in vitro." Ann N Y Acad Sci **855**: 223-5.

Silver WL (1991). The common chemical sense. The neurobiology of taste and smell. Finger TE and Silver WL. Malabar, FL, Krieger**:** 65–87.

Sleeman MW, Anderson KD, Lambert PD, Yancopoulos GD and Wiegand SJ (2000). "The ciliary neurotrophic factor and its receptor, CNTFR alpha." Pharm Acta Helv **74**(2-3): 265-72.

Sleeman MW, Garcia K, Liu R, Murray JD, Malinova L, Moncrieffe M, Yancopoulos GD and Wiegand SJ (2003). "Ciliary neurotrophic factor improves diabetic parameters and hepatic steatosis and increases basal metabolic rate in db/db mice." Proc Natl Acad Sci U S A **100**(24): 14297-14302.

Slotnick B, Glover P and Bodyak N (2000). "Does intranasal application of zinc sulfate produce anosmia in the rat?" Behav Neurosci **114**(4): 814-29.

Soudais C, Laplace-Builhe C, Kissa K and Kremer EJ (2001). "Preferential transduction of neurons by canine adenovirus vectors and their efficient retrograde transport in vivo." FASEB J.: 01-0321fje.

Suzuki N (1984). "Anterograde fluorescent labeling of olfactory receptor neurons by Procion and Lucifer dyes." Brain Res **311**(1): 181-185.

Suzuki Y, Schafer J and Farbman AI (1995). "Phagocytic cells in the rat olfactory epithelium after bulbectomy." Exp Neurol **136**(2): 225-33.

Thoenen H and Sendtner M (2002). "Neurotrophins: from enthusiastic expectations through sobering experiences to rational therapeutic approaches." Nat Neurosci **5 Suppl**(50): 1046-50.

Thorne RG, Emory CR, Ala TA and Frey 2nd WH (1995). "Quantitative analysis of the olfactory pathway for drug delivery to the brain." Brain Res **692**(1-2): 278-282.

Thorne RG and Frey 2nd WH (2001). "Delivery of Neurotrophic Factors to the Central Nervous System: Pharmacokinetic Considerations." Clinical Pharmacokinetics **40**(12): 907-946.

Thorne RG, Hanson LR, Ross TM, Tung D and Frey Ii WH (2008). "Delivery of interferon-[beta] to the monkey nervous system following intranasal administration." Neuroscience **152**(3): 785-797.

Thorne RG, Pronk GJ, Padmanabhan V and Frey 2nd WH (2004). "Delivery of insulin-like growth factor-I to the rat brain and spinal cord along olfactory and trigeminal pathways following intranasal administration." Neuroscience **127**(2): 481-496.

Tomlinson AH and Esiri MM (1983). "Herpes simplex encephalitis : Immunohistological demonstration of spread of virus via olfactory pathways in mice." Journal of the Neurological Sciences **60**(3): 473-484.

Trotier D, Eloit C, Wassef M, Talmain G, Bensimon JL, Doving KB and Ferrand J (2000). "The vomeronasal cavity in adult humans." Chem Senses **25**(4): 369-80.

van den Berg MP, Verhoef JC, Romeijn SG and Merkus FW (2004). "Uptake of estradiol or progesterone into the CSF following intranasal and intravenous delivery in rats." Eur J Pharm Biopharm **58**(1): 131-5.

Vassar R, Chao SK, Sitcheran R, Nunez JM, Vosshall LB and Axel R (1994). "Topographic organization of sensory projections to the olfactory bulb." Cell **79**(6): 981-91.

Venero JL, Hefti F and Knusel B (1996). "Trophic effect of exogenous nerve growth factor on rat striatal cholinergic neurons: comparison between intraparenchymal and intraventricular administration." Mol Pharmacol **49**(2): 303-310.

Venkatraman G, Behrens M, Pyrski M and Margolis FL (2005). "Expression of Coxsackie-Adenovirus receptor (CAR) in the developing mouse olfactory system." Journal of Neurocytology **V34**(3): 295-305.

Vig PJS, Subramony SH, D'Souza DR, Wei J and Lopez ME (2006). "Intranasal administration of IGF-I improves behavior and Purkinje cell pathology in SCA1 mice." Brain Res Bull **69**(5): 573-579.

von Bartheld C (2000). Tracing with Radiolabeled Neurotrophins Neurotrophin Protocols. Rush RA. Clifton, N.J., Humana Press. **169:** 288.

von Bartheld C, S. (2004). "Axonal transport and neuronal transcytosis of trophic factors, tracers, and pathogens." Journal of Neurobiology **58**(2): 295-314.

von Bartheld CS (1998). "Radio-iodination of neurotrophins and their delivery in vivo: advantages of membrane filtration and the use of disposable syringes." Journal of Neuroscience Methods **79**(2): 207-215.

Wagner JP, Black IB and DiCicco-Bloom E (1999). "Stimulation of Neonatal and Adult Brain Neurogenesis by Subcutaneous Injection of Basic Fibroblast Growth Factor." J. Neurosci **19**(14): 6006-6016.

Weiss DG and Buchner K (1988). Axoplasmic transport in olfactory receptor neurons. Molecular neurobiology of the olfactory system Margolis FL and Getchell TV. New York, Plenum Press**:** 217-236.

Weiss P and Holland Y (1967). "Neuronal Dynamics and Axonal flow, II. The olfactory nerve as model test object." Proc Natl Acad Sci U S A **57**(2): 258-264.

Xiao X, Li J, McCown TJ and Samulski RJ (1997). "Gene Transfer by Adeno-Associated Virus Vectors into the Central Nervous System." Exp Neurol **144**(1): 113-124.

Yang J-P, Liu H-J, Cheng S-M, Wang Z-L, Cheng X, Yu H-X and Liu X-F (2008). "Direct transport of VEGF from the nasal cavity to brain." Neurosci Lett. **In Press, Corrected Proof**.

Yoffey JM (1958). "Passage of fluid and other substances through the nasal mucosa." J Laryngol Otol **72**(5): 377-84.

Young W-J, Smith SM and Chang C (1997). "Induction of the Intronic Enhancer of the Human Ciliary Neurotrophic Factor Receptor (CNTFRalpha) Gene by the TR4 Orphan Receptor. A Member of Steroid Receptor Superfamily." J. Biol. Chem. **272**(5): 3109-3116.

Youngentob SL, Pyrski MM and Margolis FL (2004). "Adenoviral vector-mediated rescue of the OMP-null behavioral phenotype: enhancement of odorant threshold sensitivity." Behav Neurosci **118**(3): 636-42.

Yu Y-P, Xu Q-Q, Zhang Q, Zhang W-P, Zhang L-H and Wei E-Q (2005). "Intranasal recombinant human erythropoietin protects rats against focal cerebral ischemia." Neurosci Lett. **387**(1): 5-10.

Zhang ET, Richards HK, Kida S and Weller RO (1992). "Directional and compartmentalised drainage of interstitial fluid and cerebrospinal fluid from the rat brain." Acta Neuropathol **83**(3): 233-9.

Zhao H, Otaki JM and Firestein S (1996). "Adenovirus-mediated gene transfer in olfactory neurons *in vivo*." Journal of Neurobiology **30**(4): 521-530.

Zhou XF and Rush RA (1996). "Endogenous brain-derived neurotrophic factor is anterogradely transported in primary sensory neurons." Neuroscience **74**(4): 945-53.

Zucker LM and Zucker TF (1961). "Fatty, a new mutation in the rat." J Hered **52**(6): 275-278.

Zucker TF and Zucker LM (1963). "Fat Accretion and Growth in the Rat." J. Nutr. **80**(1): 6-19.